THE APPLICATION OF DUAL ENERGY X–RAY TRANSMISSION SORTING TO THE SEPARATION OF COAL FROM TORBANITE

Hayley Strydom

A dissertation submitted to the Faculty of Engineering and The Built Environment, University of the Witwatersrand, in fulfillment of the requirements for the degree of Master of Science in Engineering

Johannesburg, 2010

DECLARATION

I declare that the dissertation is my own unaided work. It is being submitted to the Degree of Master of Science in Engineering to the University of the Witwatersrand, Johannesburg. It has not been submitted before for any degree or examination to any other university.

…….

Hayley Strydom

On this the……day of… ……. Year

Dedicated to my wonderful family, in thanks for all their love and continuous support
Ivan, Myra and Tristan Strydom
Colleen Cheesman- My Mother

ACKNOWLEDGEMENTS

Work related to ore sorting has become a real passion of mine from my first introduction to it as a graduate engineer at Mintek. I feel that this is in a way, my unique opportunity to express my enthusiasm for the topic from my own point of view- an opportunity to put onto paper what I know, in a way that others may understand the concepts and appreciate them as much as I do. I would therefore like to thank Professor Rosemary Falcon and Lionel Falcon for their constant encouragement to complete this work and to Mr Carl Bergmann for his support.

The author would like to acknowledge assistance of the Central Energy Fund for providing financial assistance, use of their Mikrosort X-Tract Sorter and for permission to publish this work. In addition, I would like to thank the Minerals Processing Division at Mintek for financial assistance as part of their Science Vote research scheme and for use of their facilities and equipment.

ABSTRACT

Dual Energy X-Ray Transmission (DE-XRT) Imaging is a multi-sensor technique employed to conduct particle-by-particle sorting. The system makes use of a dual energy x-ray line scan sensor, which generates images of the transmitted x-rays, similar to images generated for suitcase inspection in airport security applications. The dual energy x-ray system allows for rapid approximation of atomic number range, which is utilised to evaluate the mineral and maceral content. The process is independent of particle surface condition, and can thus be utilised as a dry process.

A unique application of this technology is in the removal of torbanite from a coal deposit located in Mpumalanga, South Africa. The separation of coal and torbanite by conventional gravity separation techniques is often difficult, due to the overlapping densities of torbanite and coal. Preliminary laboratory DE-XRT testwork results on high quality coal and torbanite products were promising. In order to evaluate the separation of typical ROM material on pilot scale, a production scale Mikrosort X-Tract Sorter was purchased. This was the first DE-XRT sorter available in South Africa, and was housed at Mintek. A 150t sample was provided from a box cut adjacent to the coal deposit under investigation in order to conduct bulk and pilot sorting tests.

Clear distinctions between the coal, torbanite and shale fractions were observed using this technique. The sorter feed (-80mm+20mm) could be upgraded from a CV of 22MJ/kg to 28MJ/kg. Ash content could be reduced from 26% to 10%. Petrographic analysis of the coal product indicated that a high purity coal product was attainable (91% by volume) at a mass yield of 42.9% to the coal product, with shale and mixed humic/sapropelic coal as contaminants. Under these conditions, torbanite contamination was marginal.

Thermogravimetric analysis (TGA) of the torbanite product derived from testwork indicated that volatiles release occurred as two separate but overlapping events. At a temperature of approximately 450°C, maximum release of volatiles occurred for the torbanite sample. At approximately 550°C all volatile material has been removed from the sample. This is favourable, as cracking starts to increase at a high rate from a 450-500°C. The most valuable and useful diesel fraction is allowed to boil up to 395°C. The heavy diesel product could potentially be utilised by Sasol Secunda to upgrade excess light diesel product.

The capability to process coarse materials (-80mm+20mm) allows for throughputs in excess of 40t/hr. Consequently, this technique may be applied in simpler coal upgrading processes, such as coal deshaling in arid regions.

TABLE OF CONTENTS

LIST OF FIGURES

LIST OF TABLES

LIST OF ABREVIATIONS

CEF	Central Energy Fund
CV	Calorific Value
DE-XRT	Dual Energy X-Ray Transmission Sorting
DMS	Dense Medium Separation
HPGR	High Pressure Grinding Rolls
PLC	Programmable Logic Computer
TGA	Thermogravimetric Analysis
ROM	Run of Mine

1 INTRODUCTION

Electronic ore sorting was initially introduced as a means of separating ore from gangue as early as the 1940's. Computer processing speeds of the first sorting units were initially very slow and cumbersome, resulting in very low throughputs. As a result, the application of ore sorters in the mining industry was limited to specialist applications, such as radiometric sorting for upgrading of gold ores and x-ray fluorescent sorting of diamondiferous gravels. By the early 2000's processing speeds had improved dramatically, allowing optical sorting units utilised in the recycling industry to process up to 150 tons of scrap per hour. This also revived interest in the use of sorting as a tool for preconcentration in the mining industry. As a result, sorting units are widely utilised in the industrial minerals industry worldwide. Typically sorters can process materials within the size range -200mm +15mm at a throughput in excess of 150 tons per hour. Smaller size ranges can be processed for specialised applications, but at reduced flow rates.

Sorting technology has experienced rapid advancement during the last decade. The technology offers the mining industry a wide variety of sensors which can be utilised individually or in combination to identify properties such as conductivity, response to near infra-red and ultraviolet light and translucence. The most exciting of these is Dual Energy X-Ray Transmission Sorting (DE-XRT). Originally derived from x-ray detection units used for inspection of suitcases in airport security applications, the dual energy x-ray system allows for rapid approximation of atomic number range, which is utilised to evaluate mineral and maceral content. This includes degraded plant material, alginate and other components of coal and oil shale. As this process is insensitive to surface condition (e.g. the presence of dust), the process can be operated completely dry. In addition, as relative atomic number forms the basis of separation, this technique can be utilised for applications where standard minerals processing techniques have been deemed unfeasible.

An example of this is the separation of coal from torbanite. Torbanite is a very fine grained intermediate between coal and oil shale and is characterised by the presence Botryococcus-related alginite (Han et al, 1999). As a result of its composition, torbanite yields paraffinic and olefinic hydrocarbons when retorted. It is therefore a very lucrative commodity for the production of synfuel.

A number of torbanite reserves have been identified in South Africa. However, few of these have been exploited. In many instances, the torbanite is located as a seam of varying depth between two layers of high grade coal. The value of both coal and torbanite products are severely compromised by contamination with the other. The separation of these two commodities from one another is thus imperative for the financial success of such a mining undertaking. Studies conducted in the 1970's indicated that selective mining would not be financially feasible. In addition, it was noted during these studies that the density of torbanite and coal could overlap significantly. This ruled out the use of gravity based coal processing techniques, such as Dense Medium Separation (DMS) and spirals. Evaluation of such deposits (including the deposit near Kinross evaluated for this project) was terminated owing to lack of a suitable processing route.

With the introduction of Dual Energy X-Ray Sorting for applications such as the deshaling of coal, interest in the use of this technology for the separation of coal from torbanite was generated. Hand selected samples of torbanite and coal from a deposit located near Kinross were submitted to CommoDas GmbH in Wedel, Germany for preliminary DE-XRT laboratory testwork. The outcome of these tests was encouraging. However, it was recognized that a more detailed examination (in the form of a pilot scale campaign) was required to determine the performance of this technology on Run-of Mine (ROM) material. This would not only demonstrate the impacts of poor liberation on the separation, but would also allow for examination of the quality of products which could be attained on a bulk sample of material.

At that time, the technology was only available in Germany where logistics did not allow for bulk testing. A production scale sorting unit was purchased by the Central Energy Fund (CEF) to conduct a pilot scale evaluation of this technology. The unit was installed at Mintek for the duration of the testwork program. This was the first industrial scale x-ray transmission sorter to be installed in South Africa. A sample of 150 tons of typical ROM material was mined from a box-cut at an adjacent mine for testwork purposes.

This report documents results attained from process optimization and pilot scale sorting campaign.

2 INTRODUCTION TO DUAL ENERGY X-RAY TRANSMISSION SORTING

2.1 Ore Sorting- an Alternative Technique for Upgrading of Minerals

Global trends towards environmentally sustainable ore processing have resulted in a great deal of interest in the development of dry processing alternatives to conventional processing techniques. Optical sorting techniques are very energy efficient and require minimal quantities of water for operation. Other sorting techniques such as x-ray sorting can be conducted completely dry. It has been observed that operating costs of sorting units can be lower than those of conventional mineral processing units, making ore sorters a viable prospect for future mineral processing circuits.

The earliest form of ore sorting dates back to the stone-age, where banded iron stone was hand sorted from waste by ancient metal workers, based on distinct visual characteristics (Wills, 1992). Based on personal experience, it has been noted that hand sorting is still a prevalent technique utilised in small scale mining operations throughout Africa.

The first sorting units were developed in the early 1940's, and were utilised up until the late 1970's (Salter and Wyatt, 1991). Process rates of these units were slow, often allowing only for the processing of one rock at a time. As average throughputs of these units were low, sorting units were only feasible for niche markets, such as radiometric sorting of gold ores and x-ray fluorescence sorting of diamondiferous gravels (Sivamohan and Forssberg, 1991).

With the advent of more sophisticated computer technology, optical sorting units found a wide variety of application in the recycling industry. Interest in the use of sorting technology as a tool for the mining industry was rekindled in the early 2000's when sorters capable of processing in excess of 150 tons per hour were introduced for various applications in the mining industry. As a result of rapid development of this technology, a wide variety of sensors are currently available within the electromagnetic spectrum, as presented in Figure 1.

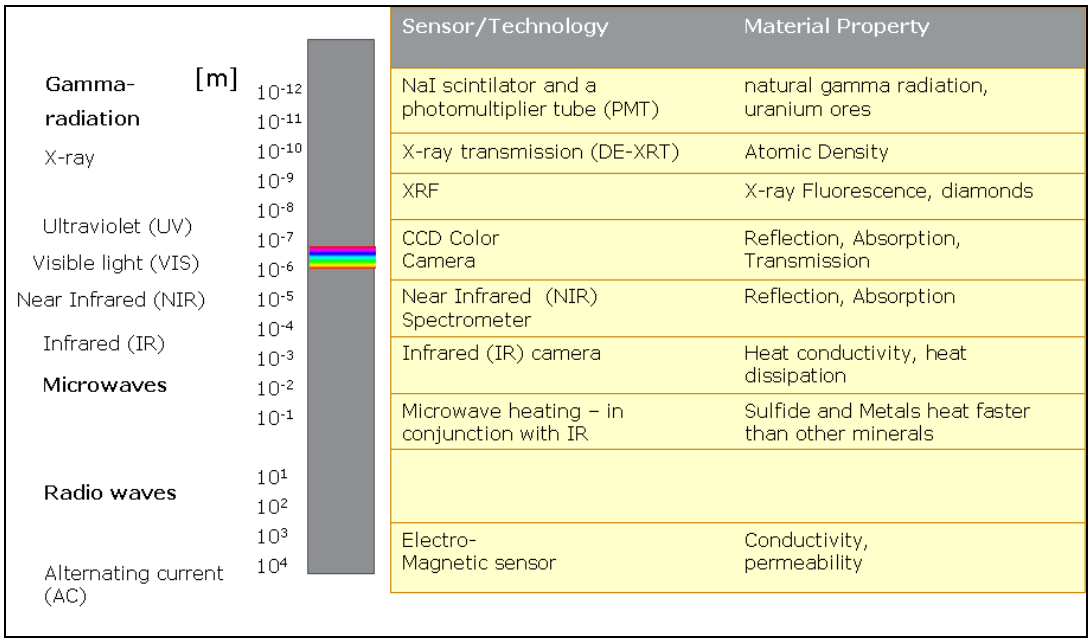

Sensor/Technology	Material Property
NaI scintilator and a photomultiplier tube (PMT)	natural gamma radiation, uranium ores
X-ray transmission (DE-XRT)	Atomic Density
XRF	X-ray Fluorescence, diamonds
CCD Color Camera	Reflection, Absorption, Transmission
Near Infrared (NIR) Spectrometer	Reflection, Absorption
Infrared (IR) camera	Heat conductivity, heat dissipation
Microwave heating – in conjunction with IR	Sulfide and Metals heat faster than other minerals
Electro-Magnetic sensor	Conductivity, permeability

Figure 1: Sensors Available Within the Electromagnetic Spectrum (Courtesy of CommoDaS, GmbH, 2009)

The sorting process consists of four distinct mechanisms, as demonstrated in Figure 2 (CommoDas, 2006):

1. *Particle Presentation Mechanism*. This is the most crucial system, as this ensures that particles report to the detection zone in a monolayer and are well spaced from one another. The detection system needs a clear image of each individual particle presented for analysis. Overlapping particles are treated as single elements.
2. *Detection System.* This can consist of a single sensor or multiple sensors working in conjunction with each other. Typically, an image of the particles passing through the sensor is taken in a "line by line" fashion. This allows for a high resolution image to be obtained. An x-ray scintillation crystal sensor can capture up to 2500 lines per second.
3. *Processing System.* The data acquired in this process is transferred to the Programmable Logic Controller (PLC), which analyses the captured images at a maximum rate of 10 000 particles per second. The prescribed algorithm is then applied to the particle to determine if it is to be rejected or accepted. The position and size of particles to be rejected is determined, and the PLC then controls the ejection of material by activating an appropriate number of valves in the correct position. The valves control a series of air jets, which facilitate separation.

4. *Ejection System.* A number of mechanisms have been utilized to perform the ejection of particles, including gate systems. The most popular is particle-by-particle ejection utilising pneumatic valves. Such a system typically consists of an array of 256 air jets, which are capable of rapid ejection of materials. This system allows for selective ejection of individual particles.

Legend	
1	*Material Feed*
2	*Vibratory Feeder*
3	*Free Fall Acceleration*
4	*Sensor*
5	*Data Processing*
6	*Air pressure*
7	*Accept/Reject Streams*
8	*Network Control Interface*

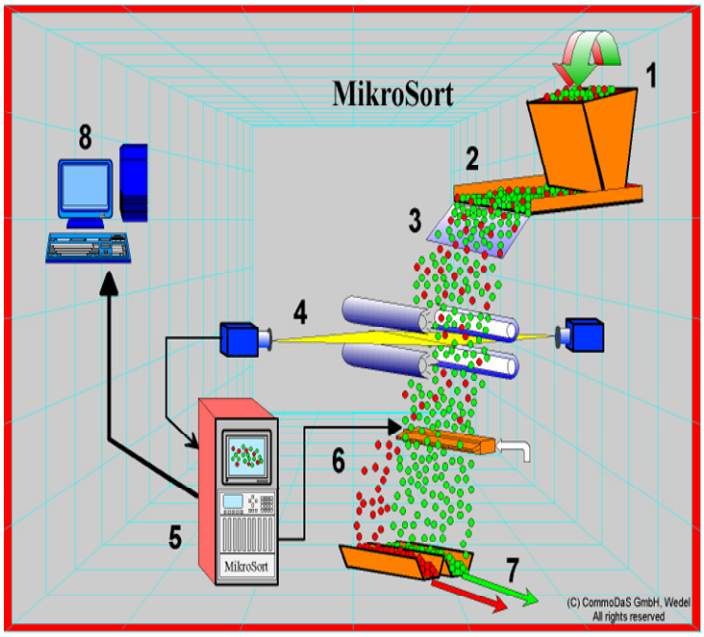

Figure 2: Typical Sorting Mechanism (Courtesy of CommoDas GmbH, 2006)

Ore sorter design and available throughput vary from manufacturer to manufacturer. The most typical designs are:

- Chute based systems, where particles are scanned in free fall. This design is preferred for optical sorting applications, as it allows for double sided scanning of particles. Particles of up to 250mm can be processed by this unit, which can have throughputs of up to 200 tons per hour.
- Belt driven sorters, where particles are presented to the sensor on a conveyor belt, travelling at the same velocity. This is the preferred method of processing materials utilising alternative sorting sensors. Recommended top size for these types of units is 80-100 tons per hour at a throughput of up to 100 tons per hour.

2.2 Identification of Minerals by X-Ray Transmission Theory

X-rays are transmitted through material at varying degrees, depending on the density of the material. Materials absorb a proportion of the radiation resulting in a reduction in the intensity of the x-ray. This phenomenon, referred to as *transmission damping*, can be explained by x-ray transmission theory.

Lambert's Law indicates that transmission damping is a function of the density and thickness of the material through which the beam passes, as presented in Equation 1 (Platt, 1999):

$$I_{\text{det}} = I_o e^{-\mu(\lambda)\rho d} \qquad [1]$$

Where I_{det} = detected intensity

I_o=intensity of undisturbed beam

$\mu(\lambda)$ = mass absorption co-efficient $\alpha \frac{Z^2}{(h\upsilon)^3}$ (Koningsberger, 1988)

ρ= solid density

d= thickness of irradiated material

Mass absorption co-efficient of all elements at various wavelengths are available in literature.

Mass absorption co-efficients for minerals and mixed element materials are determined from the sum product of the elemental composition and the mass absorption co-efficient of that element. For example, the mass absorption co-efficient of a particle with n elements is determined from:

$$\mu_{eff} = \sum_{i=1}^{n} f_i \mu_i \qquad [2]$$

where μ_{eff} = mass absorption co-efficient of the particle, as is independent of state or phase

f_i= the mass fraction of element i

The detected intensity is an exponential function of the thickness of the irradiated material. As significant variations in particle thickness are anticipated for scrap and mineral sorting, the use of a single energy wave (monochromatic imaging) to identify minerals would be

inaccurate. Observing the effects of two or more different wavelengths would rule out the effects of particle thickness.

Dual energy x-ray transmission involves the use of a high energy and low energy x-ray beam (i.e. two beams of different wavelengths). Mass absorption co-efficients vary as the wavelength of the x-ray beam varies. The extent of the change is dependant on atomic number of the material into which the x-rays are absorbed (Fox, 2004).

Application of Lambert's Law to dual energy absorption is presented as (De Jong & Harbeck, 2005):

$$\frac{I_1}{I_2} = e^{-\rho d \Delta\mu} = (e^{-\rho \Delta\mu})^d = C_m{}^d \qquad [3]$$

where $I_1; I_2 = \frac{I_{\text{det } 1;2}}{I_{01;2}}(\lambda_{1;2)})$ = dimensionless detected intensities at two different wavelengths

C_m = constant dependant only on the material properties and chosen wavelength.

As a result, if the Cm of two materials is different, these materials can be distinguished from one another. Measurement of I_1 and I_2 can thus be utilised to evaluate Cm (and hence approximate the atomic number of the material). Particle thickness can be determined by solving Lambert's Law for the high and low energy levels.

De Jong and Harbeck (2005) suggested that by comparing and plotting the degree of transmission of x-rays through particles at two different energy levels, a transmission curve specific to that material type could be generated. Various grades of the material type would have a separate transmission curve. This theory was examined utilizing binary mixtures of Zinc and Lead Sulphide, as demonstrated in Figure 3 and 4 respectively. Such curves could be derived for various grades of a particular element.

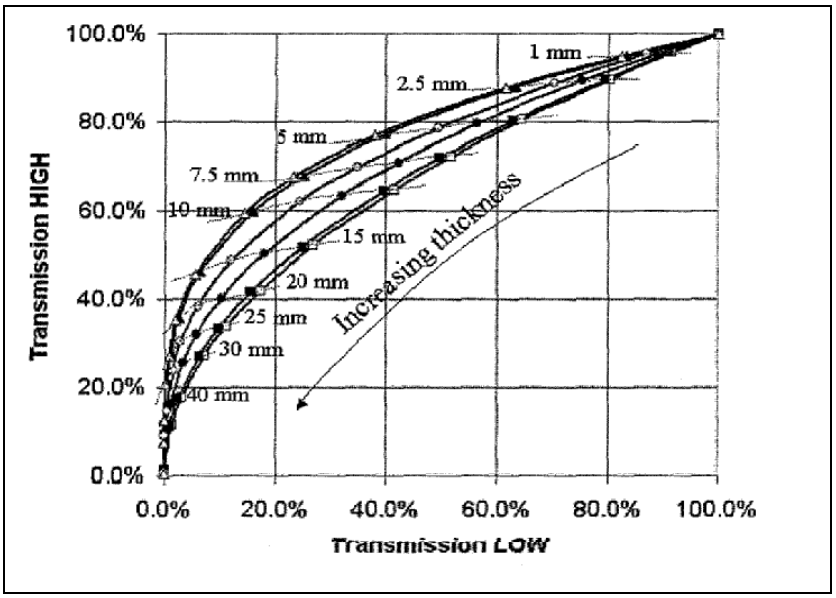

Figure 3: Theoretical DE-XRT Transmission Curve for 124/62kV for variation in ZnS content (De Jong and Harbeck, 2005)

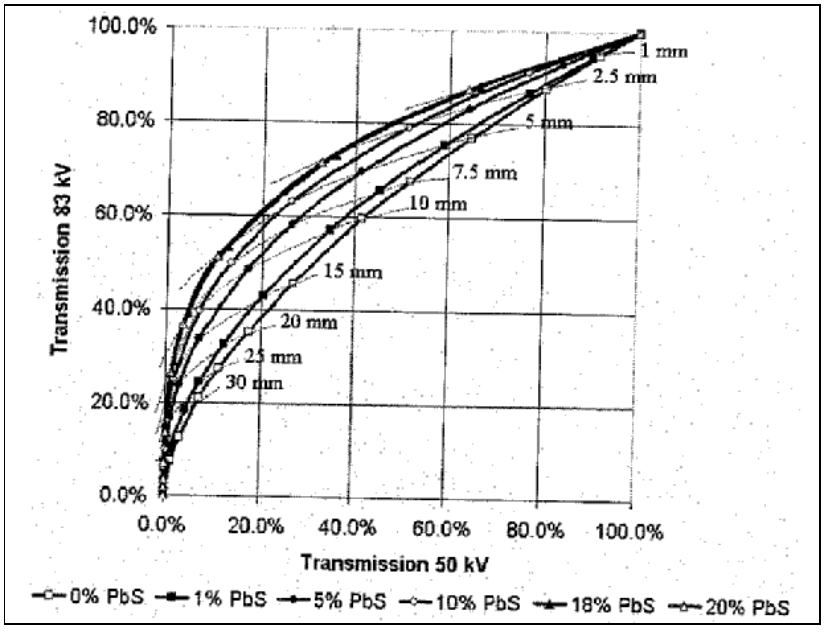

Figure 4: Model Calculation of PbS mixtures at 110kV/62kV and at 83kV/50kV (De Jong and Harbeck, 2005)

De Jong and Harbeck (2005) demonstrated that materials can be distinguished from one another if their curves on the transmission graphs do not coincide. This concept of a unique transmission curve per ore type forms the foundation of Dual Energy X-Ray Transmission Sorting.

Images produced by the transmission of x-rays through objects can provide a great deal of information regarding their density i.e. an object of low density appears brighter than a denser object on the x-ray film. It is a technique widely utilized in the medical and airport security industries. By examining the brightness produced by materials at two different x-ray intensities, a "visual" interpretation of Figure 3 and 4 can be derived. This is referred to as a *Sorting Calibration Curve*, and is presented in Figure 5.

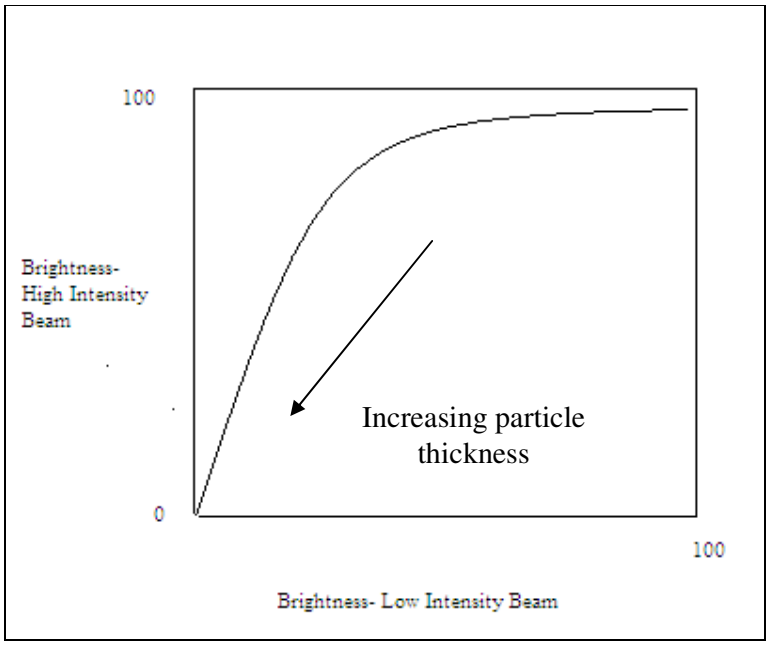

Figure 5: Representation of Typical Dual Energy X-Ray Transmission Sorting Calibration Curve, Adapted from Transmission Curves

Calibration curves are generated by taking images of typical examples of the material to be sorted. The images are broken into a number of small sub-units, called pixels. The pixels are compared to a standard brightness scale, and the number of pixels reporting to the various brightness levels on both high and low x-ray intensity images is plotted as indicated in Figure 5. The curve is produced by use of linear regression through the plotted points. This curve represents the average density composition of the target material within the processing size range. Section 2.3 presents how this curve is applied in order to facilitate separation.

2.3 Principals of Dual Energy X-Ray Transmission Sorting

This section presents the operating principles of Dual- Energy X-Ray Transmission Sorters.

2.3.1 Image Generation

Imaging techniques similar to those available for the security and medical fields are utilized. The process of capturing images is as follows:

- X-rays are generated by an x-ray tube, placed at the top of the unit, as indicated in Figure 6.
- The x-rays strike the material as it passes through the detection zone. X-ray transmission through the material is then captured by a dual energy line scan x-ray sensor. The sensor consists of an array of scintillation crystals that capture the number of counts on each element for the array.
- An image of the object is generated in a "line by line "fashion, similar to optical sorting. A typical example of such an image is presented in Figure 7. According to Harbeck (2004), the resolution obtained by the x-ray sensor is similar to that obtained by standard optical sorting units.
- A high x-ray intensity and low x-ray intensity image of each particle to be sorted is generated for analysis.

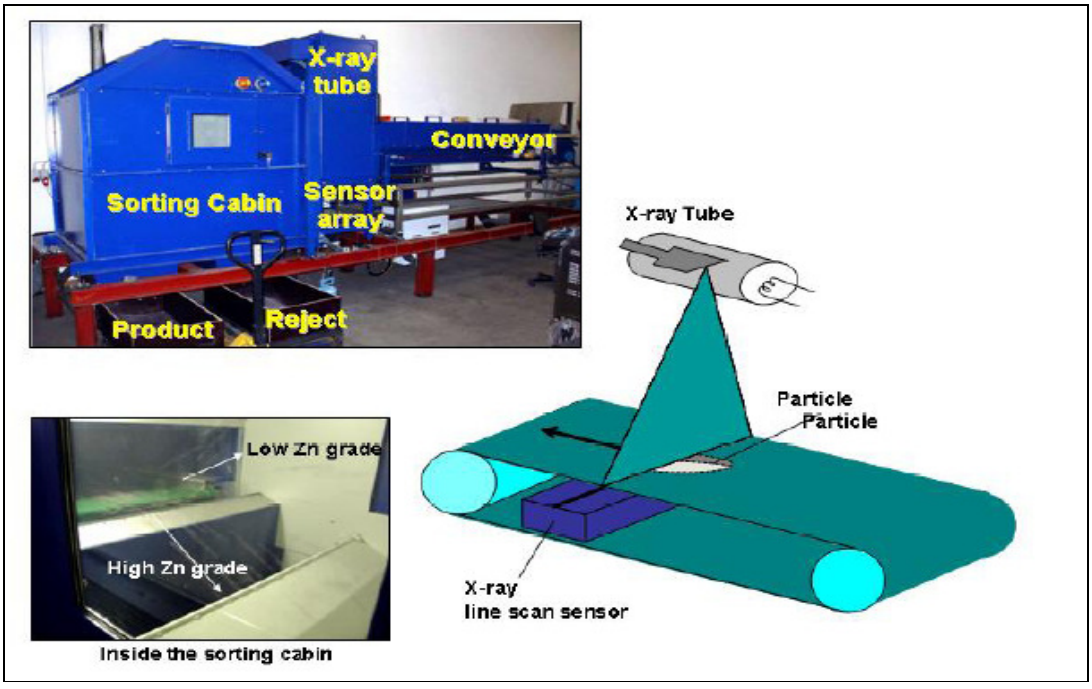

Figure 6: Principle of X-Ray Detection with on-belt sensor geometry (CommoDaS , 2004)

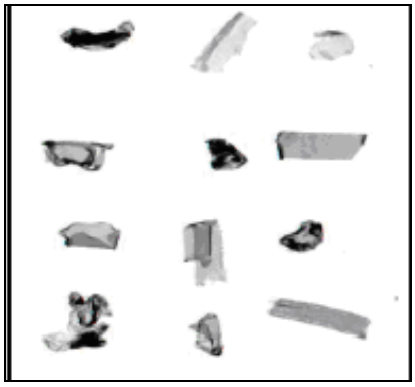

Figure 7: Typical Image Generated By the DE-XRT Process (de Jong et al, 2003)

2.3.2 Image Analysis and Product Quality Control

The analysis of images in order to facilitate separation is conducted using an algorithm consisting of two components, viz:

- Calibration curve for target mineral, as presented in Section 2.2
- Rejection criteria, defined as percentage of high density material allowable into the coal product. The quality of the required product is controlled by establishing rejection criteria. Suitable values for rejection criteria are typically determined through process optimization based on final product specifications and mass yield requirements.

The calibration curve for the target material is used to classify the materials present within each particle as high or low density. The area above the calibration area is assigned as the high density (blue) zone. The calibration curve area, as well as the area below is defined as the low density (red) zone, as demonstrated in Figure 8.

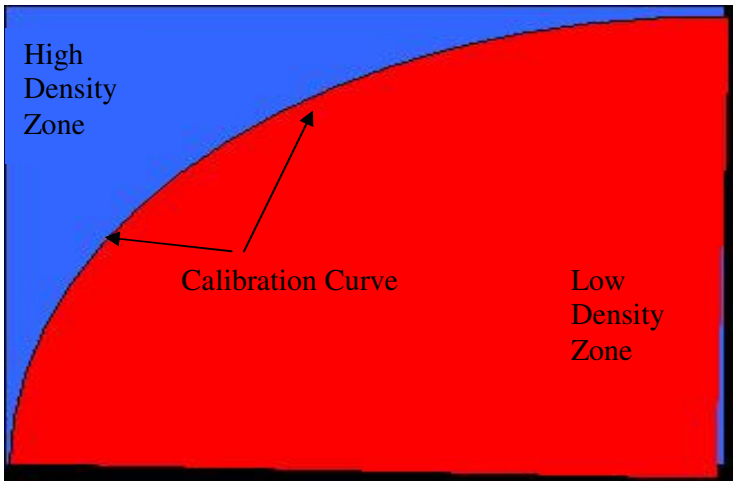

Figure 8: Representation of High and Low Density Zones

Both the high and low intensity image of each particle is divided into pixels. The brightness of each pixel within the particle is evaluated, and is plotted on the calibration curve. The pixels within a particle are assigned as blue or red, depending on their position on the calibration curve. The percentage of pixels reporting to the high (blue) and low (red) density zones are recorded. The rejection criteria are applied to each particle and the decision to accept or reject the particle is made.

Information regarding the size and position of particles on the conveyor belt, as well as the overall decision to accept or reject a particle is relayed from the PLC to the valve bank.

2.3.3 Particle Ejection

Particle ejection is conducted in a similar fashion to the standard CommoDaS optical sorting units described in Section 2.2 and will not be discussed in great detail. Ejection is conducted by means of a bank of air valves placed above the feed conveyor. An appropriate number of valves are then opened, according to the estimated size of the particle to be ejected. Air jets displace the particle from the stream leaving the feed conveyor into a separate collection bin. Accepted material passes over a splitter bar into a collection bin. Harbeck(2004) indicates that operating speeds of the x-ray sorting units are comparable to standard optical sorting units.

2.4 Advantages of Utilizing DE-XRT

Dual energy x-ray transmission sorting has a number of advantages over other available sorting equipment. The images produced provide information on the internal structure, texture and shape of the particle. Because particle volume is detected as opposed to surface layer, the process is insensitive to surface coatings and dust (Delgado and Stenmark, 2005). It can therefore have application as a dry processing technique. This could be advantageous to the coal processing industry for the following reasons (De Korte, 2009):-

- A number of South African coal deposits are in arid regions, where water supply is limited.
- Coal quality, especially in terms of heat content, is retained as the coal remains dry during processing.
- No slurry is produced which reduces the risk of groundwater contamination. Risk of groundwater contamination still exists in terms of run off from the discard coal dump.
- Potential exists for underground processing, thus reducing the amount of material required for hoisting.

In addition to this, sorting can be conducted on materials where little visual distinction is observed, as is the case with the separation of torbanite from coal.

3 LITERATURE REVIEW

3.1 Dual Energy X-Ray Transmission Sorting for Recycling Applications

Application of x-ray transmission sorting to various recycling applications is an ongoing research initiative of the Delft University of Technology in the Netherlands, and is well documented for the following applications:-

- Recovery of lightweight non-magnetic metals from scrap. Dalmijn and De Jong (2004) utilised DE-XRT to identify and separate magnesium from aluminium scrap. This research also demonstrated that wrought aluminium could be distinguished from cast aluminium, as demonstrated in Figure 9. Mesina et al (2007) demonstrated that the combination of electromagnetic and x-ray transmission sorting was very effective for metal separation and recovery of non-ferrous scrap.

- Estimation of calorific value of packed mixed waste, based on DE-XRT scan information (Dalmijn and De Jong, 2004).
- Sorting of shredder residue, resulting in the recovery of metals, solid recovered fuel, polymers and inorganic filler matter. Metal recovery from the shredder residue was possible, and it was noted that the ash content, calorific value of the resulting solid recovered fuel could be improved. PVC and polymers coated in flame retardant could be successfully rejected from the solid recoverable fuel, resulting in reduced concentration of harmful elements, including bromine and chlorine (Bakker, 2009).

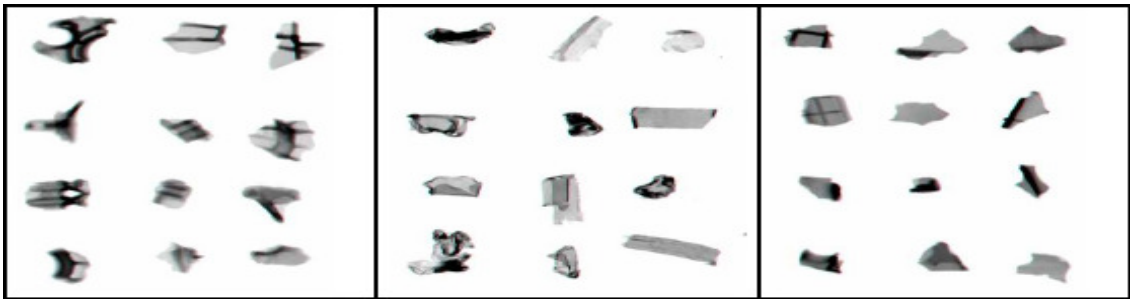

a) b) c)

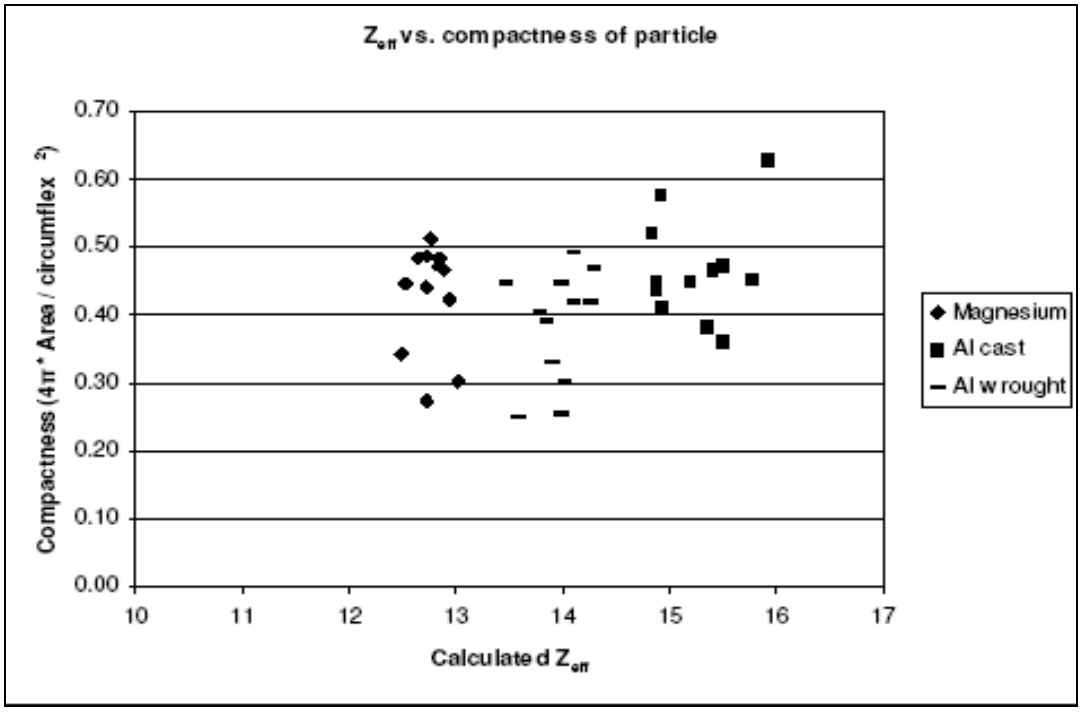

Figure 9: X-Ray Transmission Images and Analysis Results for a) Magnesium, b) Wrought Aluminium and c) Cast Aluminium (Dalmijn and De Jong, 2004)

According to Bruno (2009), x-ray transmission sorting can be successfully implemented in plastic sorting applications. Units such as the VinylCycle (National Recovery Technologies) are very effective in separating PVC polymers from PET plastics.

3.2 Dual Energy X-Ray Transmission Sorting of Minerals

The use of x-ray transmission imaging as a means of sorting base metal sulphides from gangue was first presented by Harbeck (2004). Initial work was conducted utilising mono-energetic transmission, but progressed to dual-energy transmission once this demonstrated to be more feasible (Harbeck, 2004). De Jong and Harbeck (2005) examined the degree of resolution and accuracy attainable by transmission sorting. Utilising binary ZnS;PbS/SiO_2 mixtures (0%, 1%, 5% 10%,18% and 20%), it was ascertained that:-

- Resolution was dependant on feed size, type of material and grade.
- Typically detection accuracy was better at lower grades. There was some correlation between the average atomic number of the material examined and the detection accuracy
- Transmission curves such as those presented in Section 2.2 could be prepared for all mineral types and compositions. A separation was feasible provided that the transmission curves of the two materials did not coincide.

As a result of this work, the use of dual energy x-ray transmission sorting was successfully demonstrated for number of mineral applications, including:-

- Nickel sulphide ores, such as pentlandite (Riedel, (2006); Allen and Gordon, (2009))
- Copper sulphide ores, such as chalcopyrite and bornite (Von Ketelhodt, 2009)
- Gold ores, where gold is associated with narrow veined pyrite (Von Ketelhodt, 2009)
- As alternative technology to x-ray fluorescence for diamond sorting (Von Ketelhodt, 2009)
- Separation of copper and cobalt metal from slag

Based on the author's opinion, the success of any ore sorting venture is highly dependant on the liberation of the material to be examined. It is therefore important to evaluate the validity of sorting on a case by case basis.

3.3 Dry Processing of Coarse Coal by Dual Energy X-Ray Transmission Sorting

Delft University of Technology has been utilising financial grants from the European Coal and Steel Community to investigate the feasibility of coal upgrading by x-ray sorting technology. Preliminary work conducted on Saarwilligen coal demonstrated that shale could clearly be distinguished from coal, as illustrated in Figure 10.

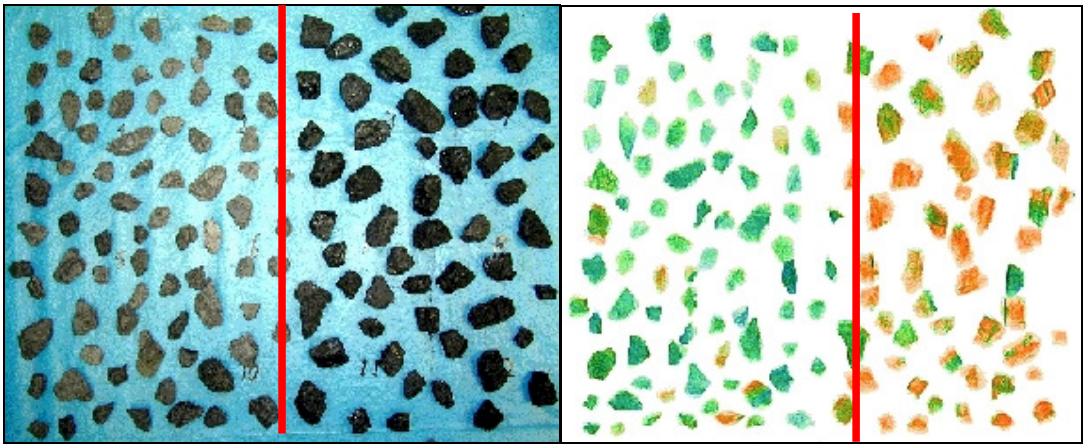

Figure 10: Dual Energy XRT images of Shale (left) and Coal (right) from Saarwillingen, Germany (De Jong,van Houwelingen and Kuilman 2003)

Further samples from Saarwillingen were utilised to establish x-ray transmission performance on materials of various size fractions, as presented in Figure 11 . The images were utilised for online washability and size distribution analysis, as presented in Figure 12.

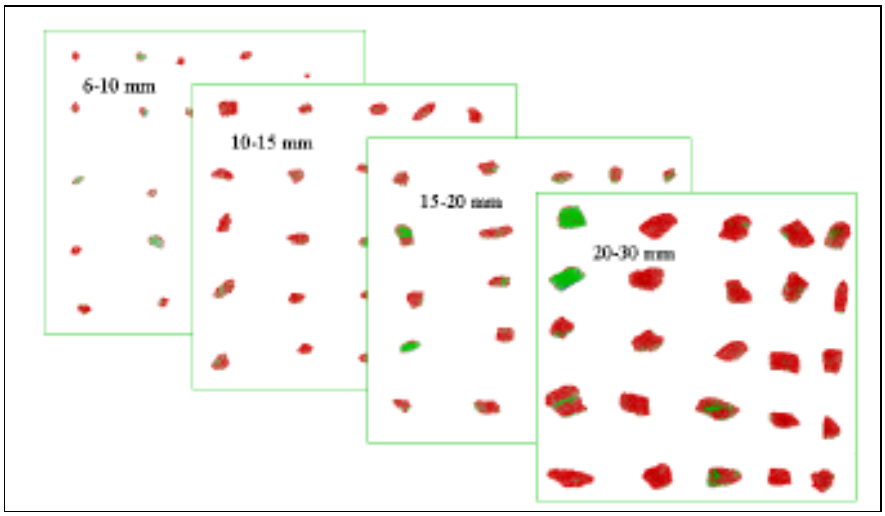

Figure 11: XRT Coal/Shale scans of four different size fractions of Saarwellingen coal product. Shale contamination is presented in green (De Jong, van Houwelingen and Kuilman 2003).

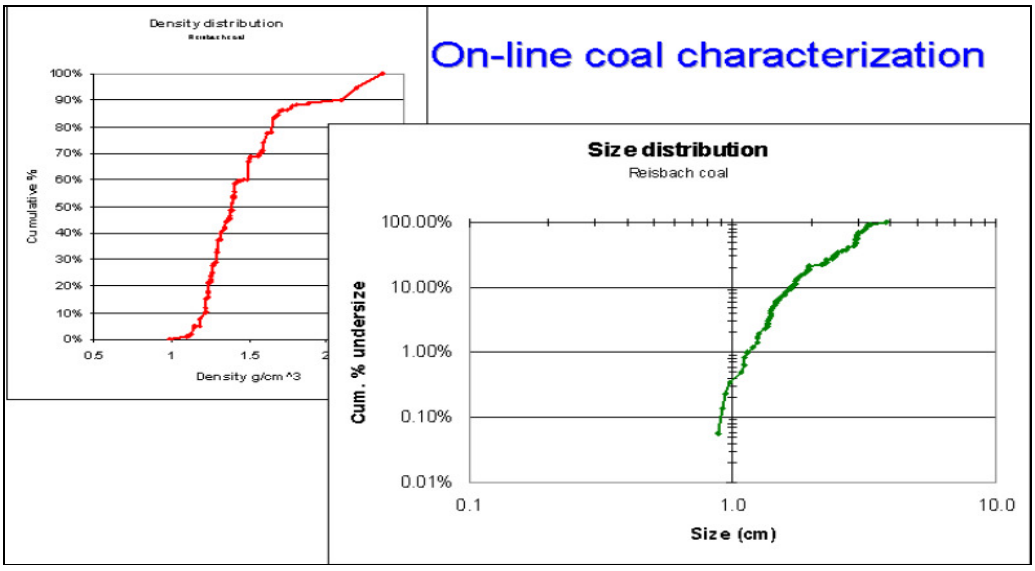

Figure 12: On-Line XRT Analysis (Size Distribution and Washability) for Saarwilligen Coal-Reisbach Seam (De Jong, van Houwelingen and Kuilman, 2003).

The final phase of testwork conduced by Delft University of Technology on deshaling of coal was to evaluate and compare three deshaling techniques:

- Jigging
- Electromagnetic separation
- Dual energy x-ray transmission

The testwork utilised laboratory scanning equipment to determine detection efficiencies of electromagnetic and XRT of coal fractions of various densities. This testwork was conducted in conjunction with L3 communications (USA). The data attained was utilised to produce partition curves for various d_{50} values by varying the threshold of the amplitude (electromagnetic separation) and frequency (x-ray sorting), as presented in Figure 13. It should be noted that the test was conducted at laboratory scale, and that 100% ejection accuracy was assumed.

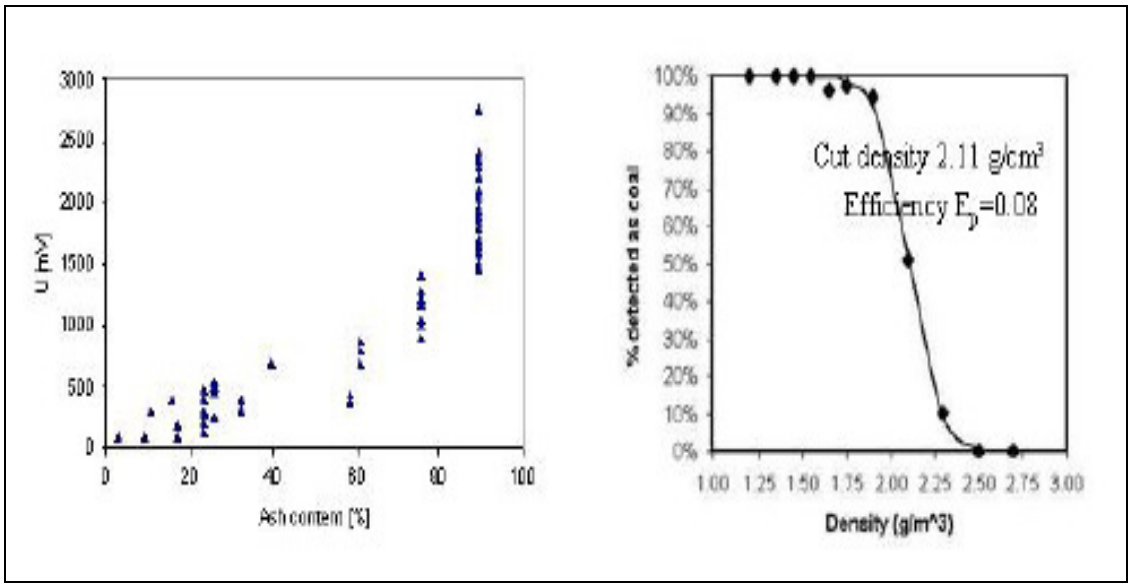

Figure 13: Ash determination and partition curves derived from laboratory scale XRT scans (De Jong and Harbeck, 2005)

Efficiency of electromagnetic deshaling was determined to be with an Ep range of 0.1-0.15. According to De Jong and Harbeck (2005), this is comparable to wet jigging of coal (Ep = 0.1), and is better than proposed dry processes, such as tabling and pneumatic jigs (0.15<Ep<0.03). The separation efficiency of x-ray sorting was evaluated as 0.02<Ep<0.09 for cut points between 1.4< d_{50}< 2.0, and was noted to be more efficient than electromagnetic deshaling.

Although both processes could not match DMS cyclone efficiencies (Ep<0.02), it should be noted that DMS cyclones are limited in terms of the top size that can be processed, whereas x-ray sorters can be applied to material up to 80mm in size.

Several small pilot scale testwork campaigns were conducted by De Jong (2006) on three samples:

- ROM coal from the Ruhr region of Germany (Sample A)
- A coal sample from the Saar region, with poor washabilty as a result of poor liberation (Sample B)
- A sample of non-European origin with good washability results (Sample C)

Results attained are summarised in Table 1.

Description	Sample A	Sample B	Sample C
Feed Ash Content (%)	23.6	17.9	4.6
Product Ash Content (%)	8.3	14.7	1.5
Mass pull to Product(%)	73.5	80.8	97.1
Waste Ash Content (%)	64.3	32.0	52.2

Table 1: Summary of Pilot Scale Coal Testwork

The following observations were made:

- Results attained for ROM material indicated that results comparable to washing can be attained.
- Efficiency of the sorting process was less at smaller size fractions (<10mm) due to limitations in resolution, as well as the carry over of small shale particles into the product bin by the air from the valves.
- The performance and viability of DE-XRT sorting was dependant on the liberation and washability of the material. It is thus important to evaluate the potential of XRT coal sorting on a case-by-case basis.

Pilot scale deshaling testwork was conducted at Mintek on coal samples derived from the Dolan Colliery. De Korte (2009) indicated that the efficiencies at cut points of 1.6 and 2.0 produced a separation efficiency (Ep) of 0.14 and 0.25 could be attained respectively. This is in line with efficiencies attained by other dry processing techniques.

4 FORMULATION OF PROBLEM

4.1 Review of Previous Testwork

The production of relatively pure products was imperative to the financial viability of exploiting the torbanite and coal deposit under investigation. As torbanite and coal have overlapping densities, standard minerals processing routes were deemed unfeasible. An innovative solution to the separation of coal from torbanite was therefore required.

Dual Energy X-Ray Transmission Sorting applications for the coal industry were the result of collaborative work between the Delft University of Technology (Holland) and CommoDas GmbH (Germany). The development of process for the deshaling of coal and upgrading of coal products for niche market is well documented (Dalmijn (2004), Harbeck (2004), de Jong, van Houvelingen and Kuilman (2003, 2004), de Jong, Dalmijn and Kattentidt (2003)

,Harbeck and De Jong (2005) and de Jong (2006)). Much of this work presented reflects progress made on a laboratory scale. Their combined efforts have culminated in a full scale investigation of coal upgrading for niche markets at the Amsterdam port.

An initiative to investigate novel techniques for the separation of coal from torbanite was established in the 2000's, after promising results were obtained from ore sorting techniques for coal applications. Laboratory scale testwork was conducted at the CommoDas GmbH laboratory in Wedel, Germany during the course of 2004/2005. Hand selected specimens of torbanite and coal were provided for testwork purposes. A number of sorting sensors were examined, including:

- Optical sensors
- Ultraviolet sensors
- Near Infrared sensors
- X-ray transmission sensors

Examination of images derived via x-ray transmission indicated that differences in average atomic density could be identified. These images are presented in Figure 14. Torbanite was characterized by the speckled appearance in the images.

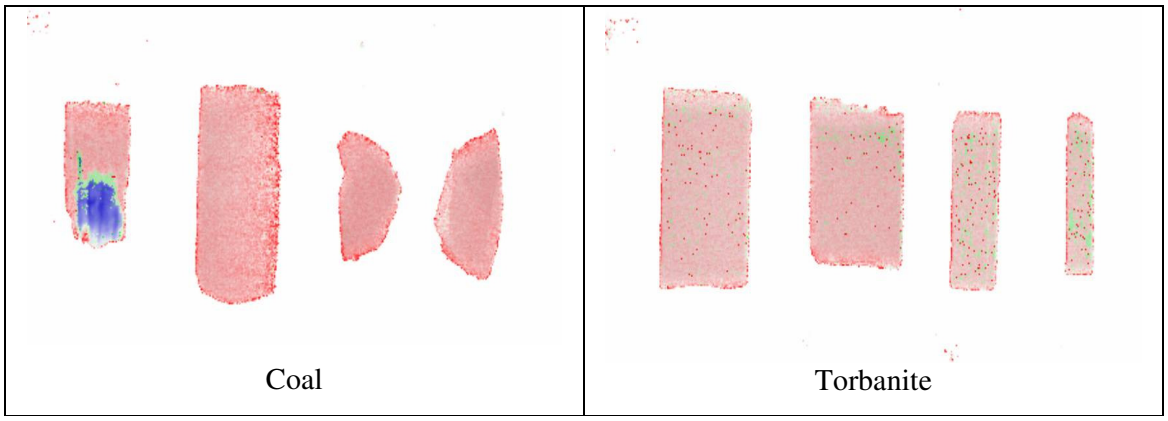

Figure 14: Dual energy x-ray transmission images of coal and torbanite.

Preliminary data analysis derived from these images is presented in Figure 15.

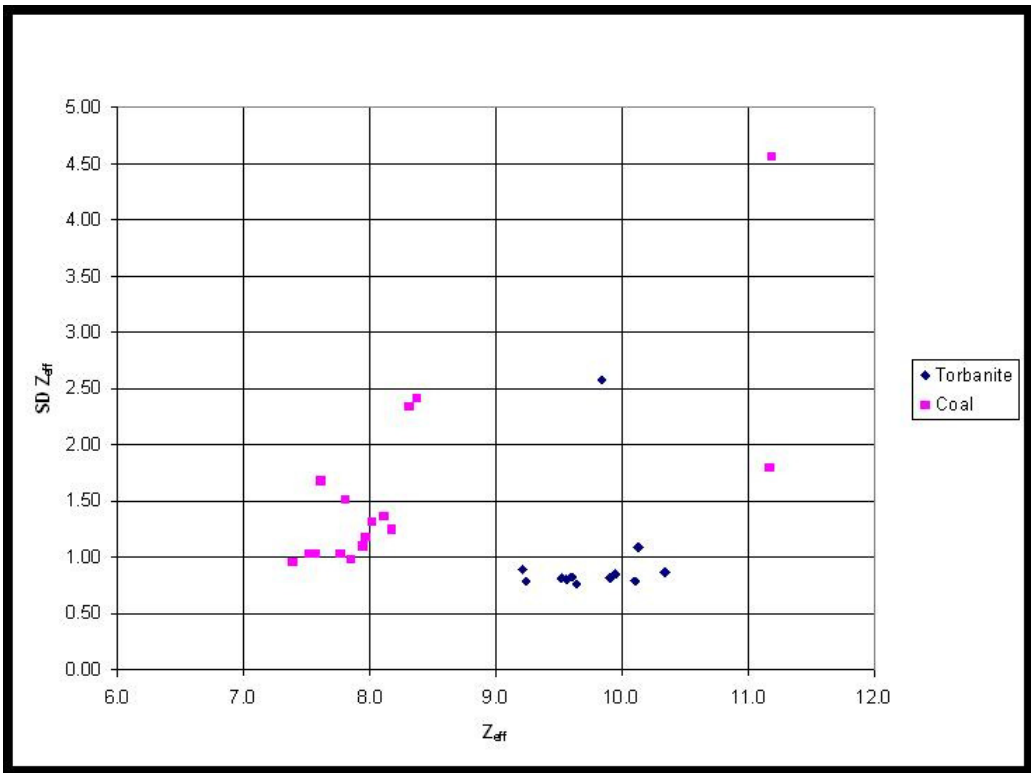

Figure 15: Classification of Coal and Torbanite by Relative Atomic Number, as Determined by Dual Energy X-Ray Transmission

Based on results from Figure 15, the coal samples provided to CommoDaS generally had an effective atomic number ranging between 7.0 and 8.0. The torbanite tended to occur at an atomic number ranging from 9.0 to 10.0, thus facilitating a separation. As a result of these promising findings, a calibration curve for the separation of coal from torbanite was derived, as presented in Section 2.2.

These promising findings highlighted the need for further investigation to address the following concerns:

- The sample utilized to conduct the testwork was not representative of typical feed material. Samples provided for testwork were high quality specimens of coal and torbanite. It was anticipated that the ore to be mined would contain a substantial proportion of unliberated material and may contain inclusions such as pyrite. The impacts of these on the sorting process could not be quantified from the preliminary testwork program.
- The process had not been demonstrated at production scale or pilot scale. Testwork at such scale could not be accommodated at CommoDas.

- Laboratory scale testwork could not provide data regarding the performance of the sorting process, such as product purity and associated mass yields.
- Sorter efficiency could not be quantified on laboratory scale
- Retorting performance of torbanite product could not be established.

In order to address these concerns, a pilot scale investigation was required. A full scale Mikrosort X-Tract sorting unit was purchased by the project sponsors, and was housed at Mintek for the testwork campaign.

4.2 Overall Study Objectives

The objectives of the pilot scale program were as follows:

- Characterisation of feed material, including washability analysis
- Set-up and commissioning of a pilot scale Dual Energy X-Ray Sorter
- Validation of previous testwork conducted on pure coal and torbanite samples
- Investigation of the range of products attainable and associated mass yields
- Process Optimisation
- Process Demonstration at Pilot Scale in order to produce sufficient material for retorting testwork

4.3 Research Questions

The research program addressed the following questions:

- Can Dual Energy X-Ray Transmission Sorting Technology be utilized to produce a coal product of high purity?
- Does the torbanite product produced as a result potentially have a market?
- What are the impacts of unliberated material on the quality of the separation process and on the quality of coal and torbanite that can be attained?
- What are the ranges of products that can be attained and the associated mass yields?

4.4 Hypothesis

Good differentiation between coal, torbanite and shale can be noted through the use of Dual Energy X-Ray Transmission. This differentiation is significant enough to effect a separation between the three materials.

5 PLANT INSTALLATION AND COMMISSIONING

5.1 Plant Layout and Process Description

A production scale Mikrosort ® X-Tract DE-XRT Sorter was acquired from CommoDas GmbH by the project sponsors.

The sorting unit consists of six modules, including:

- Feed Chute (with frame) , designed to ensure that the material reports to the feed conveyor in a monolayer
- Feed conveyor belt and frame
- Sorting mechanism, including x-ray tube, and sensor arrays. The sensor arrays are located under the feed conveyor belt.
- Electrical power supply for x-ray source and water cooling
- Pneumatic system, incorporating valves for ejection of particles
- Switch cabinet with control unit (MGC41) for x-ray system
- Process Logic Controller

A mini plant incorporating the required ancillary equipment such as conveyor belts, feeders and compressors was established at Mintek. The layout of the plant is presented in Figure 16 and Table 2.

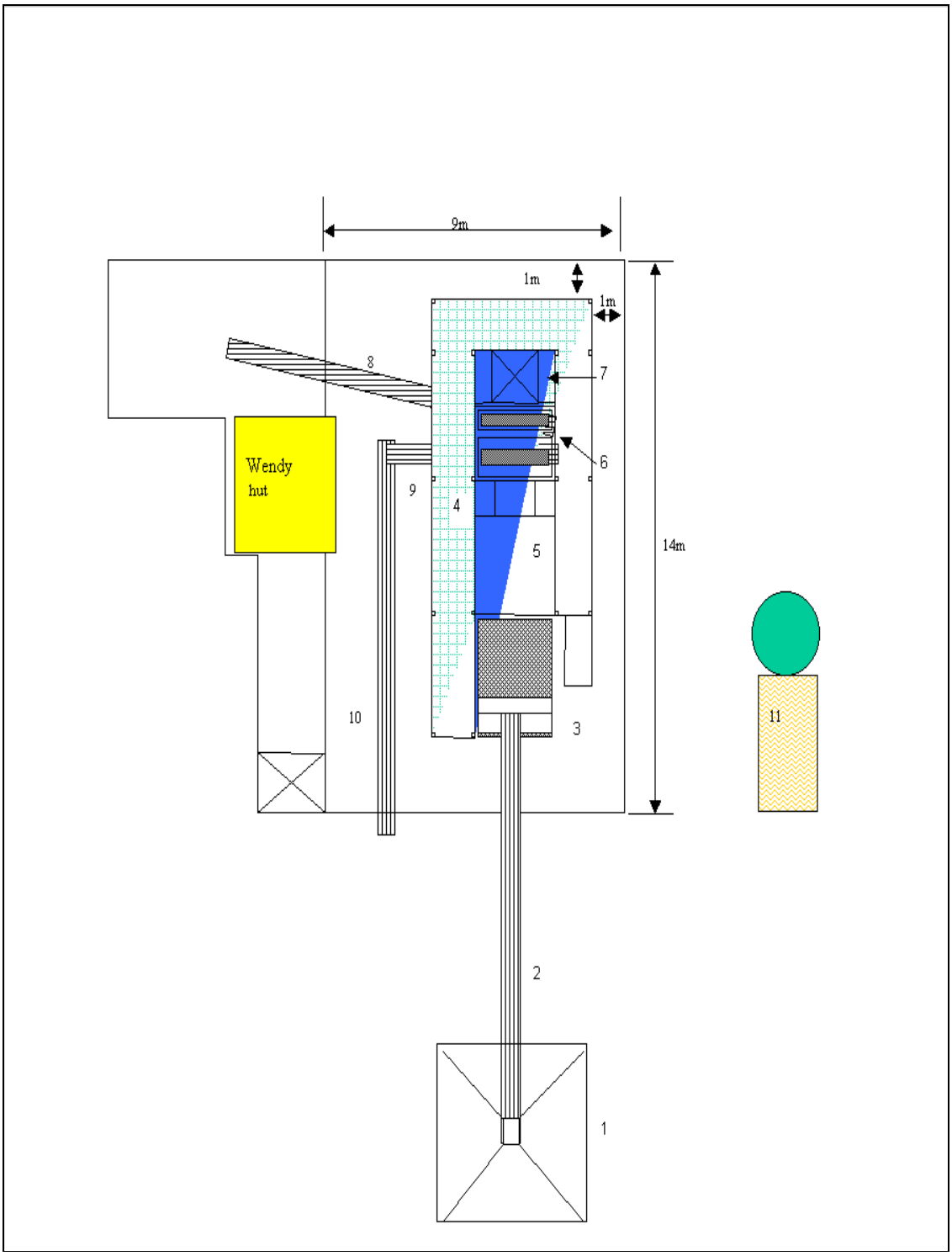

Figure 16: Layout of X-ray Sorter

Item No.	Description
1	Feed Hopper
2	Feed Conveyor – 10m
3	Joest Vibratory Pan Feeder
4	Sorter Support Frame
5	Sorter Conveyor
6	Sorting Mechanism
7	Control Panel
8	Reject Conveyor-10m length
9	Accept Conveyor 1 – 7m length
10	Accept Conveyor 2 – 10m length
11	Compressor and Receiving Tank

Table 2: Annexure to Figure 16

Feed material is crushed and pre-screened to –80mm+20mm prior to sorting. The sample is loaded into the hopper via forklift. The material is then passed to the feed conveyor and vibrating feed pan. The vibrating pan and lip ensure that the material presents to the conveyor belt in a monolayer and minimizes lateral movement of particles from the belt. Once on the belt, the sample is transported to the detection zone at a speed of 3m/s.

As the material passes through the detection zone, data relating to the material is captured. The data captured is relayed to the PLC, which applies an appropriate algorithm to the data, identifies materials to be rejected and activates the appropriate number of valves to reject the required particles. Material to be rejected is ejected from the stream of particles by air jets located underneath the particle stream. Rejected material is collected in a separate bin and is transported via conveyor to the reject stockpile. Material to be accepted is collected and transported to the accept stockpile by means of two accept conveyors.

5.2 Mechanical Commissioning

Mechanical optimization was conducted by passing rock samples of various size and mass through the sorter and observing how the sample behaved through the detection and ejection zones. Two simple algorithms were applied:

- Rejection of all materials to ensure that delay times and selected air pressure were appropriate
- Accept all materials in order to establish if splitter position is appropriate.

Adjustments were made as required based on the visual observations of each test.

6 EXPERIMENTAL PROCEDURE

6.1 Overview of Scope of Work

The scope of work was extensive and included:

- Sample preparation
- Feed characterization
- Small scale sorting test (+- 1 ton per test) for validation of previous testwork and for process optimization
- Pilot scale testwork on a 150 ton sample, operating parameters to be based on results of process optimization tests

A schematic overview of the testwork procedure is presented in Figure 17.

6.2 Feed Preparation

Mintek received 150 tons of coal and torbanite rich material which had been pre-crushed and screened to a size range of -80mm+10mm. The sample was bagged and weighed for accounting purposes.

As the optimal processing size for the Mikrosort X-tract Unit is +20mm, the sample was dry screened at 20mm. The sample of -10mm material has been dry screened at 0.5mm for feed characterization purposes. This resulted in four size fractions, viz.:

- -80mm+20mm
- -20mm+10mm
- -10mm+0.5mm
- -0.5mm

The -20mm+10mm, -10mm+0.5mm and -0.5mm material was blended using cross cut technique and representative sub-samples were removed for feed characterization purposes.

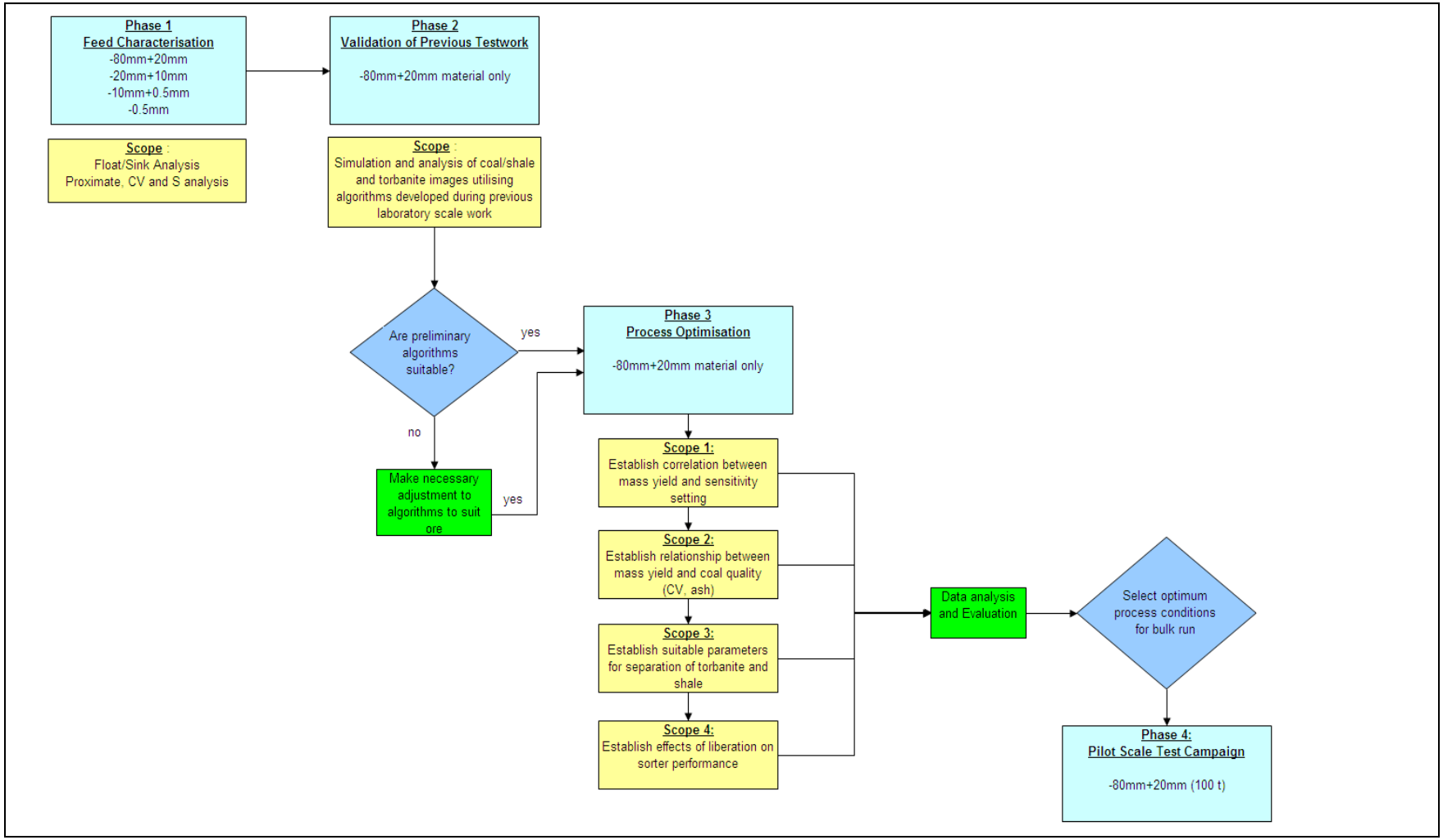

Figure 17: Schematic Overview of Testwork Objectives

The -80mm+20mm material was focused upon for the testwork campaign. This sample was blended by cross cut technique, and a 30 ton representative sample was removed, and split into 1 ton samples for process optimization testwork.

6.3 Feed Characterisation

The feed material in the pre-screened size fractions were submitted to Witlab for the following analyses:

- Proximate analysis
- Calorific value (CV)
- Sulphur and Types of Sulphur
- Ash Constituents and Ash Fusion Temperature
- Washability by "Float/Sink" Analysis at cut points ranging from 1.3 to 1.8 in increasing intervals of 0.05.

Full suite petrographics were conducted by Ms Vivien Du Cann (CSIR).

6.4 X-Ray Sorting Testwork

6.4.1 Validation of Previous Testwork

As part of the previous testwork campaign, a calibration curve as presented in Section 2.2 was derived for the separation of pure coal from pure torbanite. It was essential to ensure that the designed algorithms were applicable to the sample received. This was a major concern at the outset of the testwork, as it was suspected that the ROM sample received would contain unliberated materials (including shale/coal mixtures and torbanite coal/mixtures) as well as pyrite inclusions.

The aim of this phase of testwork was to confirm if this calibration curve was suitable for the separation of a typical ore and to make appropriate adjustments to the rejection criteria where necessary in order to separate the ore appropriately. The most effective means of doing this was to capture linescan images of typical coal, torbanite and shale material and examining the impacts of applying the calibration curve to the images.

A sub-sample of the feed material was screened into the following size fractions:

- +75mm
- -75mm+40mm
- -40mm+20mm

These fractions were hand sorted into coal, shale and torbanite fractions with assistance from staff from the samples origin. Care was taken to ensure that samples of dull and bright coal were included in the coal samples. Each of these samples was photographed and numbered for identification purposes. They were placed on sheets of brown paper and were passed through the x-ray unit in order to take x-ray transmission images. The previously devised algorithm was then applied to the samples by means of the Mikrosort® simulation package. The images were scrutinized in order to determine if the algorithms were appropriate for use on this sample.

6.4.2 Process Optimisation Testwork

Process optimisation testwork was conducted in order to examine:

- The range of coal and torbanite products that could be attained by adjusting the rejection criteria
- The effects of liberation on sorter performance
- The feasibility of separating shale from torbanite

The major focus of the work was on optimising the quality of the coal product, without compromising on the mass yield to coal product.

The matrix of tests conducted is presented in Table 3. This table presents the objective of each test as well as the parameters adjusted per test.

Test No.	Test Type	Objective	Size Fraction	Rejection Criteria
1	Coal from Torbanite and Shale	Sorter Performance Test 1	-80mm+20mm	Reject if >70% Blue Pixels
2	Coal from Torbanite and Shale	Sorter Performance Test 2	-80mm+20mm	Reject if >60% Blue Pixels
3	Coal from Torbanite and Shale	Sorter Performance Test 3	-80mm+20mm	Reject if >53% Blue Pixels
4	Coal from Torbanite and Shale	Sorter Performance Test 4	-80mm+20mm	Reject if >80% Blue Pixels
5	Coal from Torbanite and Shale	Liberation Effects	-50mm+20mm	Reject if >80% Blue Pixels
6	Shale from Torbanite	Clean Torbanite Product	Shale Removal	Reject if >95% Blue Pixels

Table 3: Optimisation Test Matrix

For consistency, each test was conducted on a 1 ton sample. Feed flowrate was restricted to 3 t/hr in order to minimize sorter error. The torbanite and coal products from each test were collected and weighed. Sub-samples were removed for CV, Ash and proximate analysis. These test products were submitted for full suite petrographic analysis.

6.5 Pilot Scale Testwork

Pilot scale sorting conditions were selected based on the results obtained in the optimisation phase of testwork. Factors considered were coal product quality and mass yields to coal product. The pilot scale testwork program was conducted in two separate stages, namely:

- Separation of Coal from Shale and Torbanite
- Separation of Torbanite from Shale

The decision to conduct the separation as two separate processing steps was derived from observations made during process simulation for validation of laboratory scale tests.

A basic process flowsheet for the pilot scale campaign is presented in Figure 18.

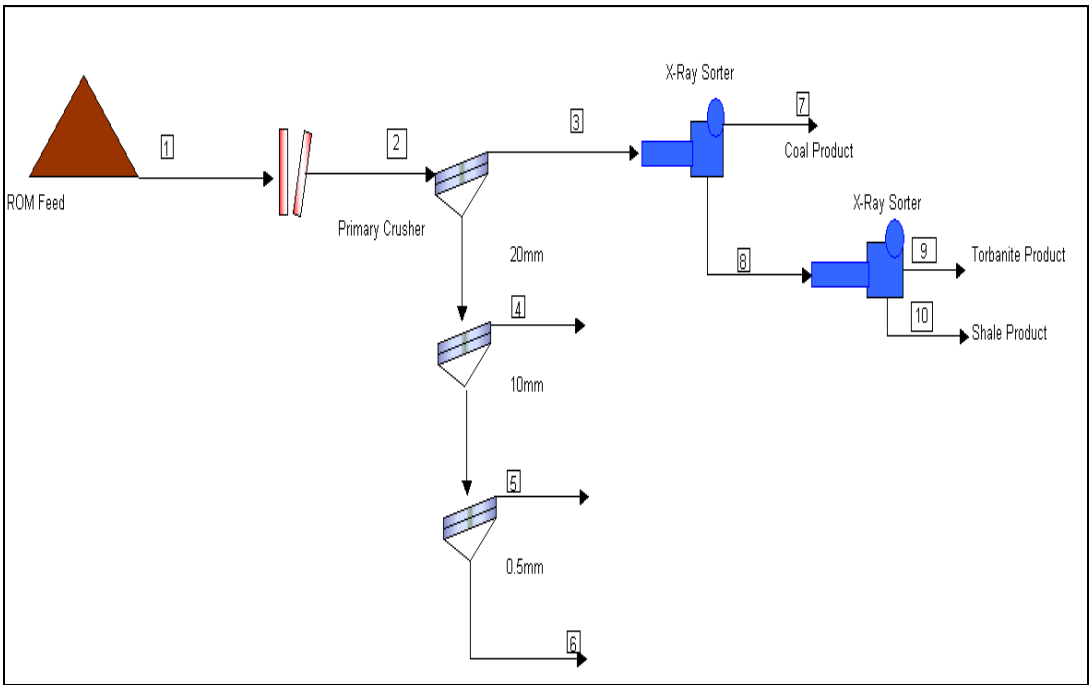

Figure 18: Two Stage Sorting Process

The sorting plant was operated at an average feed rate of 20 t/hr, which was the maximum feed rate possible with the available equipment. Target mass yield to coal product was derived from the optimisation testwork, and was confirmed by flowrate measurement on an hourly basis. Sub-samples of both products produced were removed on an hourly basis and were composited at the end of every 24 hour running period. At the conclusion of the tests, all composited samples of coal, shale and torbanite were blended individually and submitted for the following analyses:

- Full suite petrographic analysis
- Proximate and CV
- Ash Analysis and Ash Fusion Analysis
- Sulphur and Forms of Sulphur
- Trace Element Analysis

Thermogravimetric Analysis (TGA) analysis was conducted on representative sub-sample of the coal, torbanite and shale products by the Institute of Applied Minerals at the University of Pretoria. The experimental procedure for these tests is presented in Appendix D.

7 RESULTS AND DISCUSSION

7.1 Feed Characterisation

7.1.1 Chemical Composition of Feed

The chemical analysis data is presented in the form of tables and figures for comparative purposes. Full analytical data is presented in Appendix A.

The proximate analysis, calorific value (MJ/kg) and total sulphur content for the various size fractions are compared in Figure 19.

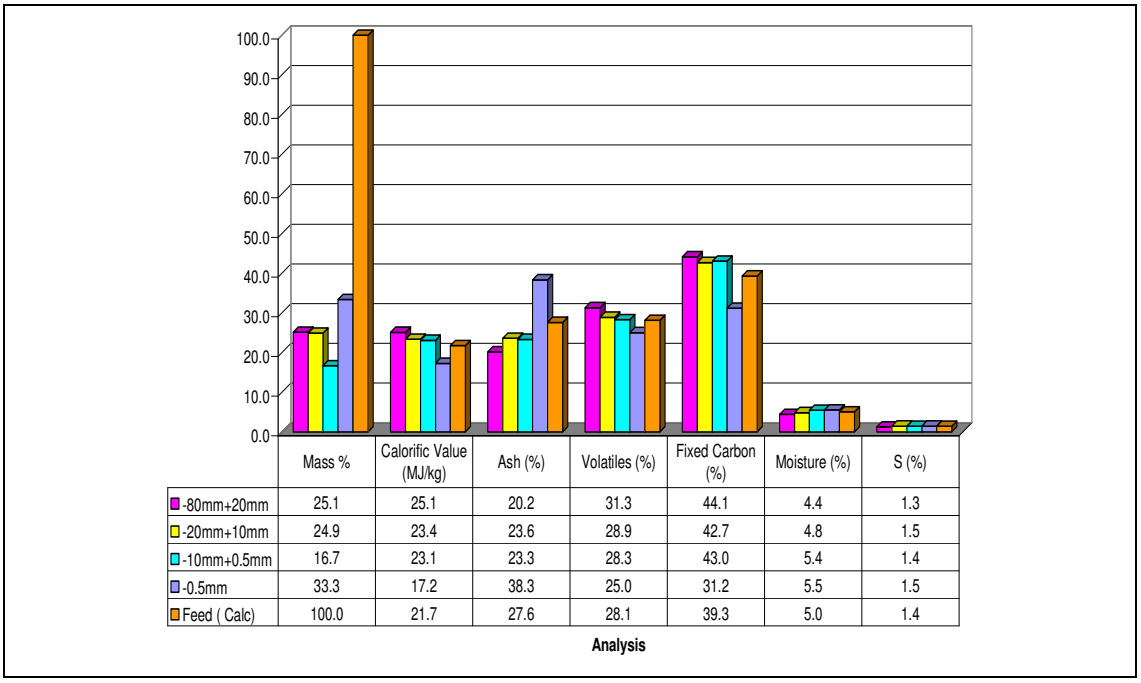

	Mass %	Calorific Value (MJ/kg)	Ash (%)	Volatiles (%)	Fixed Carbon (%)	Moisture (%)	S (%)
-80mm+20mm	25.1	25.1	20.2	31.3	44.1	4.4	1.3
-20mm+10mm	24.9	23.4	23.6	28.9	42.7	4.8	1.5
-10mm+0.5mm	16.7	23.1	23.3	28.3	43.0	5.4	1.4
-0.5mm	33.3	17.2	38.3	25.0	31.2	5.5	1.5
Feed (Calc)	100.0	21.7	27.6	28.1	39.3	5.0	1.4

Figure 19: Comparison of Proximate analysis, CV and Total S for four size fractions

Figure 19 indicated that in the size fraction of interest for this testwork program (-80mm+20mm), feed Calorific value of 25.1MJ/kg could be anticipated. This was higher than the other size fractions examined. Calorific values of the material reporting to the –0.5mm size fraction were significantly lower (17.2 MJ/kg) than the other three fractions considered. Ash content of +0.5mm material ranged between 20-24% and increased significantly with decreasing size (38.3% ash content for material reporting to –0.5mm size fraction.).

The samples received were of higher total sulphur content that average South African ROM coal samples, ranging from 1.25% to 1.47%. A substantial proportion of the sulphur present in the sample was due to the presence of pyrite inclusions within samples, as presented in Figure 20.

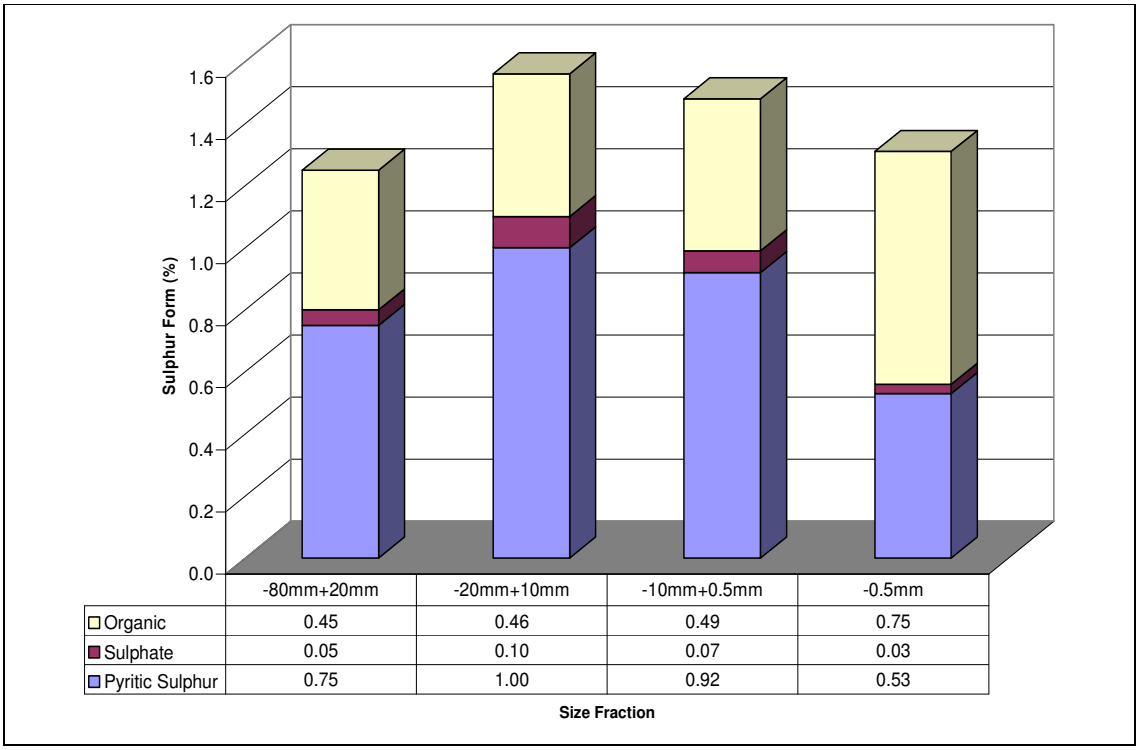

	-80mm+20mm	-20mm+10mm	-10mm+0.5mm	-0.5mm
Organic	0.45	0.46	0.49	0.75
Sulphate	0.05	0.10	0.07	0.03
Pyritic Sulphur	0.75	1.00	0.92	0.53

Figure 20: Forms of Sulphur Occurring in Feed Samples

Ash content in the sample was analysed as follows:

- Ash fusion temperature
- Ash constituent analysis

These are presented in Figure 26 and Figure 27 respectively.

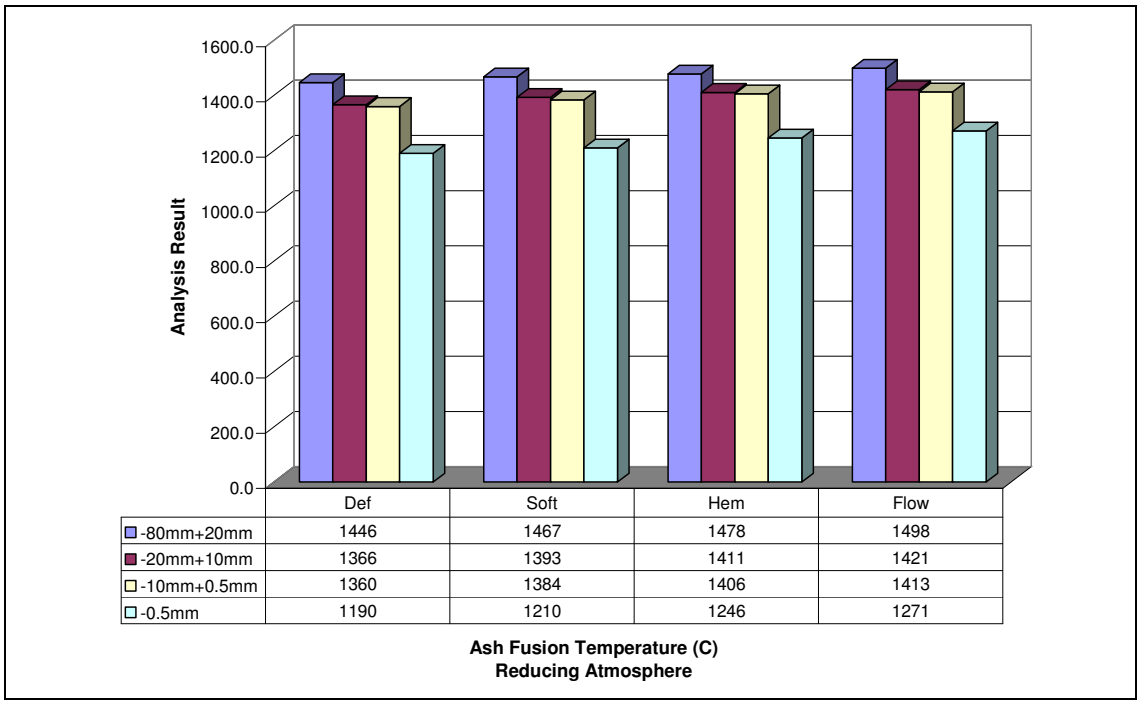

Figure 21: Ash Fusion Temperature for Four Size Fractions

Ash analysis presented in Figure 22 indicates that the composition of the ash products were consistent for all size fraction examined.

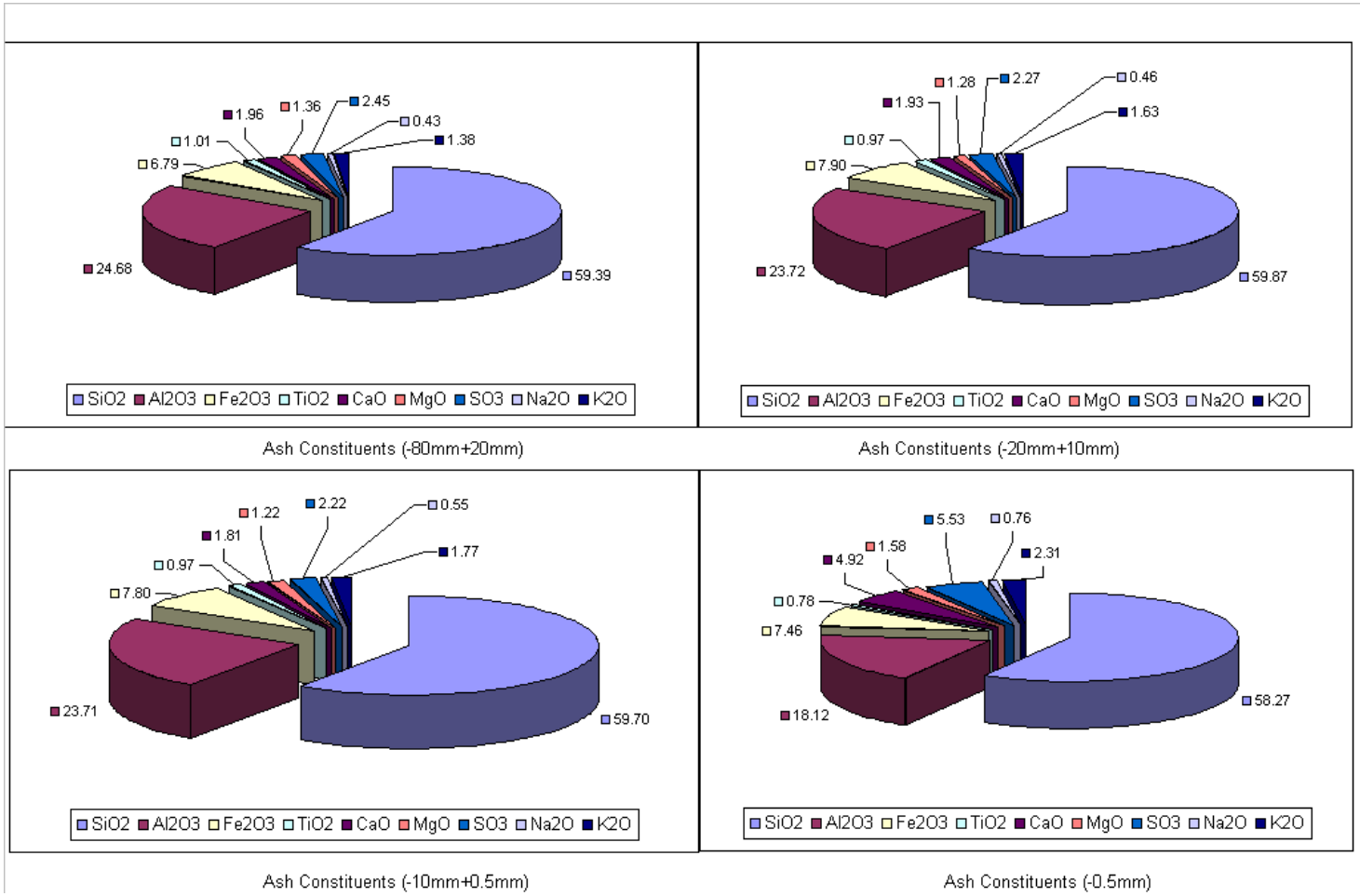

Figure 22: Variation in Ash Constituents (Major Elements)

7.1.2 Petrographic Evaluation of Feed Samples

Petrographic analysis was conducted on all size fractions. The results are presented in Figure 23.

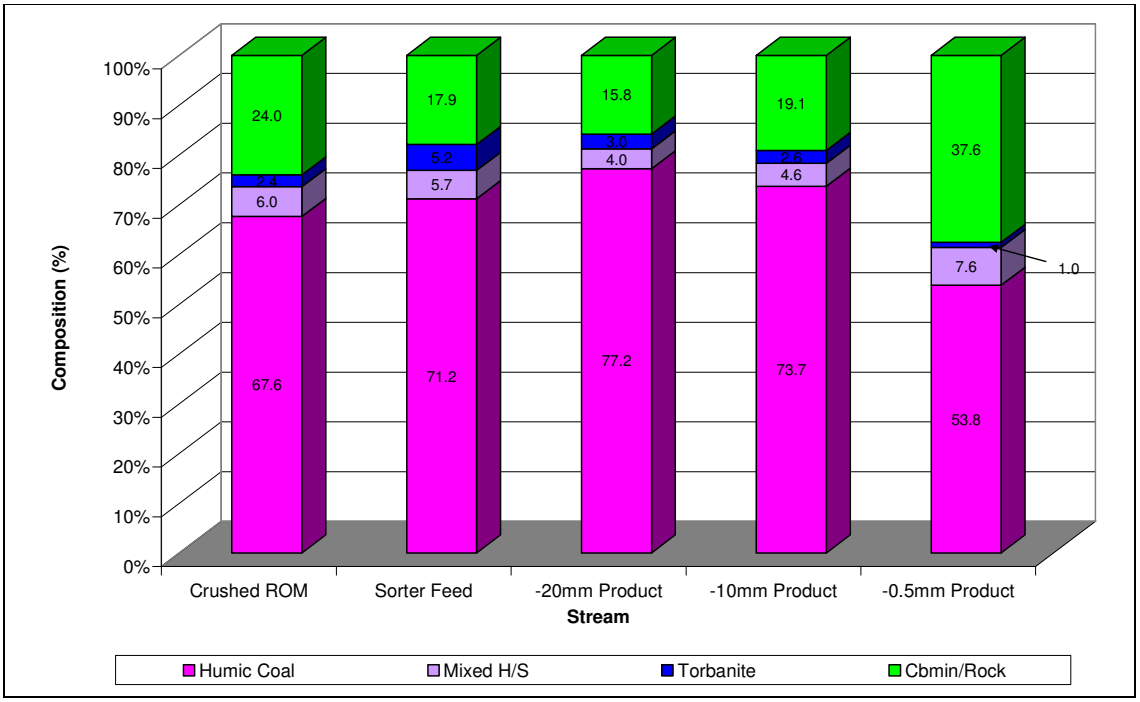

Figure 23: Summary of Petrographic Feed Analysis

Based on the results obtained in Figure 23, the following can be noted:

- The ROM sample received was a particularly coal rich sample, with torbanite accounting for approximately 2.4% of the ROM feed.
- Torbanite appeared to report preferentially to the -80mm+20mm and -20mm+10mm size fractions, with very marginal amounts (<3% of specific fraction) reporting to the -10mm+0.5mm and -0.5mm size fractions. This was anticipated, as torbanite is generally less friable than coal and is expected to break less readily than coal.
- A larger proportion of the -0.5mm material was composed of shale. This accounts for the higher ash content reported for this size fraction.

The sorter feed (-80mm+20mm) consisted predominantly of humic coal (71.2%) with approximately 5.2% of the sorter feed consisting of torbanite.

7.1.3 Washability Results

Comprehensive washability results for the –80mm+20mm, -20mm+10mm and –10mm are presented in Table 4, 5 and 6 as well as Figure 24, 25 and 26 respectively. Comprehensive washability data is presented in Appendix B.

In general, it was noted that all three size fractions tested could potentially be upgraded by gravity concentration utilising DMS. By applying a cut point of 1.40g/ml the following coal products could be attained:

- A mass yield of 54.73% would be attained for the –80mm+20mm material. The product would have a CV of 28.35MJ/kg at an ash content of 9.33%
- Similarly, the –20mm+10mm product would have a CV value of 28.24 MJ/kg with an ash content of 8.68%. Mass yield would increase to 60.79% for this size fraction.
- The –10mm+0.5mm fraction could be upgraded from a CV of 22.26 MJ/kg to 27.96MJ/kg with a mass yield of 57.22%. Ash content could be reduced from 24.04% to 8.40%.

The washability data does not provide an indication of the amount of torbanite present within the –1.4 density range, and it must be acknowledged that low density torbanite material could report to the coal product.

It was also noted that materials reporting to density fractions higher than 1.7 were ash rich, and contained in excess of 40% Ash (CV values less than 16MJ/kg). This material accounted for 15-25% of the material reporting to each size fraction. For the purposes of this exercise it was assumed that this material consists of primarily of shale.

Density Fraction	Yield %		Moisture (%)		Ash (%)		Volatile (%)		Fixed Carbon (%)		Calorific Value (MJ/kg)		Sulphur- Total (%)	
	Discrete	Cumulative	Discrete	Cumulative	Discrete	Cumulative	Discrete	Cumulative	Discrete	Cumulative	Discrete	Cumulative	Discrete	Cumulative
-1.30	0.79	0.79	6.00	6.00	5.80	5.80	35.70	35.70	52.50	52.50	29.66	29.66	0.51	0.51
-1.35+1.30	32.10	32.89	5.30	5.32	7.60	7.56	36.00	35.99	51.10	51.13	28.98	29.00	0.62	0.62
-1.40+1.35	21.83	54.73	4.90	5.15	12.00	9.33	34.10	35.24	49.00	50.28	27.37	28.35	0.65	0.63
-1.45+1.40	15.92	70.64	4.40	4.98	18.30	11.35	32.30	34.58	45.00	49.09	25.21	27.64	0.88	0.69
-1.50+1.45	2.62	73.26	4.90	4.98	21.40	11.71	29.80	34.40	43.90	48.91	23.92	27.51	1.10	0.70
-1.55+1.50	2.07	75.34	4.50	4.97	24.80	12.07	29.30	34.26	41.40	48.70	23.00	27.38	2.19	0.74
-1.60+1.55	2.18	77.52	4.30	4.95	27.40	12.50	26.70	34.05	41.60	48.50	21.74	27.22	1.80	0.77
-1.65+1.60	1.40	78.92	4.00	4.93	29.20	12.80	29.00	33.96	37.80	48.31	21.37	27.12	4.24	0.83
-1.70+1.65	1.58	80.50	4.50	4.92	34.70	13.23	23.60	33.76	37.20	48.09	18.69	26.96	3.88	0.89
-1.75+1.70	1.55	82.05	4.20	4.91	41.50	13.76	19.30	33.49	35.00	47.84	16.50	26.76	1.12	0.90
-1.80+1.75	2.71	84.76	3.60	4.87	51.20	14.96	16.80	32.95	28.40	47.22	12.29	26.29	3.46	0.98
1.80	15.24	100.00	2.70	4.54	69.10	23.21	12.00	29.76	16.20	42.50	5.58	23.14	3.36	1.34
Total	100.00		4.54		23.21		29.76		42.50		23.14		1.34	

Table 4: Washability Data for –80mm+20mm Size Fraction

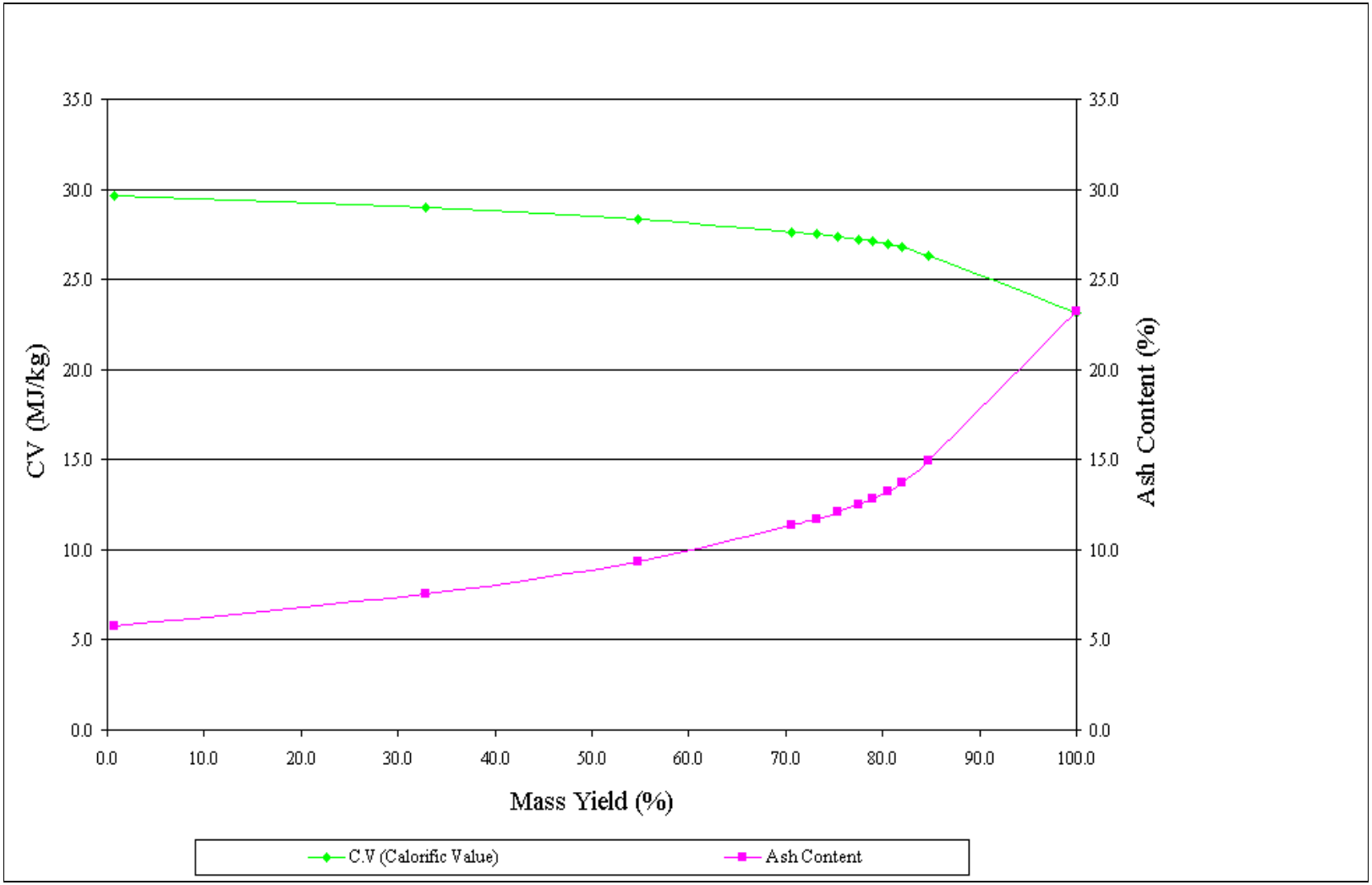

Figure 24: Cumulative Calorific Value and Ash vs. Cumulative Mass Yield for –80mm+20mm material

	Yield %		Moisture (%)		Ash (%)		Volatile (%)		Fixed Carbon (%)		Calorific Value (MJ/kg)		Sulphur- Total (%)	
Density Fraction	Discrete	Cumulative	Discrete	Cumulative	Discrete	Cumulative	Discrete	Cumulative	Discrete	Cumulative	Discrete	Cumulative	Discrete	Cumulative
-1.30	21.71	21.71	6.00	6.00	6.40	6.40	36.00	36.00	51.60	51.60	28.98	28.98	0.58	0.58
-1.35+1.30	12.79	34.50	5.70	5.89	8.00	6.99	35.10	35.67	51.20	51.45	28.54	28.82	0.49	0.55
-1.40+1.35	26.29	60.79	5.60	5.76	10.90	8.68	33.20	34.60	50.30	50.95	27.48	28.24	0.56	0.55
-1.45+1.40	9.06	69.84	4.90	5.65	16.90	9.75	32.30	34.30	45.90	50.30	25.70	27.91	0.68	0.57
-1.50+1.45	3.10	72.94	5.00	5.62	20.80	10.22	29.70	34.11	44.50	50.05	24.13	27.75	0.83	0.58
-1.55+1.50	2.56	75.51	4.80	5.60	24.30	10.70	27.80	33.89	43.10	49.82	22.88	27.58	0.84	0.59
-1.60+1.55	1.61	77.11	4.70	5.58	27.70	11.05	25.90	33.73	41.70	49.65	21.63	27.46	1.08	0.60
-1.65+1.60	1.31	78.42	4.70	5.56	32.60	11.41	23.20	33.55	39.50	49.48	19.46	27.33	1.53	0.61
-1.70+1.65	1.71	80.12	4.50	5.54	36.70	11.95	20.60	33.27	38.20	49.24	18.21	27.13	1.44	0.63
-1.75+1.70	1.39	81.51	4.40	5.52	40.40	12.43	18.80	33.03	36.40	49.02	16.45	26.95	1.42	0.65
-1.80+1.75	4.80	86.32	3.80	5.43	52.90	14.68	16.10	32.09	27.20	47.80	11.96	26.12	2.88	0.77
1.8	13.68	100.00	3.30	5.13	60.30	20.93	14.90	29.73	21.50	44.21	8.65	23.73	6.03	1.49
Total	100.00		5.13		20.93		29.73		44.21		23.73		1.49	

Table 5: Washability Data for –20mm+10mm

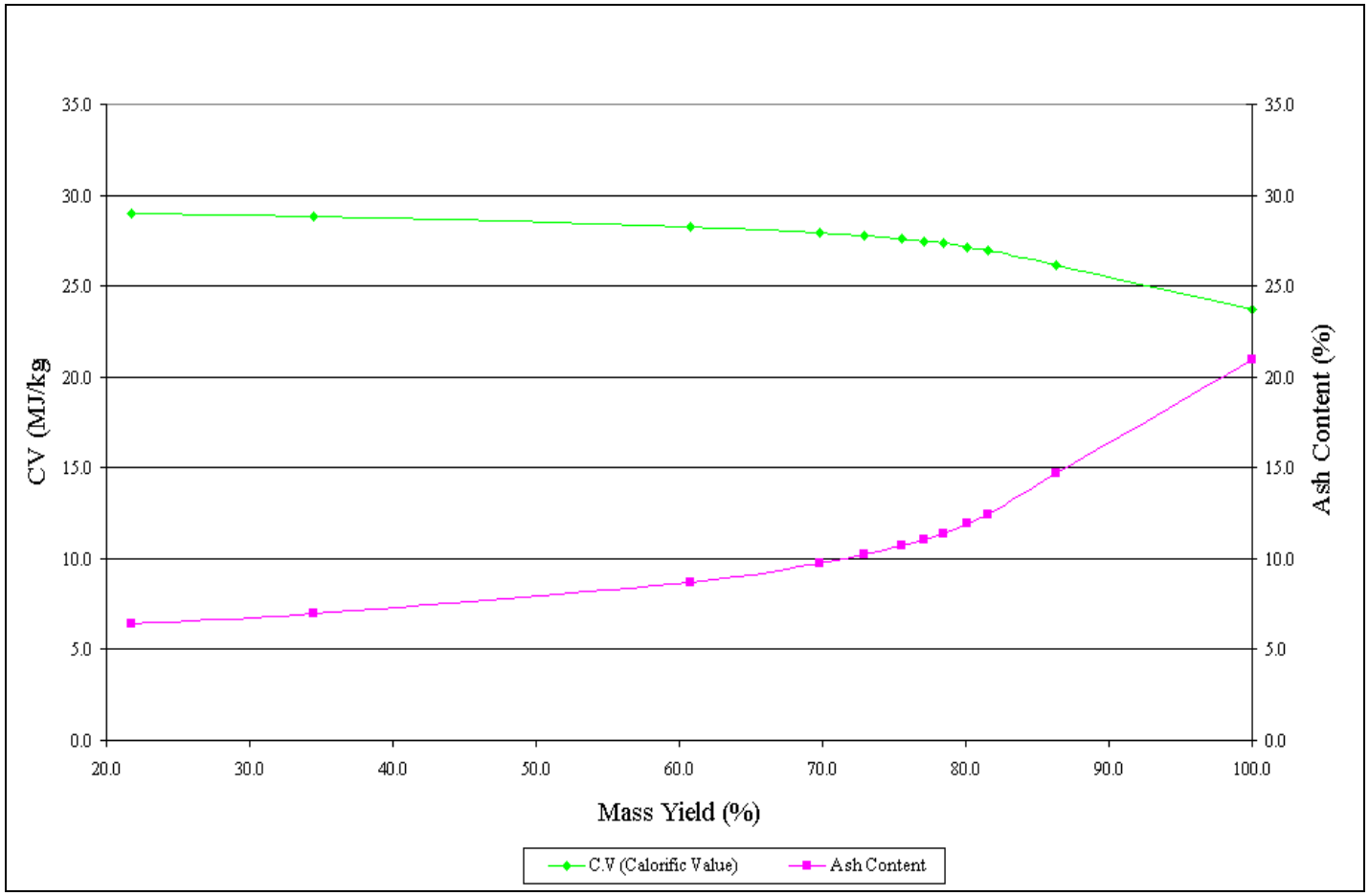

Figure 25: Cumulative Calorific Value and Ash vs. Cumulative Mass Yield for –20mm+10mm Material

	Yield %		Moisture (%)		Ash (%)		Volatile (%)		Fixed Carbon (%)		Calorific Value (MJ/kg)		Sulphur- Total (%)	
Density Fraction	Discrete	Cumulative	Discrete	Cumulative	Discrete	Cumulative	Discrete	Cumulative	Discrete	Cumulative	Discrete	Cumulative	Discrete	Cumulative
-1.30	16.88	16.88	6.40	6.40	5.20	5.20	34.30	34.30	54.10	54.10	28.80	28.80	0.61	0.61
-1.35+1.30	20.99	37.87	5.30	5.79	8.20	6.86	34.10	34.19	52.40	53.16	28.14	28.43	0.58	0.59
-1.40+1.35	19.35	57.22	5.70	5.76	11.40	8.40	33.00	33.79	49.90	52.06	27.03	27.96	0.50	0.56
-1.45+1.40	6.76	63.98	5.20	5.70	15.90	9.19	32.90	33.69	46.00	51.42	25.34	27.68	0.53	0.56
-1.50+1.45	3.75	67.73	5.00	5.66	19.90	9.78	29.70	33.47	45.40	51.08	24.11	27.48	0.59	0.56
-1.55+1.50	2.60	70.33	5.10	5.64	23.90	10.30	27.70	33.26	43.30	50.80	22.38	27.30	0.81	0.57
-1.60+1.55	1.68	72.01	4.60	5.62	30.30	10.77	24.60	33.06	40.50	50.55	19.94	27.12	0.53	0.57
-1.65+1.60	1.55	73.56	4.60	5.60	30.90	11.20	23.90	32.86	40.60	50.35	19.64	26.97	1.11	0.58
-1.70+1.65	1.71	75.27	4.50	5.57	37.20	11.79	20.10	32.57	38.20	50.07	17.42	26.75	0.64	0.58
-1.75-1.70	1.64	76.91	4.10	5.54	40.50	12.40	18.30	32.27	37.10	49.79	16.31	26.53	0.57	0.58
-1.80-1.75	4.63	81.54	4.10	5.46	50.30	14.55	16.90	31.40	28.70	48.60	12.30	25.72	1.02	0.61
+1.80	18.46	100.00	2.80	4.97	65.90	24.03	14.20	28.22	17.10	42.78	6.96	22.26	4.91	1.40
Total	100.00		4.97		24.03		28.22		42.78		22.26		1.40	

Table 6: Washability Data for –10mm+0.5mm Material

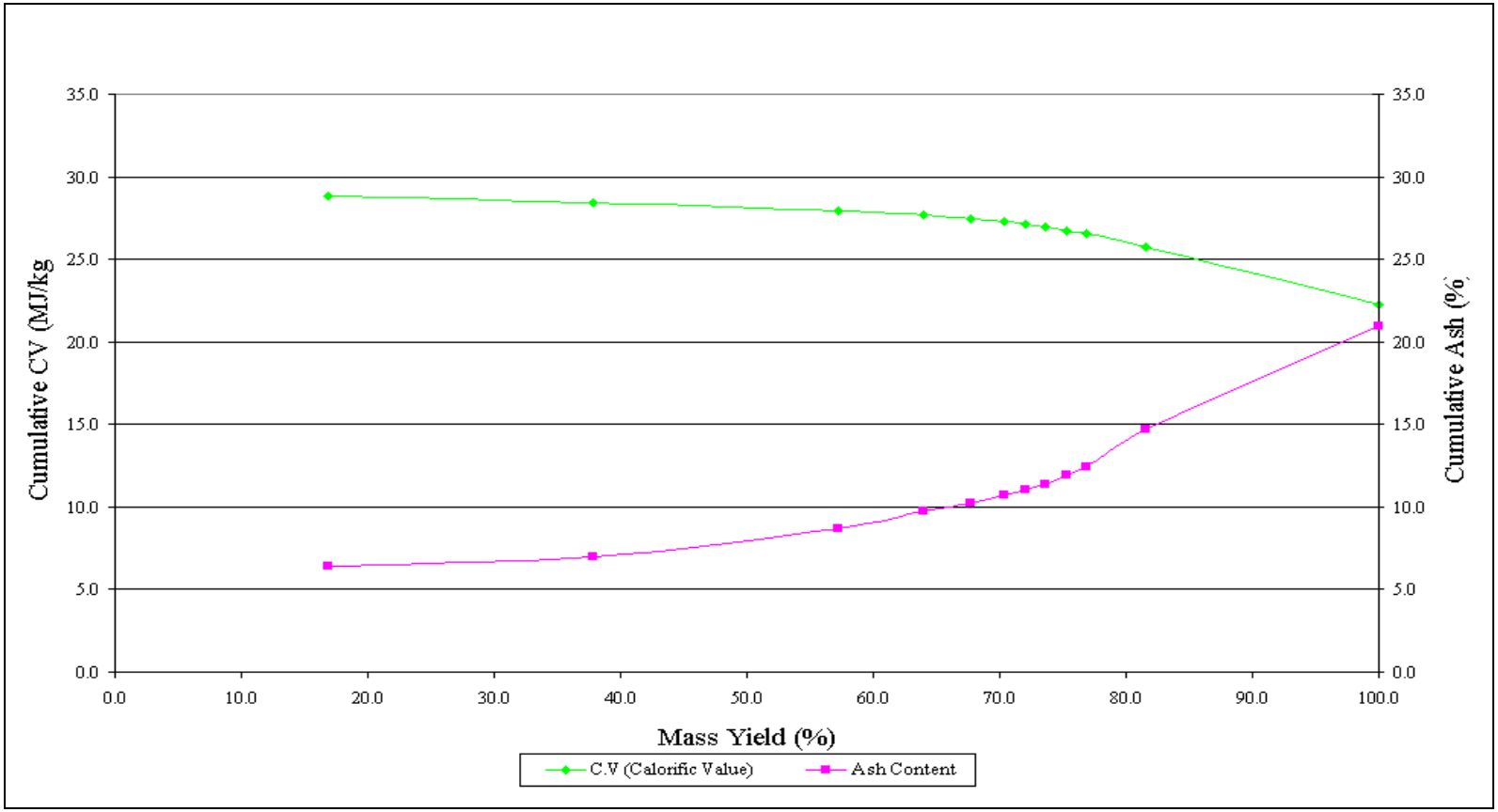

Figure 26: Cumulative Calorific Value and Ash vs. Cumulative Mass Yield for –10mm+0.5mm Material

7.2 Validation of Preliminary Laboratory Testwork

7.2.1 Observations Derived from Simulation Results

X-Ray Transmission images of typical coal, torbanite and shale samples (-80mm+20mm), hand picked from the ROM stockpile are presented in Table 7. The calibration curve derived from well liberated coal and torbanite samples during laboratory tests at CommoDaS in Wedel was applied to these images, utilising the Mikrosort® simulation package. Simulated images with density classifications in red/blue are also presented in Table 7.

Qualitative analysis of the simulation images proved to be adequate in order to draw conclusions regarding the suitability of the calibration curve for separating typical ROM ore. As demonstrated in Table 7, the simulation images showed that a clear distinction between coal and torbanite could be obtained. The reason for the clear distinction is uncertain, but it is presumed to be due to the waxy nature of the torbanite material.

Observations from examination of the images included:-

- Torbanite particles displayed "speckled" characteristics consistent with laboratory scale findings. This allows for the separation of torbanite from shale.
- X-ray images clearly displayed "bands" of shale or torbanite present within the structure of the coal particles, which is characteristic of this coal deposit. A good example of this is demonstrated in Figure 27 .
- Large pyrite inclusions were also detectable in the images, as is presented in Figure 28. This implies that large inclusions could be detected and potentially rejected from the coal product in order to reduce sulphur content.

Sample	Sample Picture	X-Ray Image (Gray Scale)	Simulation Result
Coal Rich		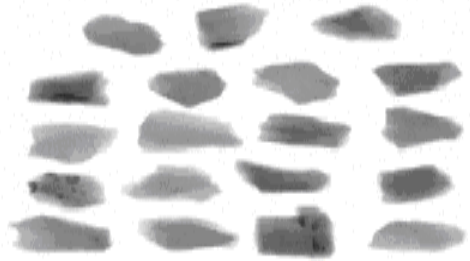	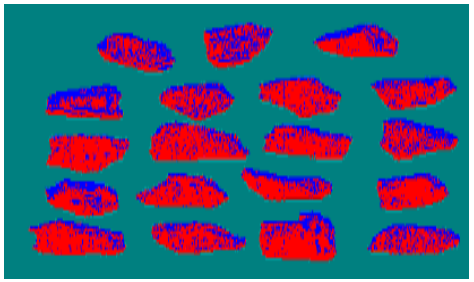
Torbanite Rich		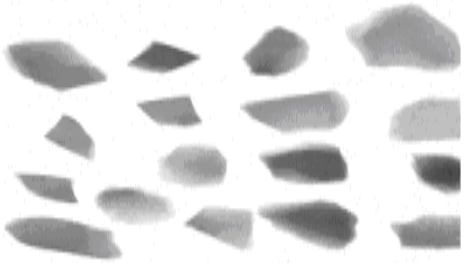	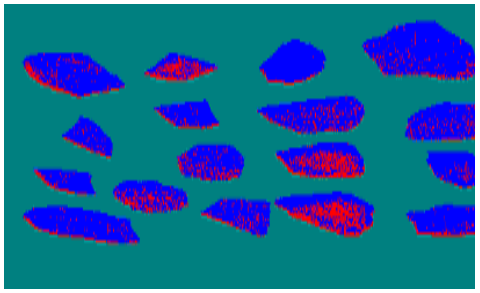
Shale Rich		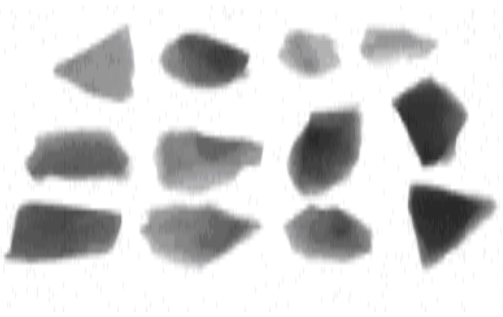	

Table 7: Simulation of Existing Algorithm for –70mm+40mm Samples

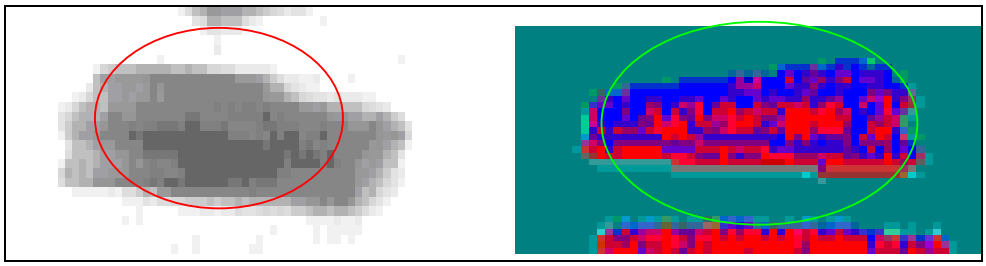

Figure 27: Band of Shale/Torbanite (Represented in Blue) Within Coal Seam (Represented in Red)

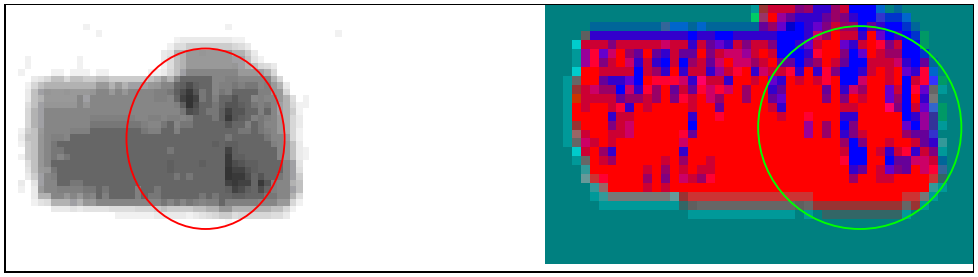

Figure 28: Coal Particle with Pyrite Inclusions (Represented in Blue)

Based on these findings, it can be concluded that the calibration curve derived from the laboratory scale investigation is adequate for the separation of typical ores, because sufficient differentiation could be attained between the coal and torbanite. However, the algorithms previously derived would need to accommodate unliberated material, which was not accounted for in the preliminary laboratory testwork. This is done by adjusting the rejection criteria of the algorithm, i.e. the percentage of blue pixels allowed to report to the coal "product stream" to a point where a suitable coal product is attained.

As both torbanite and shale are represented predominantly by high density pixels, an additional sorting step would be required in order to remove shale rich material from the torbanite product. The simulation results indicate that this could be achieved utilizing the same calibration curve by rejecting particles with very high percentages of dense material (>90%). As with the first sorting stage, the rejection criteria for the second stage should also be optimized. However, the addition of an extra sorting stage has major cost implications in terms of capital requirements. It was recommended that the effects of retorting the shale material with the torbanite be investigated initially to evaluate the necessity of the additional processing stage. For this reason, the separation of torbanite and shale is presented in this report for demonstration purposes only.

7.3 Optimization Testwork

7.3.1 Effects of Program Sensitivity on Coal Product Quality

This test series demonstrated the impacts of the program sensitivity on the quality of products that can be attained. The rejection criterion was varied to examine its effects on product quality and mass yield. The effect of increasing the percentage of blue pixels permitted to report to the product stream is presented in Figure 29 and Table 8.

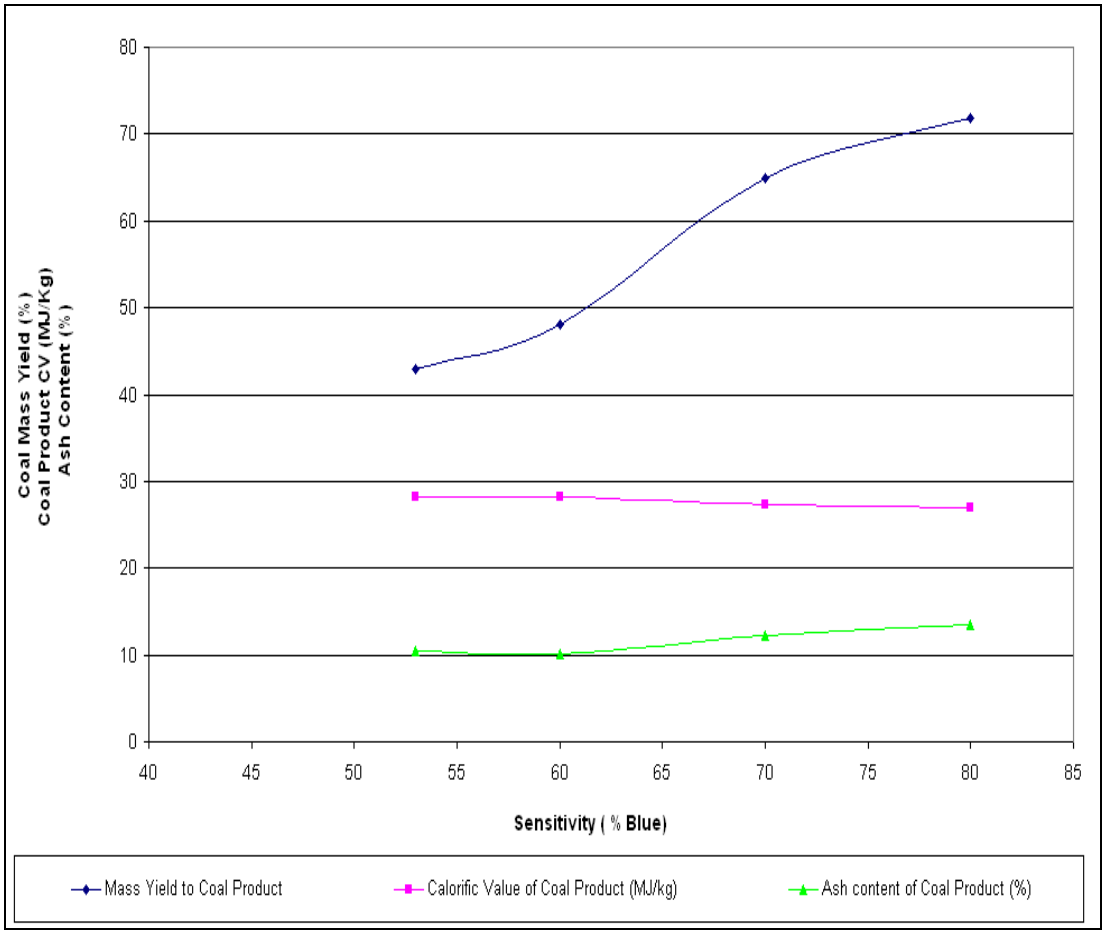

Figure 29: Variation of Mass Pull and Coal Product Quality with Changes to Sorting Criteria

As anticipated, mass yield increased as the percentage of high density material permitted to report to the coal product increased, as more material fell within the sorting criteria. This allowed for the introduction of more high density unliberated coal pieces to the coal product, resulting in increase in Ash content and reduction in Calorific Value.

TestNo.	Rejection Criteria	Stream	Mass Yield (%)	CV (MJ/kg)	Ash (%)	Moisture (%)	Volatiles (%)	Fixed Carbon (%)	Total S (%)
1	Reject >70% Blue	Coal Product	65.0	27.3	12.3	5.6	32.9	49.2	1.0
		Torbanite and Shale Product	35.0	14.5	49.2	3.6	20.8	26.4	2.5
		Reconsituted Feed	**100.0**	**22.8**	**25.2**	**4.9**	**28.7**	**41.2**	**1.5**
2	Reject >60% Blue	Coal Product	48.1	28.1	10.1	5.3	33.9	50.7	0.8
		Torbanite and Shale Product	51.9	18.7	37.3	3.8	25.3	33.6	2.6
		Reconsituted Feed	**100.0**	**23.2**	**24.2**	**4.5**	**29.4**	**41.8**	**1.7**
3	Reject >53% Blue	Coal Product	42.9	28.2	10.5	5.1	33.7	50.7	0.8
		Torbanite and Shale Product	57.1	20.0	33.6	3.8	25.9	36.7	1.7
		Reconsituted Feed	**100.0**	**23.5**	**23.7**	**4.4**	**29.2**	**42.7**	**1.3**
4	Reject >80% Blue	Coal Product	71.8	26.9	13.5	5.5	32.6	48.4	1.0
		Torbanite and Shale Product	28.2	13.1	51.6	3.3	20.1	25	2.8
		Reconsituted Feed	**100.0**	**23.0**	**24.2**	**4.9**	**29.1**	**41.8**	**1.5**

Table 8: Effect of Program Sensitivity on Product Quality

The variation of calorific value, volatiles and Ash content with mass yield to the coal product is presented in Figure 30 and 31 respectively.

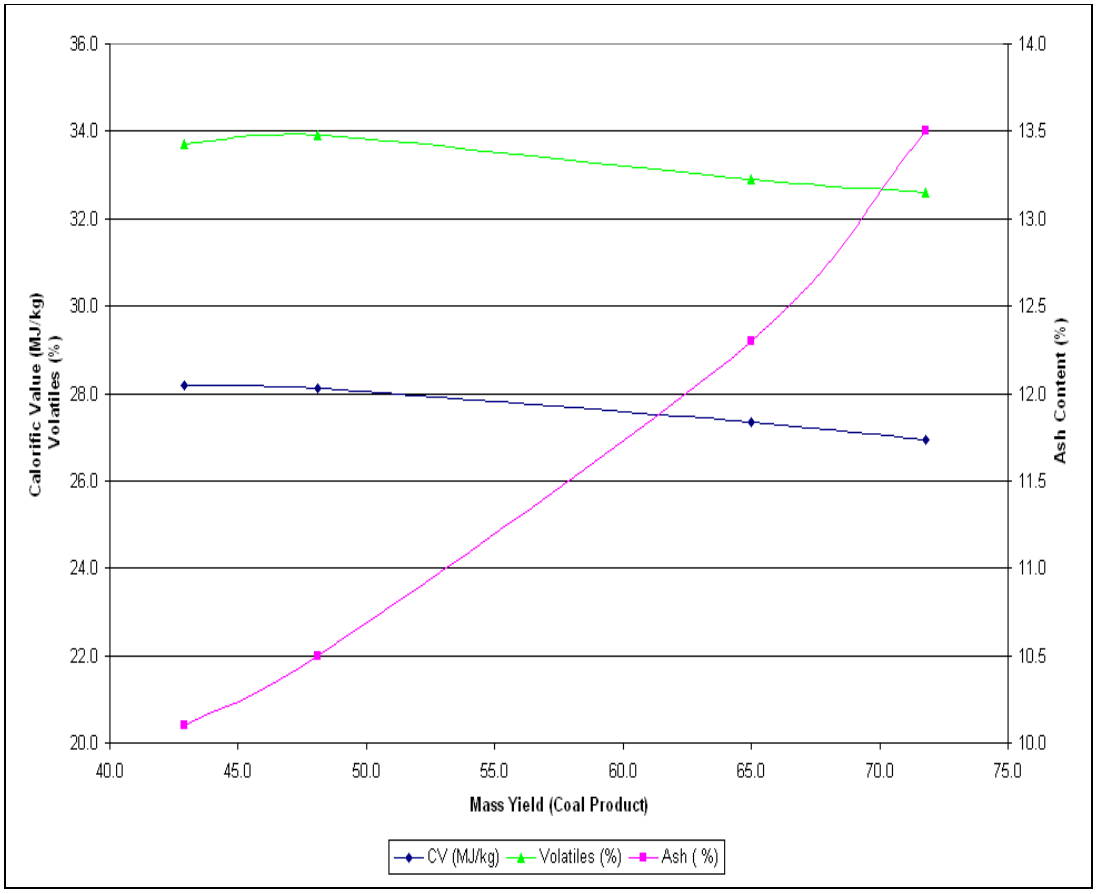

Figure 30: Variation of CV, Volatile and Ash Content of Coal Product with Mass Yield

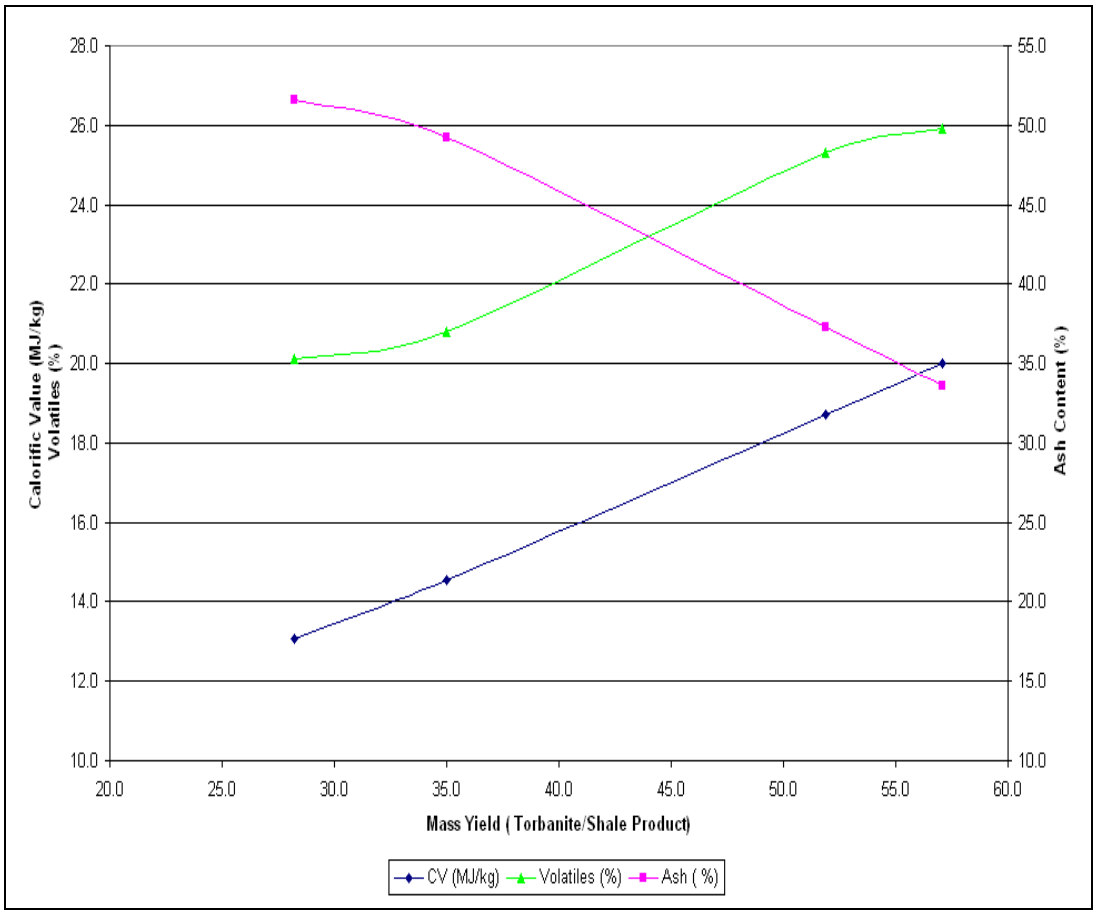

Figure 31: Variation of CV, Volatile and Ash Content of Torbanite/ Shale Product with Mass Yield

A summary of the petrographic composition of the coal and torbanite products is presented in Figure 32 and 33 respectively.

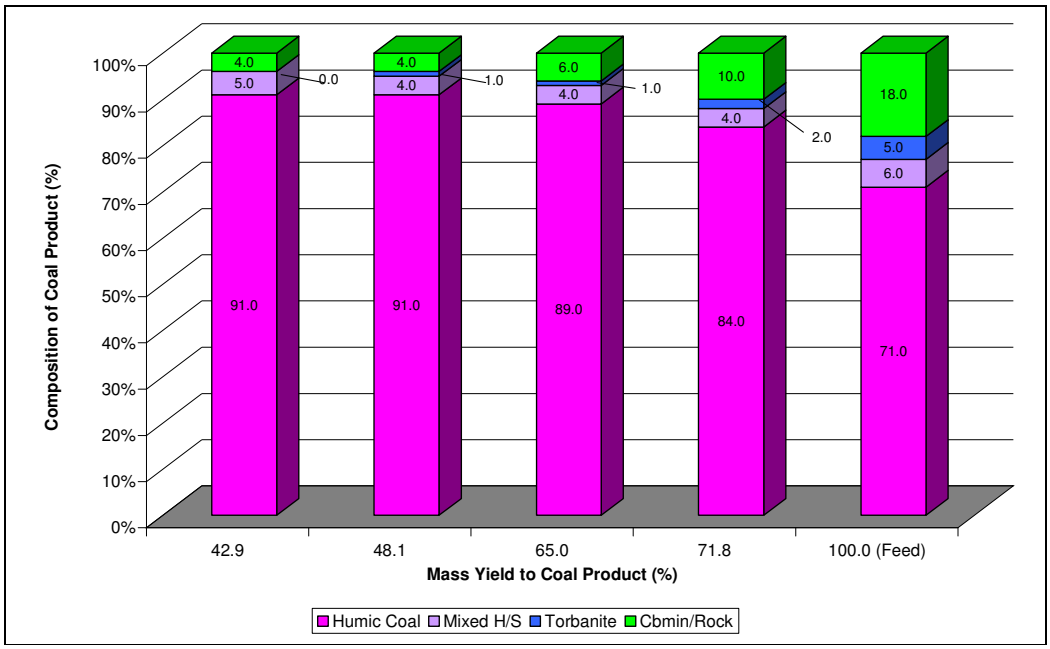

Figure 32: Variation of Coal Product Composition with Mass Yield (by Volume)

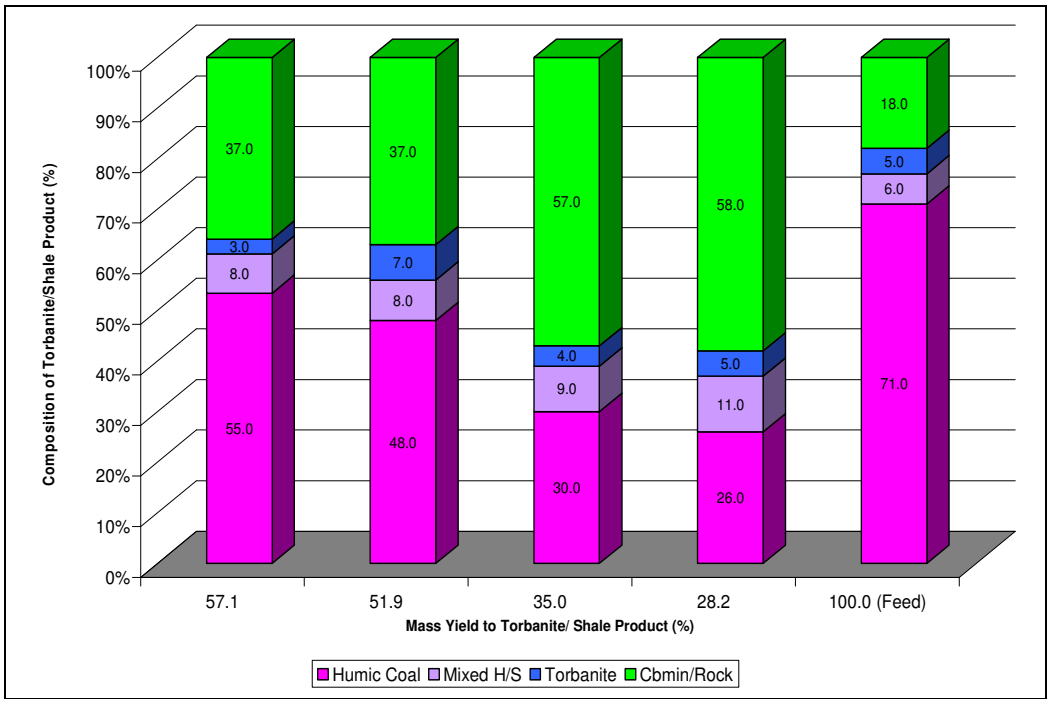

Figure 33: Variation of Torbanite/ Shale Product Composition with Mass Yield (by Volume)

Based on the sample received, a saleable quality coal can be produced up to mass yields of 48.1% to coal product. Under these conditions, products had a CV of 28.1MJ/kg at an Ash content of 10.1%. The torbanite and shale product derived would have a CV of 18.7MJ/kg and have an Ash content of 37.3%.This constituted an upgrade in coal composition from a feed stock consisting of approximately 71.0% (by volume) humic coal to 91.0% (by volume) humic coal, as illustrated in Figure 32.

Torbanite contamination in the coal product was marginal at a mass yield of 42.9%, but did increase up to 2% as mass yield to coal product was increased. The major contaminants in the coal product included interlocked particles, mixtures of humic/sapropelic coal, shale and mudstones. Such contamination accounted for between 9 and 14%, depending on the mass reporting to the coal product.

Some contamination of the coal product by interlocked and mixed humic/sapropelic coal was anticipated as a direct consequence of algorithm design. Interlocked and mixed pieces which have a higher proportion of coal would often have shale and torbanite compositions well below the rejection criteria and would therefore report to the coal product. This is demonstrated in more detail when coal recovery is discussed in Section 7.3.2.

It was observed that shale and mudstone particles that reported to the coal product were correctly placed into the torbanite/ shale product if passed through the sorting unit a second time. This suggests that these particles have been derived from interlocked particles which have broken during the vigorous ejection and handling process after sorting has taken place, or have been misplaced by sorter error.

7.3.2 Effect of Program Sensitivity on Coal and Torbanite Recovery

Figure 34 presents the distribution of the various mineral components to the coal and torbanite/shale products. This figure indicates the percentage (by volume) of coal, shale and torbanite present in the feed that reports to the coal product, as well as torbanite and shale product.

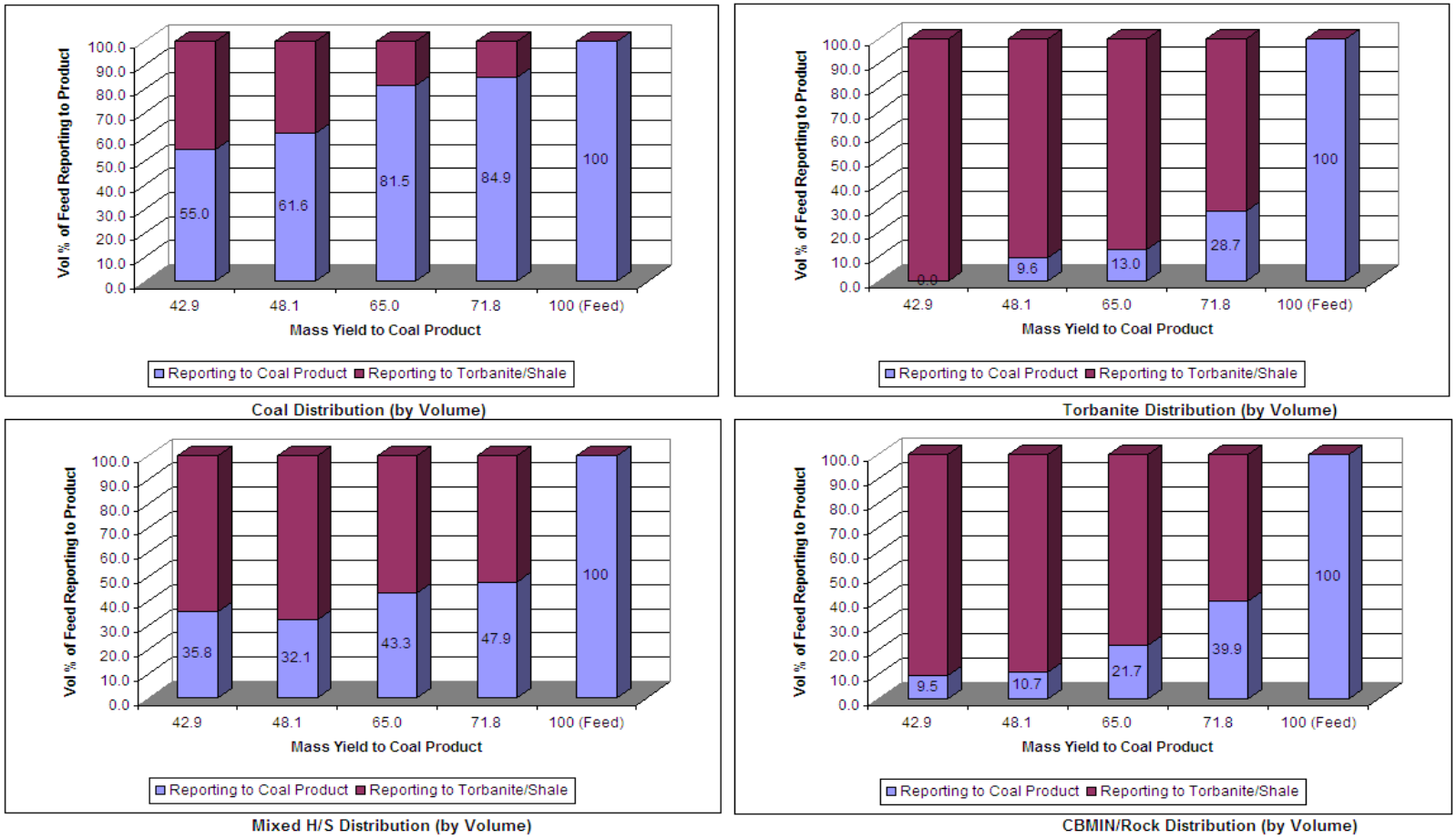

Figure 34: Recovery of Various Feed Components to Coal Product

At a mass yield of 42.9% to coal product, only 55% (by volume) of the coal present in the feed material was recovered to the coal product. It was anticipated that the primary cause of coal losses to the torbanite and shale fraction was owing to the presence of unliberated material in the ROM sample. The reason for these losses is demonstrated in Figure 35.

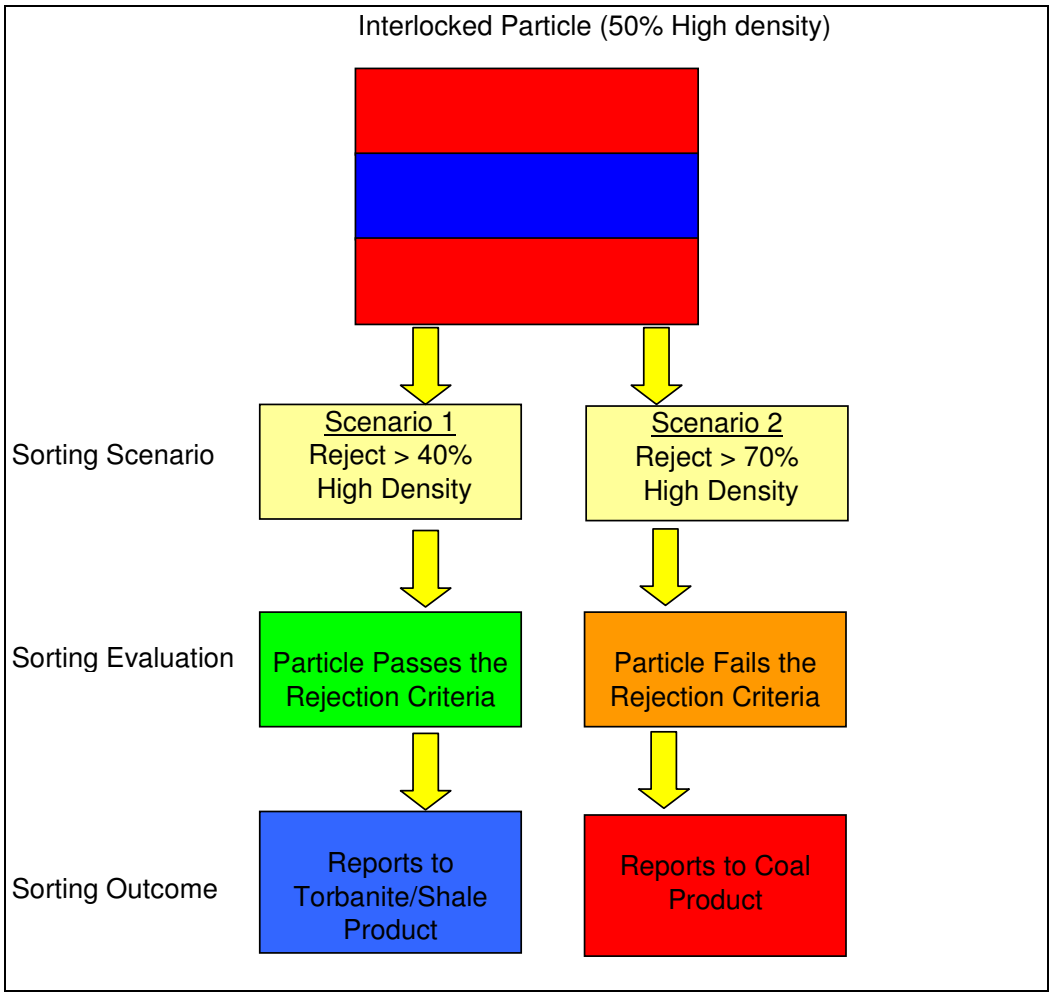

Figure 35: The Effect Of Rejection Criteria on Unliberated Material

As demonstrated in Figure 35, the proportion of shale or torbanite within unliberated particles defines whether the particle will report to the coal or torbanite fraction, based on the applied rejection criteria. In order to meet the requirements for a torbanite free, high grade coal product, low rejection criteria are required to minimize the amount of interlocked material reporting to the coal product. This has the following implications:-

- The torbanite and shale fraction will always contain some coal, as a proportion of the unliberated material will report to the torbanite and shale fraction.
- Lower grade, dull coals may also be misplaced to the torbanite/shale product, as was visually observed during this testwork program.
- Recovery of coal to the coal product would be low, as observed by the optimization testwork.

Coal recovery increased significantly as mass yield to coal product was increased (90% recovery at a mass yield of 71%.) However, the increase in mass yield resulted in the introduction of torbanite, as well as more interlocked material into the coal product. This impacted negatively on the coal product CV and Ash content.

Based on visual examination of the torbanite and shale product, it would appear that the majority of the misplaced coal samples at high mass yields to coal product contain substantial proportions of pyrite, present as bands across the length of the particle. This is further substantiated by the reduction of sulphur content of the coal product. Pyrite rich coal samples tended to report to the shale fraction during second stage processing due to their high density.

Vitreous coal was also noted to report to the torbanite and shale products at high mass yield to coal product. The presence of vitreous coal within the torbanite fraction can be beneficial in the retorting process.

7.3.3 Effect of Degree of Liberation on Sorter Performance

The effect of degree of liberation on the sorting performance is demonstrated graphically in Figure 36. This figure presents simulated x-ray images of torbanite samples at various fractions.

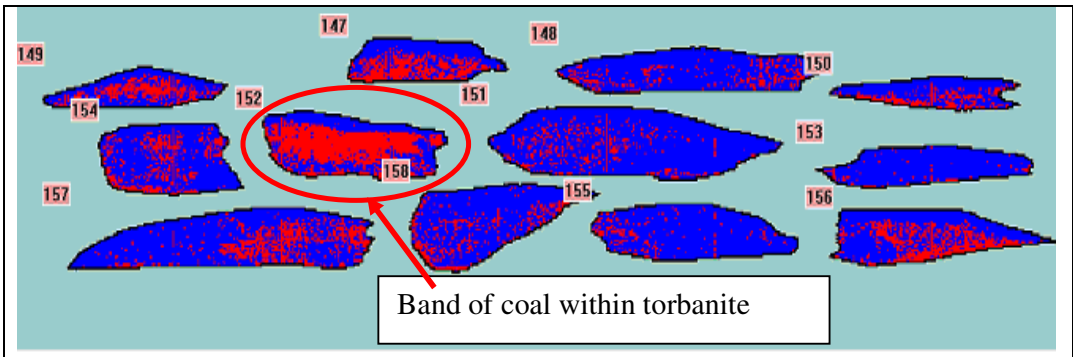

Torbanite (-80mm+70mm)

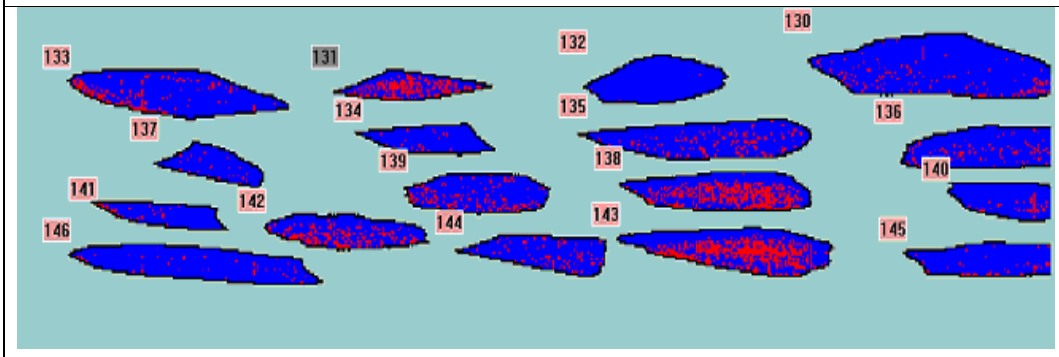

Torbanite (-70mm+50mm)

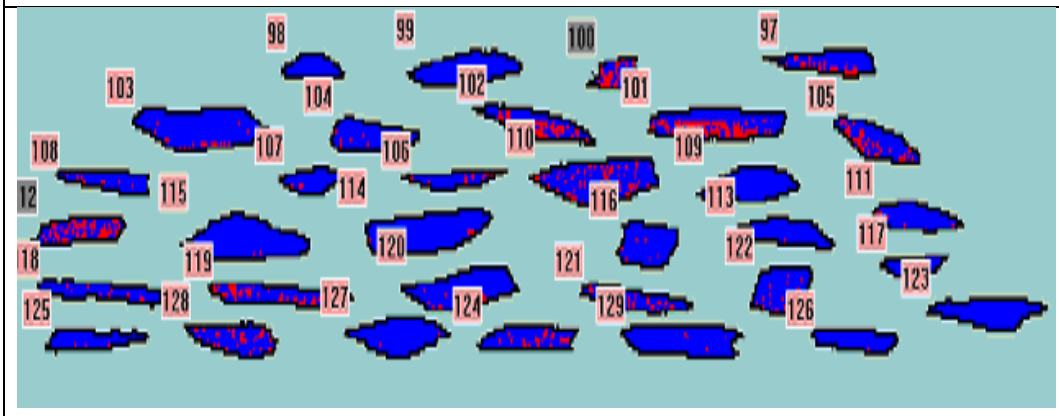

Torbanite (-50mm+20mm)

Figure 36: Simulation Images of Torbanite at Various Size Fractions

Figure 36 demonstrates that liberation in the -80mm+20mm size fraction is poor, but is significantly improved at -50mm+20mm. Reducing the top size of the material to 50mm by means of further communition would have positive impacts on the overall mass yield to coal product and coal product purity.

An additional test (Test 5) conducted on -50mm+20mm material confirmed this finding. The test was conducted at a mass yield similar to that of Test 4 (refer to Table 8) conducted on -80mm+20mm material in order to compare sorter performance. The results are compared in Figure 37.

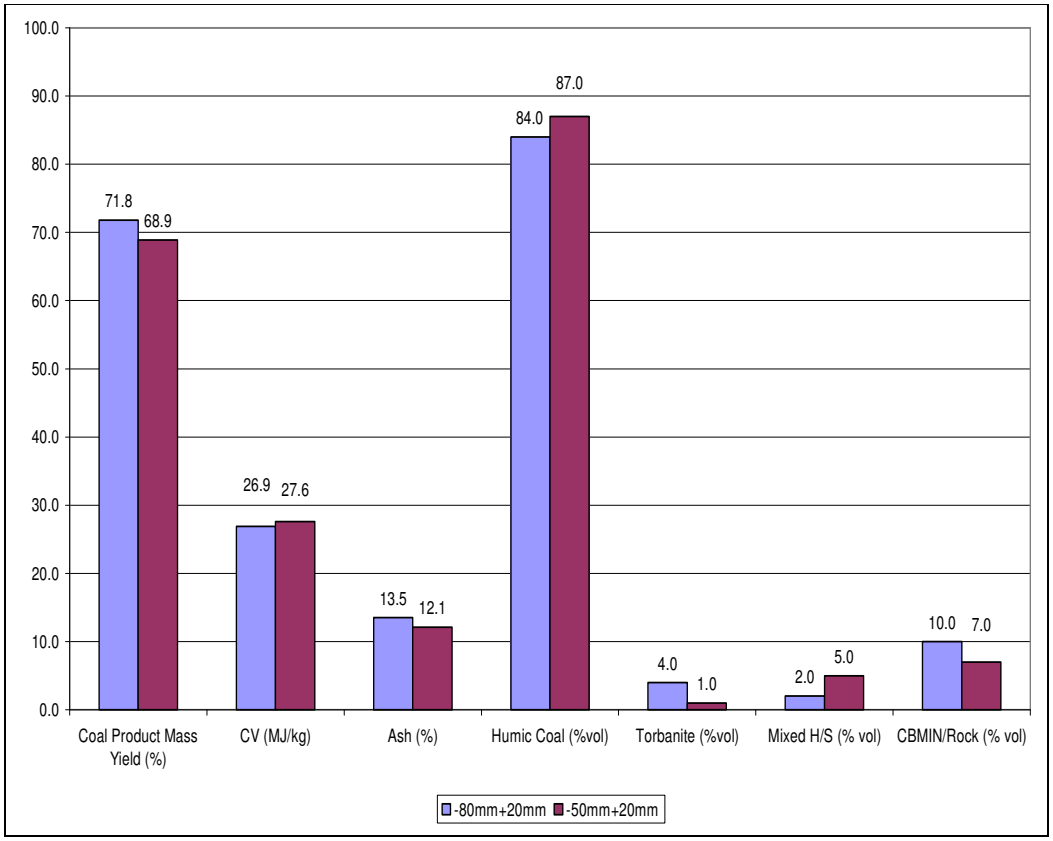

Figure 37: Comparison of Coal Product at Processing Size Ranges of -80mm+20mm and -50mm+20mm

The results of Test 5 indicated that at similar mass yields to coal product:-

- Calorific value could be improved from 26.9MJ/kg to 27.6 MJ/kg. Ash content could be reduced from 13.5% to 12.1% by reducing the top size from 80mm to 50mm
- Torbanite and shale content could be reduced by 3%.

It is recommended that further optimisation of the processed size fraction be conducted, including examination of various crushing techniques, as this may improve the sorter performance significantly.

7.4 Deshaling of Torbanite Product

As discussed in Section 7.2, the deshaling of the torbanite product was conducted only to demonstrate that the process was feasible. The deshaling test was conducted at 95% sensitivity.

The results, including petrographic analysis of the resulting products are presented in Tables 9, 10 and Figure 38.

Stream	Mass Yield (%)	CV (MJ/kg)	Ash (%)	Moisture (%)	Volatiles (%)	Fixed Carbon (%)	Total S (%)
Coal Product	68.9	27.62	12.1	4.7	33.9	49.3	0.9
Torbanite and Shale	31.1	15.2	46.4	3.2	20.0	23.3	3.4
Feed Material	**100.0**	**23.8**	**22.8**	**4.2**	**29.6**	**41.2**	**1.7**
Stage 2							
Torbanite	47.4	18.8	37.3	4.9	22.6	33.2	2.7
Shale	52.6	12.1	54.7	3.5	17.6	23.7	4.0
Torbanite and Shale	**100.0**	**15.3**	**46.5**	**4.2**	**20.0**	**28.2**	**3.4**

Table 9: Results of Deshaling Tests

		Composition (% volume)				
Stream	Mass Yield (%)	Humic Coal	Mixed H/S	Torbanite	Total Organic	Cbmin/Rock
Coal Product	68.9	87.0	5.0	1.0	93.0	7.0
Torbanite and Shale	31.1	35.6	7.8	6.3	49.7	50.3
Feed Material	**100.0**	**71.0**	**5.9**	**2.6**	**79.5**	**20.5**
Stage 2						
Torbanite	47.4	44.0	11.0	11.0	66.0	34.0
Shale	52.6	28.0	5.0	2.0	35.0	65.0
Torbanite and Shale	**100.0**	**35.6**	**7.8**	**6.3**	**49.7**	**50.3**

Table 10: Petrographic Analysis of Samples Derived From Deshaling Test

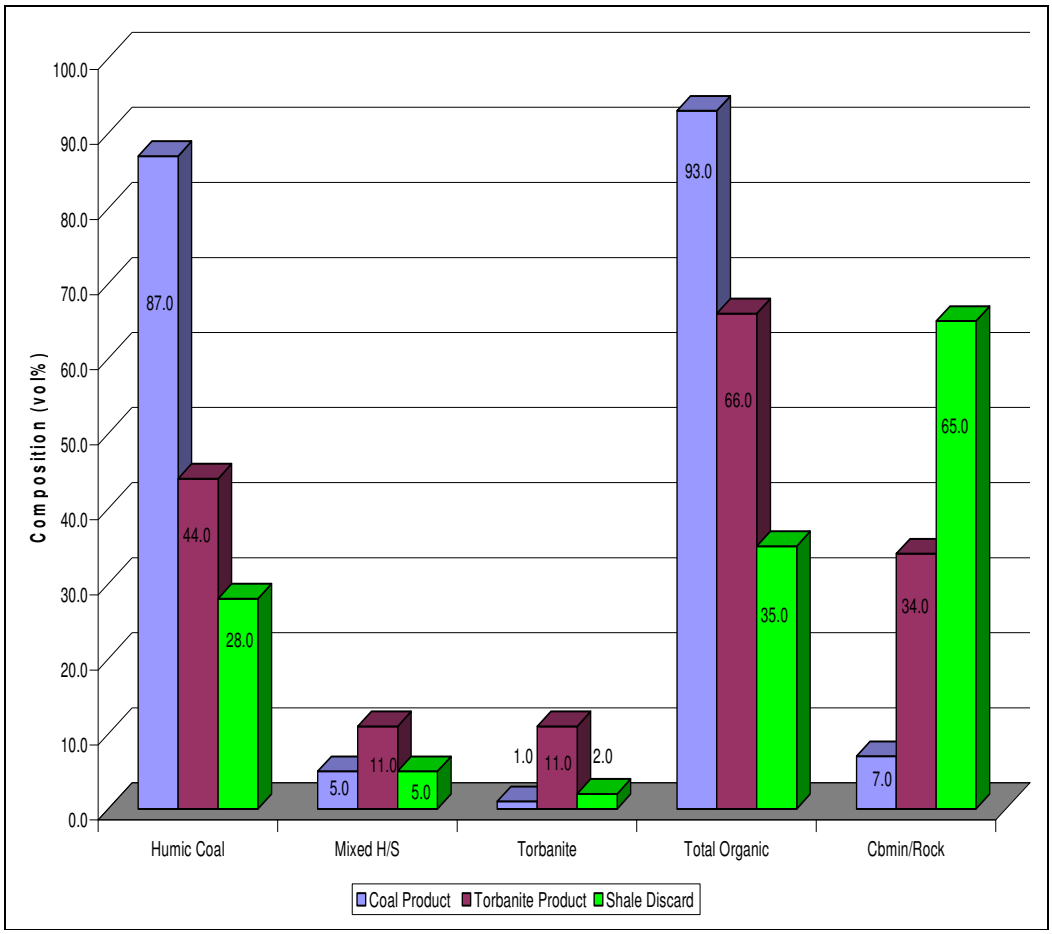

Figure 38: Summary of Petrographic Analysis- Deshaling Tests.

Based on the rock and carbonaceous mineral content of the shale product (65% by volume), and torbanite content (2%), it would appear that, in principle, the separation of torbanite from shale is feasible. It was noted that:-

- The shale discard had a calorific value of 12.1MJ/kg, and an Ash Content of 54.7%. The shale product consisted of approximately 16.4% of the -80mm+20mm sorter feed.
- The shale product has high total sulphur content (4.0% S). It is anticipated that coal material with large pyrite inclusions report to the shale fraction due to the high density of the inclusions. Other humic coal is present in the shale discard is attributed to interlocked material with very high shale compositions.
- Torbanite recovery can be improved through optimization of the selection criteria

7.5 Production of Bulk Coal and Torbanite Products

7.5.1 Overall Process Mass Balance

Pilot scale testwork was conducted using very conservative rejection criteria in order to obtain reasonable mass yields to the coal product. A rejection criterion of 60% was selected. The mass balance presented in Figure 39 takes all streams, including undersize sample that were not suitable for sorting into account. Comprehensive analysis of the products is presented in Appendix D.

A relatively small proportion of the ROM material reports to the -80mm+20mm size fraction. The sorter feed consists of approximately 25.5% of the ROM feed material. Typically, the size distribution for coal operations is approximately 50-60% reporting to the +20mm fraction. There is at present no feasible means of upgrading the finer material. As a result, only 17.2% of the ROM feed material is recoverable as a coal product and 5% of the overall feed is recoverable as a torbanite product. A means of maximizing the percentage of ROM material reporting to the feed is required to ensure that the process is financially viable.

The coal product has a calorific value of 27.6MJ/kg, with an ash content of 11.5%. As a conservative program was utilised, this grade could be improved by reducing the rejection criterion to 50%.

The grade of the shale product produced is consistent with washability results attained for the–1.75 SG fraction, and contains a calorific value of 8.9MJ/kg, 61.3% ash. This product contained 75.6% non-organic material.

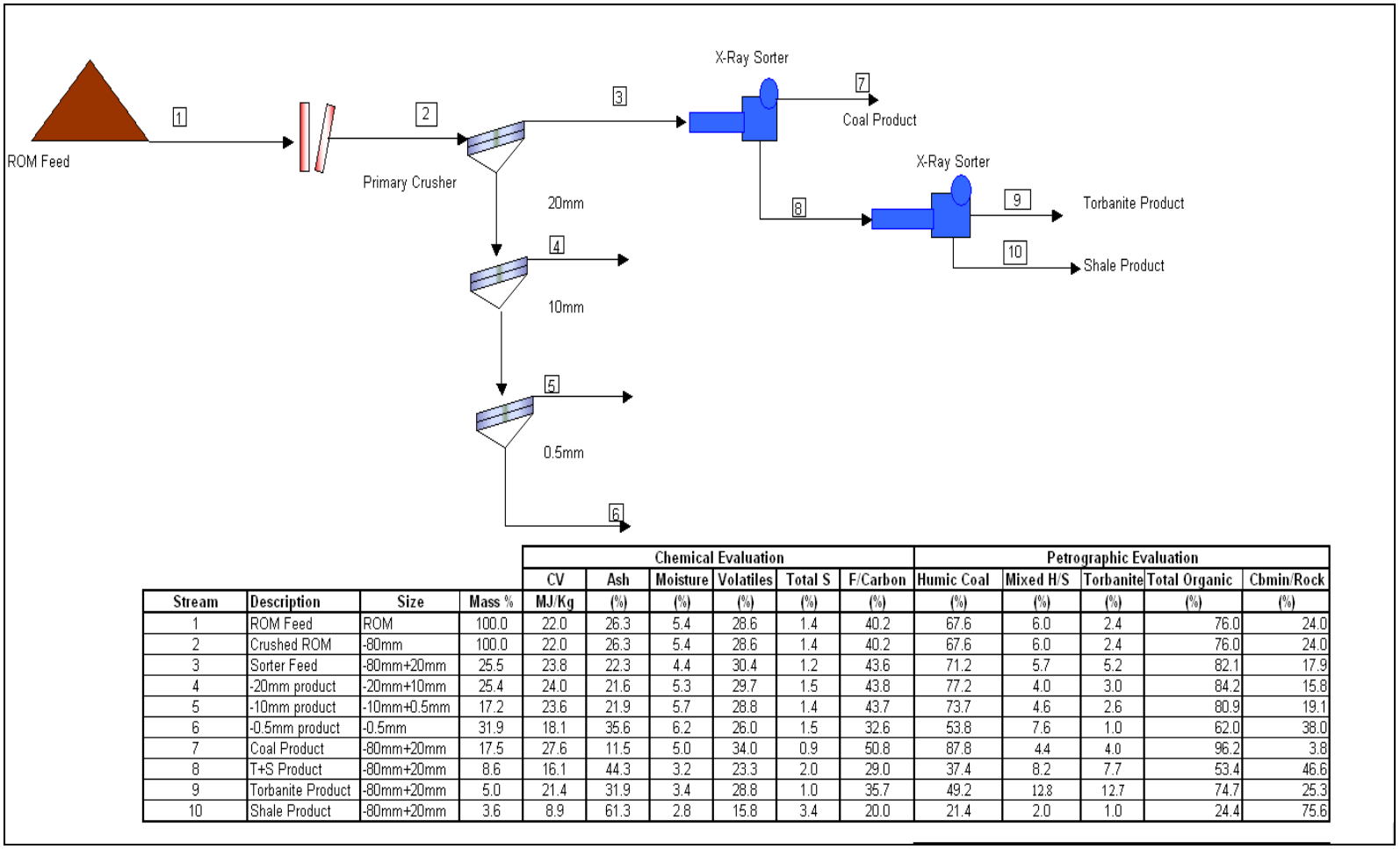

				Chemical Evaluation						Petrographic Evaluation				
				CV	Ash	Moisture	Volatiles	Total S	F/Carbon	Humic Coal	Mixed H/S	Torbanite	Total Organic	Cbmin/Rock
Stream	Description	Size	Mass %	MJ/Kg	(%)	(%)	(%)	(%)	(%)	(%)	(%)	(%)	(%)	(%)
1	ROM Feed	ROM	100.0	22.0	26.3	5.4	28.6	1.4	40.2	67.6	6.0	2.4	76.0	24.0
2	Crushed ROM	-80mm	100.0	22.0	26.3	5.4	28.6	1.4	40.2	67.6	6.0	2.4	76.0	24.0
3	Sorter Feed	-80mm+20mm	25.5	23.8	22.3	4.4	30.4	1.2	43.6	71.2	5.7	5.2	82.1	17.9
4	-20mm product	-20mm+10mm	25.4	24.0	21.6	5.3	29.7	1.5	43.8	77.2	4.0	3.0	84.2	15.8
5	-10mm product	-10mm+0.5mm	17.2	23.6	21.9	5.7	28.8	1.4	43.7	73.7	4.6	2.6	80.9	19.1
6	-0.5mm product	-0.5mm	31.9	18.1	35.6	6.2	26.0	1.5	32.6	53.8	7.6	1.0	62.0	38.0
7	Coal Product	-80mm+20mm	17.5	27.6	11.5	5.0	34.0	0.9	50.8	87.8	4.4	4.0	96.2	3.8
8	T+S Product	-80mm+20mm	8.6	16.1	44.3	3.2	23.3	2.0	29.0	37.4	8.2	7.7	53.4	46.6
9	Torbanite Product	-80mm+20mm	5.0	21.4	31.9	3.4	28.8	1.0	35.7	49.2	12.8	12.7	74.7	25.3
10	Shale Product	-80mm+20mm	3.6	8.9	61.3	2.8	15.8	3.4	20.0	21.4	2.0	1.0	24.4	75.6

Figure 39: Bulk Product Mass Balance

7.5.2 Comparison of Pilot Scale Investigation and Optimization Testwork

Figure 40 and Figure 41 compare the x-ray sorter performance at optimisation and pilot production scale. Both tests were conducted at the same sensitivity level, and provide an indication of the robustness of the sorting process.

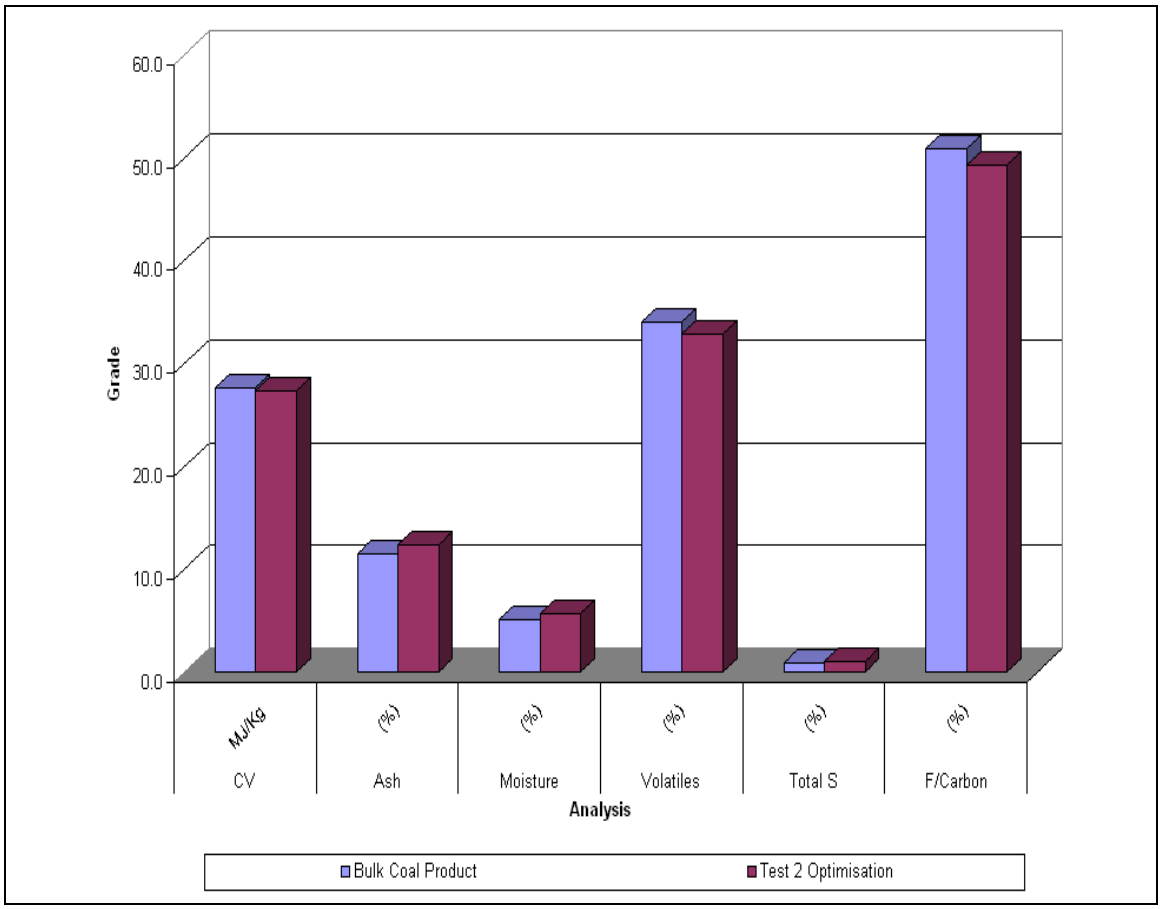

Figure 40: Chemical Comparison of the Coal Products of Optimisation Test 2 and Bulk Production Test

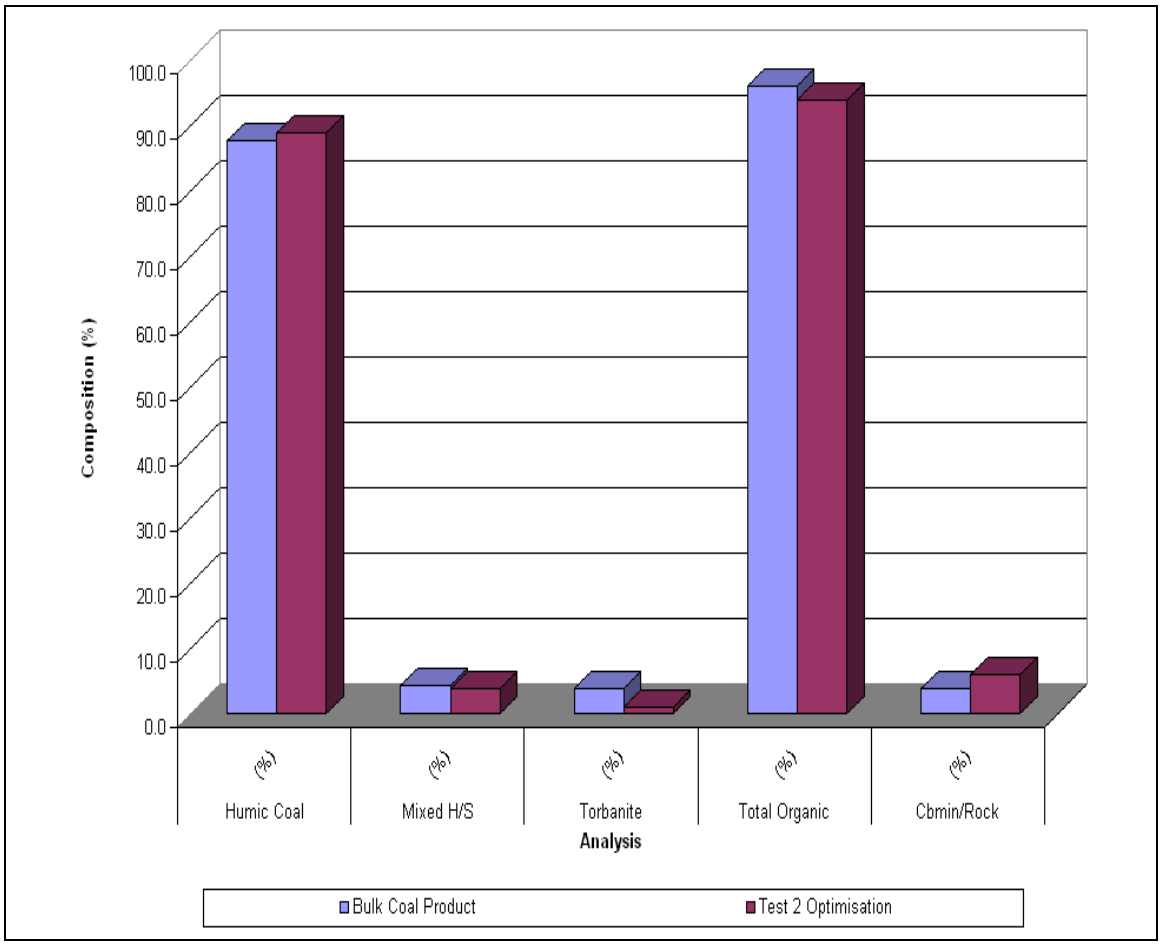

Figure 41: *Petrographic Comparison of the Coal Products of Optimization Test 2 and Bulk Production Test*

The results attained on pilot production scale (10t/hr) are consistent with those attained on optimisation scale (3 ton/hr), with the exception of the improved torbanite recovery in the bulk processing exercise. This indicates that the process is particularly robust within these process parameters.

7.6 TGA analysis of Torbanite Products

A comprehensive TGA report from University of Pretoria is presented in Appendix E.

The TGA analysis of the coal, shale and torbanite products indicate that volatiles release occurred as two separate but overlapping events. At a temperature of approximately 450°C, maximum release of volatiles occurred for the torbanite sample. At approximately 550°C all volatile material has been removed from the sample. This is favourable, as cracking starts to increase at a high rate from a 450-500°C. The most valuable and useful diesel fraction is allowed to boil up to 395°C. The heavy diesel product could potentially be utilised by the Sasol Secunda to upgrade excess light diesel product (Goosen, 2006).

8 CONCLUSIONS

Dual Energy X-Ray Transmission Sorting has been utilised successfully in the separation of Coal from Torbanite. The technique has demonstrated that differentiation between coal, torbanite and shale could be attained, and that the differentiation was significant enough to effect a separation. Calibration curves derived from high quality coal samples during preliminary laboratory testwork proved to be adequate, and did not require adjustment. However, rejection criteria established for purer coal samples were inappropriate, and required adjustment to accommodate unliberated material present in the ROM sample.

A two stage sorting process was required in order to produce a coal, torbanite and shale product. The deshaling of torbanite was conducted utilising the same calibration curve, but at a higher rejection criteria. This additional stage would have cost implications in terms of capital expenditure. It is recommended that the impact of the shale contamination in the torbanite product be investigated from a syncrude quality perspective, in order to establish the necessity of this additional processing stage.

Optimisation testwork conducted on the samples indicated that a high purity coal product could be attained. Coal products with marginal torbanite contamination could be attained at rejection criterion of 53% or less. This has not been accomplished by any other

processing technique. Based on the sample received, 42.9% of the material reporting to the sorter feed could be recovered. The product had a calorific value of 28.1MJ/kg with an ash content of 10.1%, and could therefore be a marketable product.

A number of issues arose from the proportion of unliberated material present in the sorter feed. The unliberated material reported to either the coal or torbanite fraction, depending on the ratio of coal to torbanite/shale within the particle, as well as the rejection criteria defined. This had the following impacts on sorter performance:-

- In order to produce a high grade, torbanite free coal product, low rejection criteria were required. As a result, a significant proportion of the coal present in the sorter feed was lost to the torbanite fraction.
- Low mass yields to coal product were required to produce a torbanite free product.
- Torbanite products will always contain unliberated coal/shale particles, if high purity coal products are targeted. The retorting process will therefore need to be very robust, and be able to tolerate the presence of up to 55% by volume of coal.

It was observed that reducing the processing size from -80mm+20mm to -50mm+20mm resulted in reduced coal losses, as well as improved coal quality in terms of calorific value and ash content.

The results attained from pilot scale processing of a bulk sample were consistent with results attained from optimisation tests at the same program conditions, indicting that the x-ray sorting process is robust.

TGA analysis of the resulting deshaled torbanite product from the pilot test program indicated that the heavy diesel product produced from the retorting process could potentially be utilised by Sasol to upgrade excess light diesel product.

An issue arising from the pilot sorting campaign that needs to be addressed is the low proportion of the ROM feed material reporting to the sorter feed as a result of the size distribution of the sample received. As a direct result, the coal and torbanite products represent a very small proportion of the overall ROM feed. Techniques for the separation of coal from torbanite in fine size fractions have yet to be evaluated. It is therefore

essential from a financial perspective to maximise the proportion of the ROM material reporting to the sorter.

9 RECOMMENDATIONS

A number of recommendations are proposed to address issues arising from the testwork program:-

9.1 Minimising The Proportion of Unliberated Material

An investigation into means of minimising the proportion of unliberated material into the sorter feed should be conducted. Such an investigation should include:

- Optimising the top size for the sorting process, by crushing ROM feed material to various top sizes.
- New technology such as High Pressure Grinding Rolls (HPGR) could potentially exploit the differences in breakage characteristics between coal, shale and torbanite, resulting in preferential liberation at coarse sizes.

9.2 Maximising the Proportion of ROM Material Reporting to the Sorter Feed

It is recommended that the following alternatives be investigated in order to exploit more of the available resource:-

- The size distribution of the sample received is atypical, and should be confirmed by conducting a full ROM size distribution.
- Use of alternative mining and crushing techniques should be examined, with the objective of minimising fines production.
- An investigation into the minimum processing size should be conducted. Based on the sample received, the proportion of ROM material reporting to the sorter feed could be increased from 25.5% to 51.1% by mass if reducing the bottom size for processing from 20mm to 10mm. Reduced throughput as a result of reducing the bottom processing size would also need to be considered.

- Petrographic analysis of the -0.5 mm material indicated that this consisted predominantly of coal. The potential of upgrading this size fraction by means of spirals in order to produce a clean coal product should be investigated, as this would provide an alternative means of increasing the proportion of ROM material reporting to the product.

10 REFERENCES

1. Allen, A. and Gordon, H., (2009),*X-Ray Sorting and Other Technologies for Upgrading Nickel Ore* , ALTA 2009 Nickel-Cobalt, Copper and Uranium Conference, May 2009, Perth
2. Bakker, E.J., (2009), *X-Ray Sorting of Shredder Residue: From Waste to Energy,* http://www.bk.tudelft.nl/live/pagina.jsp?id=e61f2806-476d-47e3-b6d8-245f85a1d0de, accessed June 2009
3. Bruno, E.A., (2009) *Automated Sorting of Plastics for Recycling,* http://www.p2pays.org/ref/09/08620.pdf, accessed January 2010
4. CommoDaS GmbH., (2006), *Product Brochures and Marketing Material,* Wedel, Germany
5. CommoDaS GmbH., (2009),CommoDaS *Product Brochures and Marketing Material*, Wedel, Germany
6. Dalmijn, W.L. and Jong, T.P.R de, (2004), *Developments in and the Application of Dual Energy X-Ray Transmission Sorting,* Sensorgestutzte Sortierung, Stolberg, Germany
7. De Jong, T.P.R., (2006), *DE-XRT Sorting of Coal*, Sensor Based Sorting Conference, Aachen, Germany
8. De Jong, T.P.R. Dalmijn, W.L. and Kattintidt, H.U.R., (2003), *Dual Energy X-ray Transmission Imaging for the Concentration and Control of Solids.* Proc. IMPC-2003 XXII International Minerals Processing Conference, Cape Town
9. De Jong. T.P.R. van Houwelingen, J.;Kuilmann, W., (2003) *On-line Imaging of Coal for Process Control and Dry Separation,* (Publication on University of Delft Website :- http://www.citg.tudelft.nl/live/pagina.jsp?id=1b65df55-948f-4c17-b12e-85492ff3f7e8&lang=en), Accessed November 2006
10. De Jong. T.P.R. van Houwelingen, J.;Kuilmann, W., (2004), *Automatic Sorting and Control in Solid Fuel Processing- Opportunities in European Perspective,* Geologica Belgica, [7(3-4)]

11. De Korte. GJ., (2009), *High Density Processing of Coal,* South African Coal Preparation conference, Accessed from SA Coal Preparation Society Webpage http://www.sacoalprep.co.za/Conference2009/18_High%20density%20processing%20of%20coal_J%20de%20Korte.pdf (access 31 January 2010)

12. Delgado, C. and Stenmark, A., (2005), *Technological Reference Paper on Recycling Plastics,* www.wastexchange.co.uk/document/H%20_medio_ambiente_PROVECTOS_Z5008_verc_clara_WP2_refpaper_plastic_v2.pdf (accessed November 2009)

13. Fox , N.; (2004) *X-ray Imaging for Security Applications.* www.pparc.co.uk/in/prest/2Nick_Fox.pdf, Accessed November 2006

14. Goosen, G., (2006) Personal Communication with Author via E-mail:-*Comments on TGA analysis of Torbanite Material*

15. Han, Z.; Kruge, M.A. Crelling, and J.C.;Bensley, D.F.; (1999), *Classification of Torbanite and Canned Coal- 1. Insights from Petrographic Analysis of Density Fractions,* International Journal of Coal Geology, [38(3)]

16. Harbeck, H.,(2004),*Classification of Minerals with the Use of X-ray Transmission,* Colloquim Sensorgestutzte Sortierung, Stolberg, Germany

17. Koningsberger, D.C., (1988), *X-Ray Absorption,* Wiley-Interscience, Maiden MA

18. Mesina, M.B., De Jong, T.P.R., Dalmijn, W.L., (2007) , *Automatic Sorting of Scrap With a Combined Electromagnetic and Dual Energy X-Ray Transmission Sensor,* International Journal of Minerals Processing, [4-82]

19. Platt,C.M.R.,(1991), *General Physics of Radiation in Remote Sensing,* CSIRO Office of Space Science and Applications (COSSA) Publication 026, accessed via http://ceos.cnes.fr:8100/cdrom00b2/ceos1/science/platt/pages/platt2.htm,2000, Accessed November 2007

20. Riedel,F.,(2006), Sortierung von Disseminerten Sulphiderzen mittels Rontgentransmission und Electromagnetischen Sensoren, Sensor Based Sorting Colloquiem, March 2006, Aachen

21. Salter. J.D. and Wyatt. N.P.G., (1991), *Sorting in the Minerals Industry: Past, Present and Future*, Minerals Engineering,[4(7-11)], p779

22. Sivamohan, R. and Forssberg,E. (1991), *Electronic Sorting and Other Preconcentration Methods,* Minerals Engineering, [4(7-11)], p797

23. Von Ketelhodt, L. , (2009), *Sensor Based Sorting:- New Developments,* Mintek 75th Anniversary Conference, June 2009

24. Wills, B.A., (1992), Minerals Processing Technology, 5th Edition, Pergamon Press Ltd, London, p 685-694

11 APPENDICES

11.1 Appendix A: Feed Analysis Certificates

								Ash Fusion Temperature								%	%	%
	%	%	%	%	Mj/Kg	%	%	°C Reducing Atmosphere				%	%	%	%	Pyritical	Sulfate	Organic
Sample Identity	H_2O	Ash	Volatile	F/Carbon	Cal Value	T Sulphur	Phos	Def	Soft	Hem	Flow	Carbon	Hydrogen	Nitrogen	Oxygen	Sulphur	Sulphur	Sulphur
COAL FEED +20mm	4.4	20.2	31.3	44.1	25.08	1.25		1446	1467	1478	1498	63.38	4.11	1.55	5.11	0.75	0.05	0.45
COAL FEED-20mm+10mm	4.8	23.6	28.9	42.7	23.35	1.46		1366	1393	1411	1421	59.21	3.68	1.25	5.99	1.00	0.10	0.46
COAL FEED-10mm+0.5mm	5.4	23.3	28.3	43.0	23.10	1.39		1360	1384	1406	1413	58.84	3.66	1.24	6.17	0.92	0.07	0.49
COAL FEED-0.5mm	5.5	38.3	25.0	31.2	17.24	1.47		1190	1210	1246	1271					0.53	0.03	0.75

	Ash Constituent Analyses															
	%	%	%	%	%	%	%	%	%	%	%	%	%	%	%	%
Sample Identity	SiO_2	Al_2O_3	Fe_2O_3	TiO_2	P_2O_5	CaO	MgO	SO_3	Na_2O	K_2O	Cr_2O_3	MnO	V_2O_5	ZrO_2	BaO	SrO
COAL FEED +20mm	59.39	24.68	6.79	1.01	0.06	1.96	1.36	2.45	0.43	1.38	0.02	0.02	0.02	0.04	0.07	0.05
COAL FEED-20mm+10mm	59.87	23.72	7.90	0.97	0.06	1.93	1.28	2.27	0.46	1.63	0.08	0.01	0.02	0.04	0.05	0.04
COAL FEED-10mm+0.5mm	59.70	23.71	7.80	0.97	0.06	1.81	1.22	2.22	0.55	1.77	0.05	0.01	0.02	0.05	0.06	0.04
COAL FEED-0.5mm	58.27	18.12	7.46	0.78	0.06	4.92	1.58	5.53	0.76	2.31	0.25	0.04	0.01	0.04	0.07	0.05

11.2 Appendix B : Comprehensive Washability Data

-80mm+20mm Sample

	Mass g		% Yield		% H_2O		% Ash		% Volatile		% Fixed Carbon		Cal Val - Mj/Kg		% T Sulphur	
Sample Identity	Total	Fract	Fract	Cumul	Fract	Cumul	Fract	Cumul	Fract	Cumul	Fract	Cumul	Fract	Cumul	Fract	Cumul
Mass=73.520Kg	73520															
F @ 1.30		580	0.8	0.8	6.0	6.0	5.8	5.8	35.7	35.7	52.5	52.5	29.66	29.66	0.51	0.51
F @ 1.35		23600	32.1	32.9	5.3	5.3	7.6	7.6	36.0	36.0	51.1	51.1	28.98	29.00	0.62	0.62
F @ 1.40		16050	21.8	54.7	4.9	5.2	12.0	9.3	34.1	35.2	49.0	50.3	27.37	28.35	0.65	0.63
F @ 1.45		11700	15.9	70.6	4.4	5.0	18.3	11.4	32.3	34.6	45.0	49.1	25.21	27.64	0.88	0.69
F @ 1.50		1928	2.6	73.3	4.9	5.0	21.4	11.7	29.8	34.4	43.9	48.9	23.92	27.51	1.10	0.70
F @ 1.55		1525	2.1	75.3	4.5	5.0	24.8	12.1	29.3	34.3	41.4	48.7	23.00	27.38	2.19	0.74
F @ 1.60		1606	2.2	77.5	4.3	4.9	27.4	12.5	26.7	34.1	41.6	48.5	21.74	27.22	1.80	0.77
F @ 1.65		1030	1.4	78.9	4.0	4.9	29.2	12.8	29.0	34.0	37.8	48.3	21.37	27.12	4.24	0.83
F @ 1.70		1160	1.6	80.5	4.5	4.9	34.7	13.2	23.6	33.8	37.2	48.1	18.69	26.96	3.88	0.89
F @ 1.75		1138	1.5	82.0	4.2	4.9	41.5	13.8	19.3	33.5	35.0	47.8	16.50	26.76	1.12	0.90
F @ 1.80		1996	2.7	84.8	3.6	4.9	51.2	15.0	16.8	33.0	28.4	47.2	12.29	26.29	3.46	0.98
Si @ 1.80		11200	15.2	100.0	2.7	4.5	69.1	23.2	12.0	29.8	16.2	42.5	5.58	23.14	3.36	1.34
Total		73512	100.0													

-20+10mm Sample

	Mass g		% Yield		% H_2O		% Ash		% Volatile		% Fixed Carbon		Cal Val - Mj/Kg		% T Sulphur	
Sample Identity	Total	Fract	Fract	Cumul	Fract	Cumul	Fract	Cumul	Fract	Cumul	Fract	Cumul	Fract	Cumul	Fract	Cumul
Sample Mass	52770															
F @ 1.30		11457	21.7	21.7	6.0	6.0	6.4	6.4	36.0	36.0	51.6	51.6	28.98	28.98	0.58	0.58
F @ 1.35		6750	12.8	34.5	5.7	5.9	8.0	7.0	35.1	35.7	51.2	51.5	28.54	28.82	0.49	0.55
F @ 1.40		13870	26.3	60.8	5.6	5.8	10.9	8.7	33.2	34.6	50.3	51.0	27.48	28.24	0.56	0.55
F @ 1.45		4778	9.1	69.8	4.9	5.7	16.9	9.7	32.3	34.3	45.9	50.3	25.70	27.91	0.68	0.57
F @ 1.50		1636	3.1	72.9	5.0	5.6	20.8	10.2	29.7	34.1	44.5	50.1	24.13	27.75	0.83	0.58
F @ 1.55		1352	2.6	75.5	4.8	5.6	24.3	10.7	27.8	33.9	43.1	49.8	22.88	27.58	0.84	0.59
F @ 1.60		848	1.6	77.1	4.7	5.6	27.7	11.0	25.9	33.7	41.7	49.6	21.63	27.46	1.08	0.60
F @ 1.65		689	1.3	78.4	4.7	5.6	32.6	11.4	23.2	33.6	39.5	49.5	19.46	27.33	1.53	0.61
F @ 1.70		900	1.7	80.1	4.5	5.5	36.7	11.9	20.6	33.3	38.2	49.2	18.21	27.13	1.44	0.63
F @ 1.75		733	1.4	81.5	4.4	5.5	40.4	12.4	18.8	33.0	36.4	49.0	16.45	26.95	1.42	0.65
F @ 1.80		2535	4.8	86.3	3.8	5.4	52.9	14.7	16.1	32.1	27.2	47.8	11.96	26.12	2.88	0.77
Si @ 1.80		7220	13.7	100.0	3.3	5.1	60.3	20.9	14.9	29.7	21.5	44.2	8.65	23.73	6.03	1.49
		0														
Total		52768	100.0													

-10mm+0.5mm Sample

	Mass g		% Yield		% H_2O		% Ash		% Volatile		% Fixed Carbon		Cal Val - Mj/Kg		% T Sulphur	
Sample Identity	Total	Fract	Fract	Cumul	Fract	Cumul	Fract	Cumul	Fract	Cumul	Fract	Cumul	Fract	Cumul	Fract	Cumul
Sample Mass	26030															
F @ 1.30		4361	16.9	16.9	6.4	6.4	5.2	5.2	34.3	34.3	54.1	54.1	28.80	28.80	0.61	0.61
F @ 1.35		5423	21.0	37.9	5.3	5.8	8.2	6.9	34.1	34.2	52.4	53.2	28.14	28.43	0.58	0.59
F @ 1.40		5000	19.4	57.2	5.7	5.8	11.4	8.4	33.0	33.8	49.9	52.1	27.03	27.96	0.50	0.56
F @ 1.45		1746	6.8	64.0	5.2	5.7	15.9	9.2	32.9	33.7	46.0	51.4	25.34	27.68	0.53	0.56
F @ 1.50		969	3.8	67.7	5.0	5.7	19.9	9.8	29.7	33.5	45.4	51.1	24.11	27.48	0.59	0.56
F @ 1.55		672	2.6	70.3	5.1	5.6	23.9	10.3	27.7	33.3	43.3	50.8	22.38	27.30	0.81	0.57
F @ 1.60		435	1.7	72.0	4.6	5.6	30.3	10.8	24.6	33.1	40.5	50.6	19.94	27.12	0.53	0.57
F @ 1.65		399	1.5	73.6	4.6	5.6	30.9	11.2	23.9	32.9	40.6	50.3	19.64	26.97	1.11	0.58
F @ 1.70		442	1.7	75.3	4.5	5.6	37.2	11.8	20.1	32.6	38.2	50.1	17.42	26.75	0.64	0.58
F @ 1.75		424	1.6	76.9	4.1	5.5	40.5	12.4	18.3	32.3	37.1	49.8	16.31	26.53	0.57	0.58
F @ 1.80		1196	4.6	81.5	4.1	5.5	50.3	14.5	16.9	31.4	28.7	48.6	12.30	25.72	1.02	0.61
Si @ 1.80		4770	18.5	100.0	2.8	5.0	65.9	24.0	14.2	28.2	17.1	42.8	6.96	22.26	4.91	1.40
Total		25836	100.0													

11.3 Appendix C:- Optimisation Testwork Raw Data

Test 2- Sensivity =70% Blue (Original Setting)

Stream	Mass Yield %	CV	Ash	Moisture	Volatiles	Fixed Carbon	Total S
Coal Product	65.0	27.34	12.3	5.6	32.9	49.2	1.02
Torbanite + Shale	35.0	14.53	49.2	3.6	20.8	26.4	2.47
Total	100.0	22.9	25.2	4.9	28.7	41.2	1.5

Test 3 - Sensivity =60% Blue

Stream	Mass Yield %	CV	Ash	Moisture	Volatiles	Fixed Carbon	Total S
Coal Product	48.1	28.13	10.1	5.3	33.9	50.7	0.73
Torbanite + Shale	51.9	18.73	37.3	3.8	25.3	33.6	2.62
Total	100.0	23.3	24.2	4.5	29.4	41.8	1.7

Test 4- Sensivity =53% Blue

Stream	Mass Yield %	CV	Ash	Moisture	Volatiles	Fixed Carbon	Total S
Coal Product	42.9	28.18	10.5	5.1	33.7	50.7	0.77
Torbanite + Shale	57.1	20.00	33.6	3.8	25.9	36.7	1.74
Total	100.0	23.5	23.7	4.4	29.2	42.7	1.3

Test 5- Sensitivity=80% Blue

Stream	Mass Yield %	CV	Ash	Moisture	Volatiles	Fixed Carbon	Total S
Coal Product	71.8	26.94	13.5	5.5	32.6	48.4	0.96
Torbanite + Shale	28.2	13.07	51.6	3.3	20.1	25	2.76
Total	100.0	23.0	24.3	4.9	29.1	41.8	1.5

Test 16

		Composition				
Stream	**Mass Yield %**	**Humic Coal**	**Mixed H/S**	**Torbanite**	**Total Organic**	**Cbmin/Rock**
Coal Product	68.9	87	5	1	93	7
Torbanite + Shale	31.1	35.6	7.8	6.3	49.7	50.3
Total	100.0	71.0	5.9	2.6	79.5	20.5

Stage 2

		Composition				
Stream	**Mass Yield %**	**Humic Coal**	**Mixed H/S**	**Torbanite**	**Total Organic**	**Cbmin/Rock**
Torbanite	47.4	44.0	11	11	66	34
Shale	52.6	28.0	5	2	35	65
Total	100	35.6	7.8	6.3	49.7	50.3

Test 2

		Composition				
Stream	**Mass Yield %**	**Humic Coal**	**Mixed H/S**	**Torbanite**	**Total Organic**	**Cbmin/Rock**
Coal Product	65.0	89	4	1	94	6
Torbanite + Shale	35.0	30	9.0	4	43	57
Total	100.0	68.4	5.7	2.0	76.2	23.8

Test 3

		Composition				
Stream	**Mass Yield %**	**Humic Coal**	**Mixed H/S**	**Torbanite**	**Total Organic**	**Cbmin/Rock**
Coal Product	48.1	91	4	1	96	4
Torbanite + Shale	51.9	48	8.0	7	63	37
Total	100.0	68.7	6.1	4.1	78.9	21.1

Test 4

		Composition				
Stream	**Mass Yield %**	**Humic Coal**	**Mixed H/S**	**Torbanite**	**Total Organic**	**Cbmin/Rock**
Coal Product	42.9	91	5	0	96	4
Torbanite + Shale	57.1	55	8.0	3	66	37
Total	100.0	70.4	6.7	1.7	78.9	22.8

Test 5

		Composition				
Stream	**Mass Yield %**	**Humic Coal**	**Mixed H/S**	**Torbanite**	**Total Organic**	**Cbmin/Rock**
Coal Product	71.8	84	4	2	90	10
Torbanite + Shale	28.2	26	11.0	5	42	58
Total	100.0	67.6	6.0	2.8	76.4	23.6

11.4 Appendix D: Comprehensive Product Analysis

	%	%	%	%	Mj/Kg	%	°C Reducing Atmosphere			
Sample Identity	H_2O	Ash	Volatile	F/Carbon	Cal Value	T Sulphur	Def	Soft	Hem	Flow
COAL PRODUCT	4.8	11.5	33.3	50.4	27.64	0.88	1395	1409	1418	1444
TORBANITE PRODUCT	3.4	31.8	28.9	35.9	21.40	0.97	>1550	>1550	>1550	>1550
SHALE	2.8	61.4	15.8	20.0	8.80	3.43	1404	1412	1423	1454
Lurgi -3mm x +0.5mm	5.0	28.4	27.5	39.1			>1550	>1550	>1550	>1550
Lurgi -0.5mm	4.6	32.4	26.6	36.4			1527	>1550	>1550	>1550

	Ash Constituent Analyses									
	%	%	%	%	%	%	%	%	%	%
Sample Identity	SiO_2	Al_2O_3	Fe_2O_3	TiO_2	P_2O_5	CaO	MgO	SO_3	Na_2O	K_2O
COAL PRODUCT	56.36	25.17	5.93	0.98	0.08	3.70	1.75	4.49	0.70	1.12
TORBANITE PRODUCT	62.96	26.84	3.81	1.10	0.06	1.10	1.11	1.25	0.39	1.39
SHALE	61.06	22.49	10.33	0.98	0.06	0.71	1.14	0.74	0.42	1.99
Lurgi -3mm x +0.5mm	62.41	26.49	2.98	1.15	0.07	1.29	1.12	1.57	0.48	1.35
Lurgi -0.5mm	62.60	25.86	4.05	1.07	0.05	1.27	1.25	1.64	0.39	1.44

	Trace Elements (mg/kg)									
Sample Identity	As	Ba	Bi	Cd	Co	Cr	Cu	Ga	Ge	Hg
COAL PRODUCT	1.8	62.0	0.2	0.1	4.4	11.3	6.5	7.6	5.1	0.1
TORBANITE PRODUCT	2.5	201.0	0.7	0.1	3.5	18.2	11.2	15.8	4.4	0.1
SHALE	15.9	176.0	0.8	0.2	6.4	74.0	14.9	24.9	2.7	0.3
Lurgi -3mm x +0.5mm	1.8	147.0	0.6	0.2	3.5	19.2	11.8	15.2	6.8	0.1
Lurgi -0.5mm	3.4	184.0	0.7	0.2	4.1	42.9	20.5	15.7	5.3	0.1
	Sb	Se	Sn	Sr	Th	U	V	W	Y	Zn
COAL PRODUCT	0.2	1.5	0.6	11.7	2.1	1.2	17.4	2.5	10.8	9.3
TORBANITE PRODUCT	0.3	1.4	1.0	7.9	2.1	1.9	28.5	1.7	3.1	20.2
SHALE	0.4	2.5	1.2	6.4	3.3	2.4	45.2	2.5	2.0	31.2
Lurgi -3mm x +0.5mm	0.4	1.4	1.0	9.1	1.6	1.9	31.6	1.8	3.2	16.3
Lurgi -0.5mm	0.3	1.7	1.0	9.7	2.1	2.0	36.3	1.7	3.8	21.1

11.5 Appendix E : TGA Report

TG ANALYSIS
Date 10-08-2005

Pretoria 0002 Republic of South Africa http://www.up.ac.za
Institute of Applied Materials
Tel. (012) 420 2588 Fax. (012) 420 2516

REPORT

THERMAL ANALYSIS OF COAL SAMPLES

Prepared for: **Prof Rosemary Falcon**

Prepared by: **Mila Maksa**
Institute of Applied Materials
UNIVERSITY OF PRETORIA
LYNNWOOD ROAD
PRETORIA

CONTENTS

INTRODUCTION

Prof Rosemary Falcon approached the Institute of Applied Materials at the Pretoria University for TG analysis on 3 samples for volatile content and CO_2 reactivity.

The samples were labeled:	Coal	97397
	Torbanite	97398
	Shale	97399

METHOD

Thermogravimetric analysis (TGA) implies the monitoring the weight loss of a as the temperature increases. Weight loss is dew to moisture and other volatiles, and at higher temperatures, to the degradation of the materials. This technique can be used both to examine the state of material (i.e. the presence and quantity of volatiles) and to investigate the process of degradation (identifying temperatures at which significant changes occur and, by controlling the atmosphere and / or by analyzing the products evolved obtaining information about the chemistry of the degradation process).

In the cases where various weight losses are not completely discrete, the use of the derivative thermogravimetric curve (DTG) is recommended. In DTG the rate of weight loss of the sample is recorded as a function of temperature. The DTG curve consists of a series of peaks, corresponding to the various steps in the decomposition of the sample. The area under each peak is proportional to the weight loss.

Mettler TGA/SDTA 851e was used for the analysis. It is equipped with an additional sensor to record the temperature difference between the temperature measured directly at the sample and the model reference temperature. This measuring signal is called SDTA (single DTA) and indicates for example whether transition is exothermic or endothermic, analogously to DSC.
SDTA curve can be converted to a heat flow curve (DSC) by the determination of a temperature dependent calibration function.

VOLATILE RELEASE AND REACTIVITY

Two methods were used:

1. **Volatile Release and CO_2 Reactivity**. The samples were heated in Nitrogen from 25 to 150°C at a heating rate 10°C/min and held isothermally at this temperature for 5 min. The mass loss represents the moisture in the sample. The temperature was then raised at rate 10°C/min to 1000°C and held at this temperature for 5 min. The mass loss was attributed to loss of volatile components. While temperature was maintained at 1000°C the purge gas was changed from Nitrogen to Carbon Dioxide and held at this temperature 60 min. The reactivity (mg/min) of the coal in CO_2 was determined.

Combustion. The samples were heated in air from 25 to 1000°C at rate 10°C/min. The remaining mass in the sample pan is the ash content in the sumple. The heat of

1. combustion is converted from SDTA curve, using the temperature dependent calibration function.

CONDITIONS

(a) VOLATILE RELEASE AND REACTIVITY

Measuring cell:	TGA 851e with gas controller		
Pan:	Alumina 70 µl, no lid		
Sample preparation:	The sample was used as received and ± 20 mg was carefully weighed on the Thermogravimetric analyzer.		
TGA measurement:	25-150 ºC	10 ºC/min	N_2 50 ml/min
	150 ºC	5 min	N_2 50 ml/min
	150 ºC-1000 ºC	10 ºC/min	N_2 50 ml/min
	1000 ºC	5 min	N_2 5 0ml/min
	1000 ºC	60 min	CO_2 50 ml/min

(b) COMBUSTION

Measuring cell:	TGA 851e with gas controller		
Pan:	Alumina 70 µl, no lid		
Sample preparation:	The sample was used as received and ± 20 mg was carefully weighed on the Thermogravimetric analyzer.		
TGA measurement:	25-1000ºC	10ºC/min	AIR 50ml/min

RESULTS

VOLATILE RELEASE

Typical TG and SDTA results curves are given in Figures 1 to 8. Figures 3 and 4 compare the TG and DTG properties of the three samples. Figure 3 indicates that

1. The moisture, volatiles and fixed carbon and reactivity contents increases in the order shale < torbanite < coal
2. Ash content increases in the order coal <torbanite < Shale

Figure 4 shows that the volatiles release occurs as two separate but overlapping events.

Figure 5 compares the TG CO_2 reactivity of Coal, Torbanite and Shale.

Figure 6 to 8 show the combustion in air for Coal, Torbanite and Shale.

The results of volatile components, the DTG peak temperatures (inflection point of the TG curve) are given in Table 1.

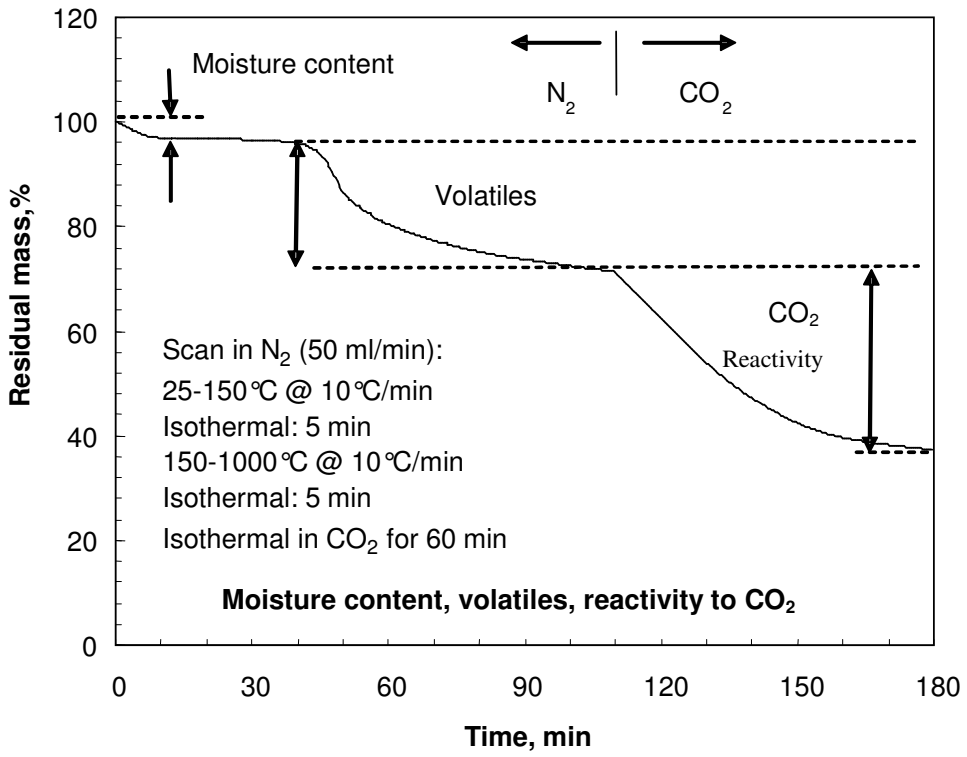

Fig. 1: TG moisture content, volatiles and the reactivity of Torbanite.

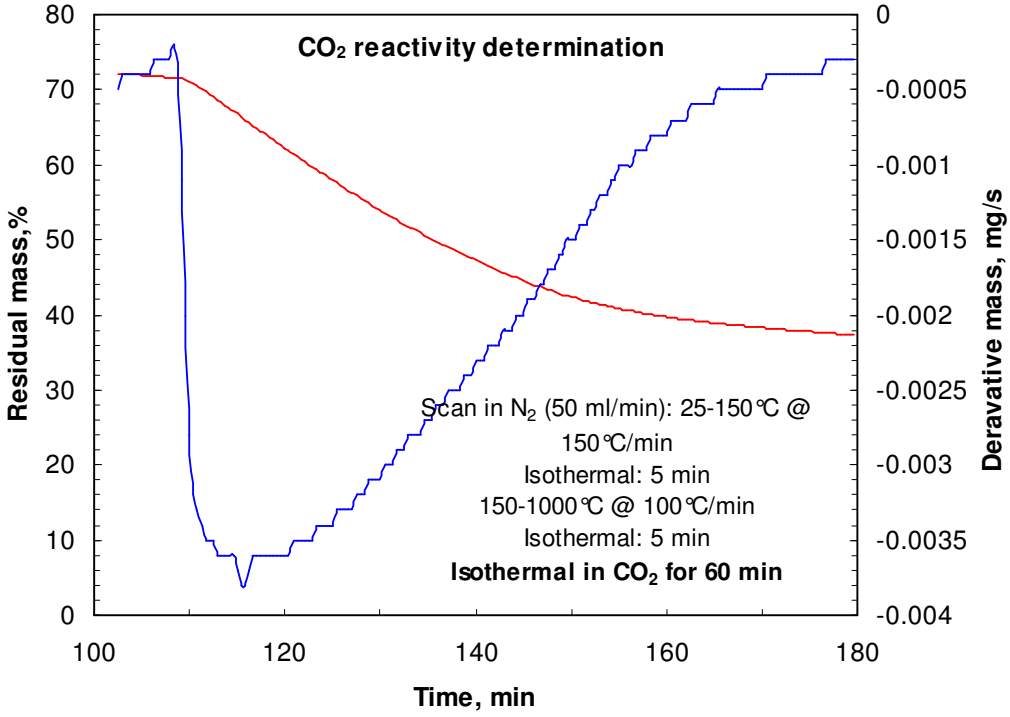

Fig. 2 TG CO_2 reactivity of Turbonite

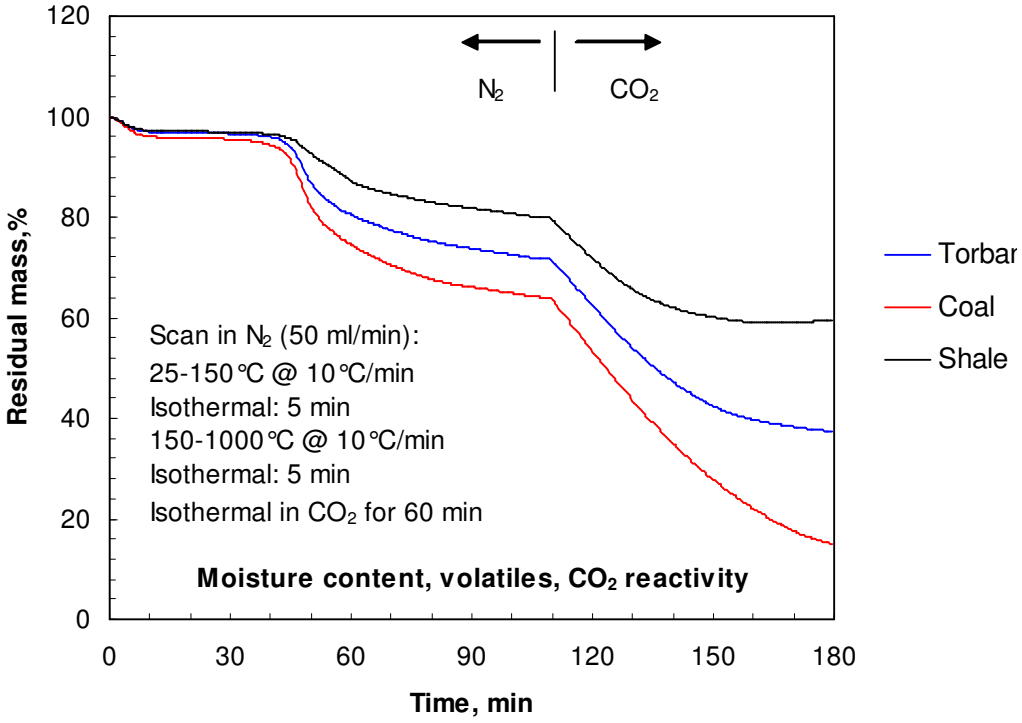

Fig. 3: TG comparison: Moisture, volatiles and CO_2 reactivity content.

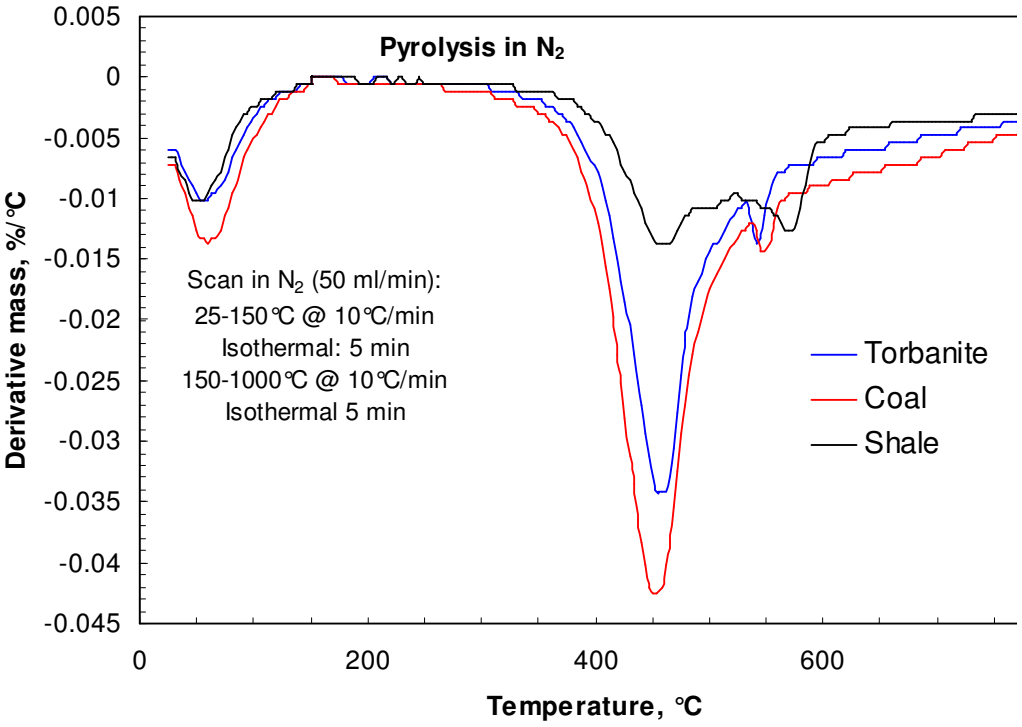

Fig. 4: DTG moisture and volatiles of Coal, Torbanite and Shale.

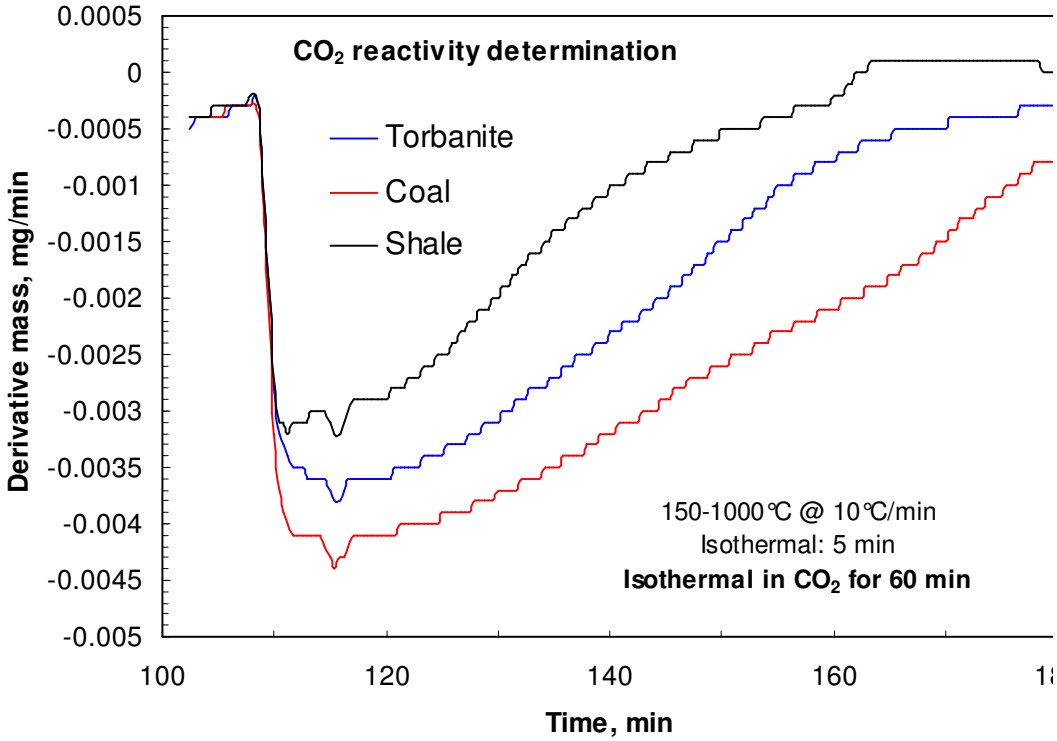

Fig. 5: TG CO_2 reactivity of Coal, Torbanite and Shale.

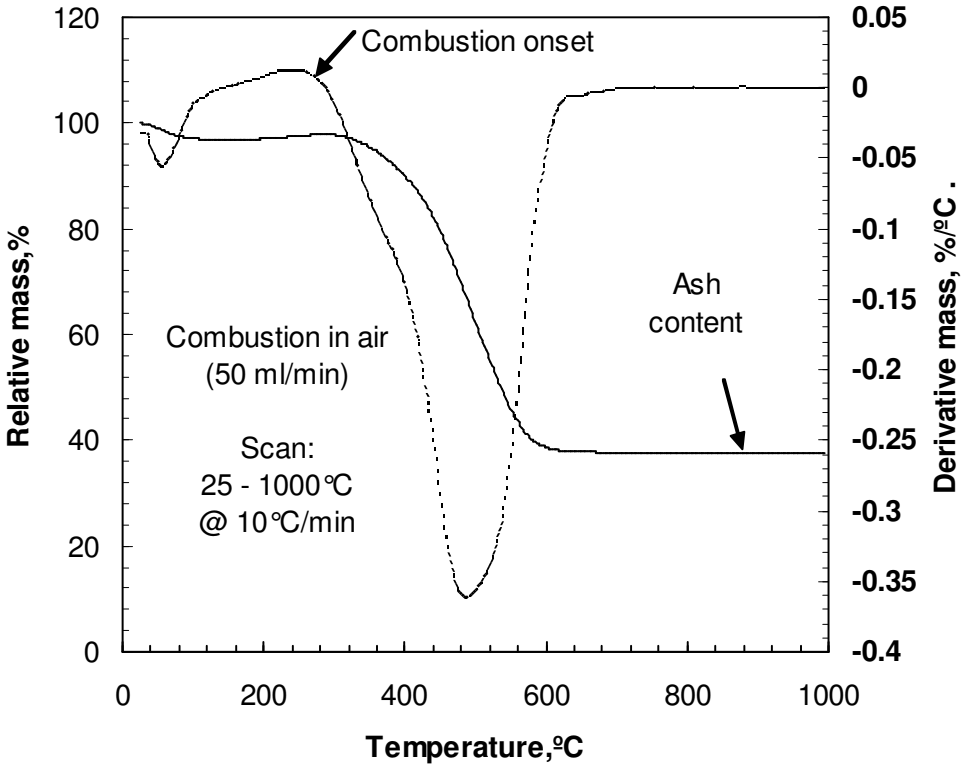

Fig. 6: TGA combustion in air of Coal

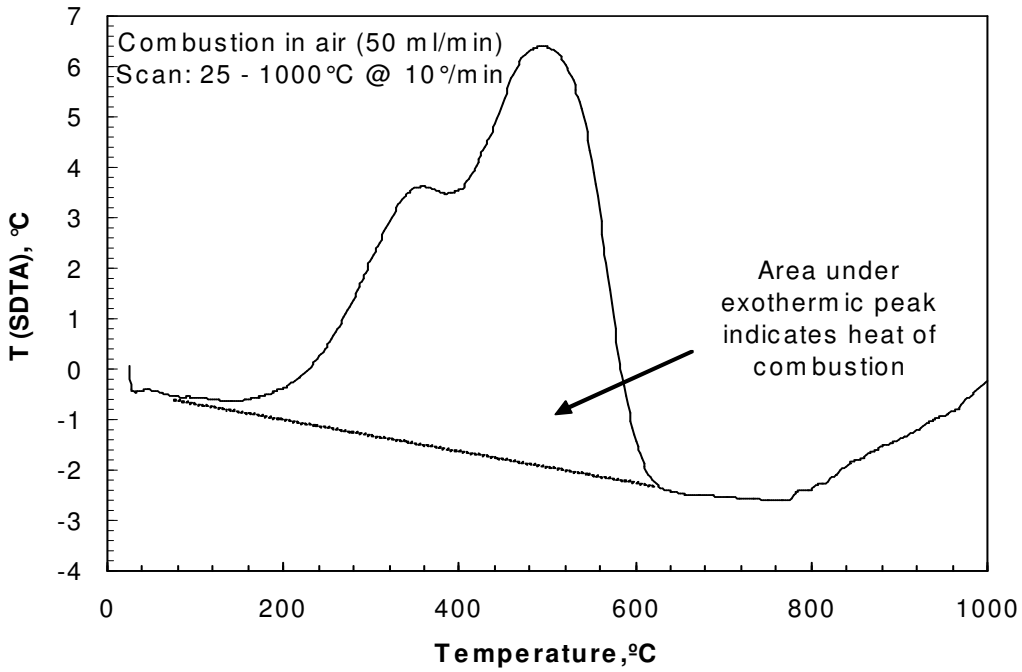

Fig. 7: SDTA combustion in air of Coal.

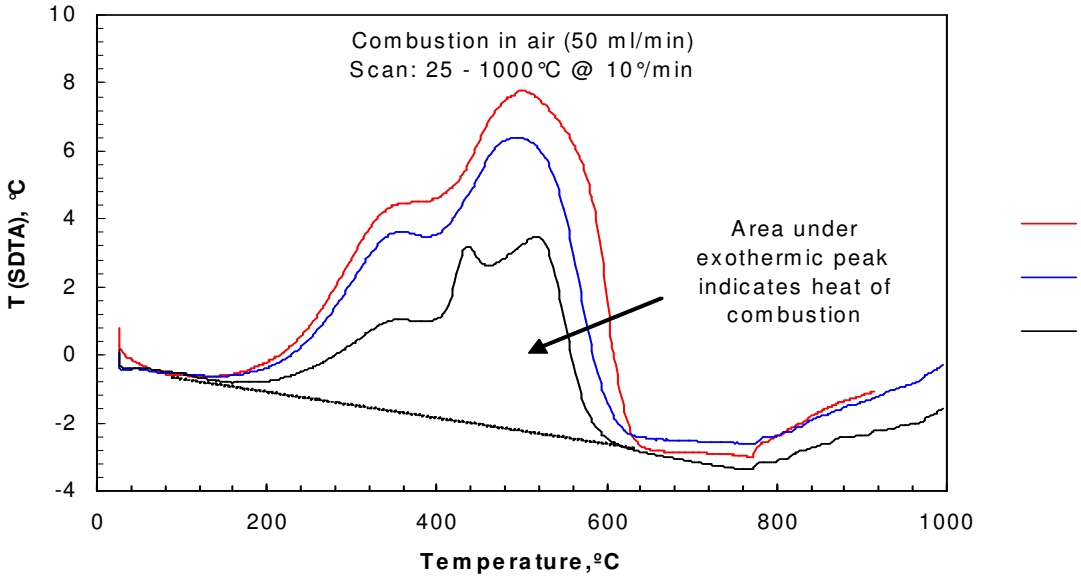

Fig. 8: Comparison SDTA combustion in air of Coal, Torbanite and Shale.

Table 1: TG/DTG results

Sample ID	Moisture %	Volatile Components % Mass loss	DTG Peak Temperature °C	Residue %
Coal 97397	4.18	31.48	58.01 452.09 548.54	63.36
Torbanite 97398	3.15	24.98	56.33 457.72 542.47	71.02
Shale 97399	2.91	17.14	49.83 458.70 571.31	79.58

SDTA curves in Nitrogen shoved an endothermic peak related to moisture and exothermic to volatiles. The middle endothermic and exothermic events (T. max.) are stated in Table 2.

Table 2: SDTA results

Sample ID	Moisture Endotherm peak Temperature ºC	Volatiles Exotherm peak Temperature ºC
Coal 97397	67.13	149.41 583.46
Torbanite 97398	74.03	149.45 572.73
Shale 97399	60.64	149.44 560.03

REACTIVITY

The results of the CO_2 reactivity are given in Table 3.

Table 3: Reactivity to CO_2

Sample ID	Reactivity in CO_2 Mass loss %	Residue %	Reactivity in CO_2 (mg/hr)
Coal 97397	48.52	14.83	3.05
Torbanite 97398	33.96	37.06	7.58
Shale 97399	20.48	59.10	11.96

COMBUSTION

The initial weight loss is due to the loss of moisture. The increase in weight at around 120-275 °C is due to oxygen absorption. Then combustion takes place over a range of temperature, leaving a residue of ash.

The TGA combustion components are given in Table 4. The DTG peak temperatures for the identification at 10ºC/min are given in Table 5.

Table 4: TGA results

Sample ID	Combustion Total Mass loss %	Ash %
Coal 97397	85.39	13.42
Torbanite 97398	62.22	37.24
Shale 97399	39.53	59.89

Table 5: DTG results

TG/DTG EVALUATION	**Coal 97397**	**Torbanite 97398**	**Shale 97399**
Temp. Range ºC	25-120	25-120	25-120
% Weight Loss	3.75	3.11	2.39
Temp. Range ºC	120-275	120-275	120-275
% Weight Gain	+1.13	+ 0.19	+ 0.43
Temp. Range ºC	275-1000	275-1000	275-1000
% Weight Loss	82.77	60.02	37.57
% ASH	13.42	37.24	59.89
Onset/Endset ºC	275.6 / 655.7	404.2 / 568.0	417.6 / 554.06
Peak Temp. ºC	504.09	492.53	435.28 / 514.78

Combustion reaction is characterized by an exothermic peak. The measured peak areas with peak temperature are listed in Table 6

Table 6: SDTA T.max.

Sample ID	Combustion Exotherm Peak ºC
Coal 97397	509.28
Torbanite 97398	504.23
Shale 97399	521.49

FULL ANALYSIS OF COAL SAMPLES

Table 7: Summary analysis of coal samples, obtained by TGA/SDTA

Sample	Moisture (%)	Volatile Material (%)	Fixed Carbon (%)	Ash (%)	Reactivity in CO_2 (mg/hr)	Heat of Combustion (kJ/g)
Coal 97397	4.18	31.48	50.92	13.42	3.05	
Torbanite 97398	3.15	24.98	34.63	37.24	7.58	
Shale 97399	2.91	17.14	20.06	59.89	11.96	

Remarks:

The fixed carbon is calculated from:

Fixed carbon = (100 - % Moisture - % Volatile material - % Ash)

The steps have been evaluated with horizontal baseline. A blank curve has been run prior to the measurement.

All onsets/endsets are based on inflectional tangents.

It should be noted that the TGA/SDTA 851e provides the results of the calibration standards in the conversion of the SDTA curve into DSC within 10%.